DOI: 10.1002/smll.200600727

The Synthesis and Fabrication of One-Dimensional Nanoscale Heterojunctions

■■*All academic titles please*■■*Aneta J. Mieszawska, Romaneh Jalilian, Gamini U. Sumanasekera, and Francis P. Zamborini**

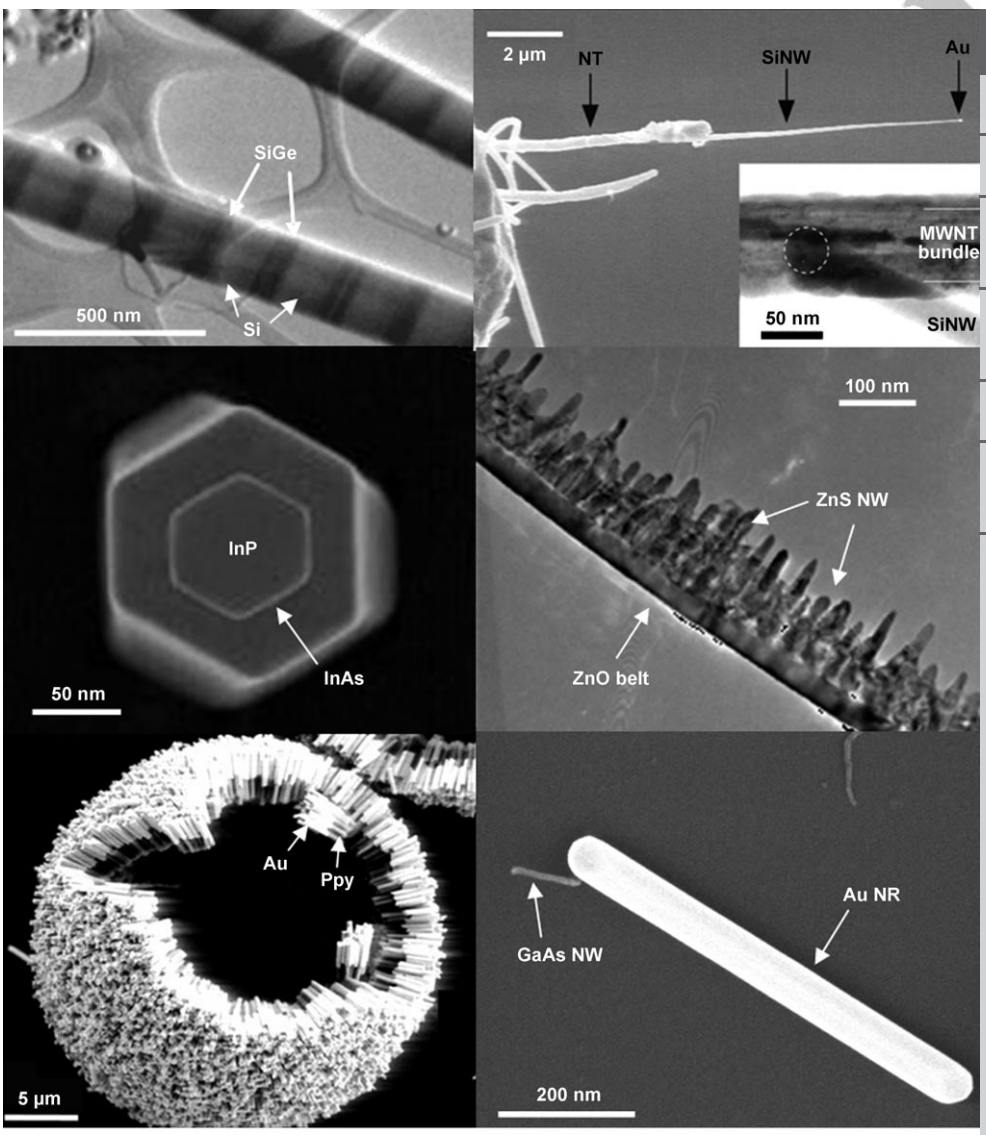

"Some examples of the wide variety of one-dimensional nanoscale heterostructures to have been synthesized."

From the Contents

Keywords:
- heterojunctions
- nanorods
- nanostructures
- nanowires
- one-dimensional (1D)

These are not the final page numbers!

NANO MICRO small

There are a variety of methods for synthesizing or fabricating one-dimensional nanostructures containing heterojunctions between different materials; such structures lead to unique properties and multifunctionality useful for a wide range of applications. Here we review recent developments in the synthesis and fabrication of such heterojunctions formed between different materials within the same 1D nanostructure or between different 1D nanostructures comprised of different materials. Structures containing 1D nanoscale heterojunctions exhibit interesting chemistry as well as size, shape, and material-dependent properties that are unique when compared to single-component materials. This leads to new or enhanced properties or multifunctionality useful for a variety of applications in electronics, photonics, catalysis, and sensing, for example. This review separates the methods into vapor-phase synthesis, solution-phase synthesis, template-based synthesis, and other approaches, such as lithography, electrospinning, and assembly. These methods are used to form a variety of heterojunctions, including segmented, core/shell, branched, or crossed, from different combinations of semiconductor, metal, carbon, and polymeric materials.&
&*text changed somewhat or swapped for TOC and Abstract. OK?*&&

1. Introduction

The synthesis of one-dimensional (1D) nanostructures[1–13] has gained a tremendous amount of attention in recent years due to their fascinating chemistry and size-, shape-, and material-dependent properties. Their interesting electronic, optical, and magnetic properties, along with small size and chemical reactivity, have led to a wide range of applications in nanoelectronics, optoelectronics, plasmonics, medical diagnostics, catalysis, drug delivery, therapeutics, separations, and chemical sensing. There are many different forms of 1D nanostructures, which are all characterized by a high aspect ratio (length-to-width). Nanorods (NRs) and nanowires (NWs) are the most common shape, differing only by their aspect ratio (AR), which is commonly defined as <20 for NRs and ≥ 20 for NWs, respectively. Other common 1D shapes include tubes, ribbons, belts, whiskers, and needles. The physical properties greatly depend upon the material, which can be metals, alloys, semiconductors, carbon, polymers, or molecular, but may also depend on shape, morphology, and structure (i.e., crystalline or amorphous).

There have been two main types of studies on the properties of 1D structures. The first includes those that measure the collective properties of a solution or solid-state assembly of numerous 1D structures. This requires the ability to synthesize large quantities of material with high uniformity and low size dispersity in order to determine the structure and size-dependent properties. For solid-state properties, it is also necessary that the material be deposited as a film or assembled into an ordered array, and depending on the property, may also require control over alignment and orientation of the assembly. One example of collective properties is the optical spectrum of a solution of metallic 1D NRs or NWs of Ag and Au, which prominently display a transverse and AR-dependent longitudinal plasmon band.[14–16] Oriented, assembled arrays of Ag NWs and NRs display high surface-enhanced Raman scattering (SERS),[17–19] fluorescence enhancement,[20] and plasmonic waveguiding properties,[21,22] for example. Semiconductor NWs and carbon-nanotube arrays display properties useful for applications in nanoelectronics,[23] optoelectronics,[24] lasing,[25] sensing,[26,27] and separations.[28]

The second type of study includes those that isolate and measure the properties of individual 1D nanostructures. Excellent examples include electronic studies of individual carbon nanotubes and Si NWs, which behave as field-effect transistors[29–32] and electronic-based chemical or biological sensors.[33–35] There are also studies on the photoconductive properties of individual semiconductor NWs[36,37] and the effect of molecular adsorption on the conductivity of individual metallic quantum wires.[38] These studies have had an

[*] ■. a. t. p. J. Mieszawska, F. P. Zamborini
Department of Chemistry, University of Louisville
Louisville, Kentucky 40292 (USA)
Fax: (+1) 502-852-8149
E-mail: f.zamborini@louisville.edu
R. Jalilian
Department of Physics, University of Louisville
Louisville, Kentucky 40292 (USA)
R. Jalilian, G. U. Sumanasekera
Department of Electrical and Computer Engineering
University of Louisville, Louisville, Kentucky 40292 (USA)

enormous impact on nanotechnology, demonstrating the great potential of these materials for a variety of applications.

A natural progression from single-component materials has been towards the synthesis and design of more complex, multicomponent 1D nanostructures. These multicomponent materials contain heterojunctions between various combinations of metals (M), semiconductors (SC), carbon (C), and polymers (P) having a nanoscale 1D morphology. The formation of 1D heterojunctions has led to materials with unique properties and multiple functionalities not realized in single-component structures that are useful for a wide range of applications. For example, the synthesis of p–n junctions formed from SC–SC 1D heterojunctions has resulted in current rectification[39] useful for logic gates, the fabrication of nanoscale photodetectors,[40] and functional light-emitting diodes (LEDs).[41] M–SC–M heterojunction NWs are photoconductive and M–M segmented 1D heterojunctions have been used for biosensing,[42] gene delivery,[43] separations,[44] and catalysis.[45] Other groups have synthesized segmented M–M 1D heterojunctions, where the different segments possess different functions and properties, leading to the assembly of higher-order superstructures.[46,47] Combining different materials into a 1D nanostructure exploits the combined benefits of the 1D morphology with the unique function of the multicomponent heterojunction.

One of the most promising applications of 1D nanostructures in general, as shown in some of the examples above, has been in the area of electronics and photonics. Their small size potentially allows for higher-density electronics, which could lead to smaller, more portable devices or those with improved speed and performance. In addition to the size benefit, the small size of the structures often leads to vastly different properties compared to their bulk or 2D counterparts due to the higher surface-to-volume ratio of the material and quantum confinement effects. These properties are often tunable by the nanostructure size and offer more desirable properties for certain applications. Heterojunctions of 1D materials offer the same size and property benefit as single-component materials, but with the added benefit of multifunctionality or new properties arising from combining different materials, such as p–n junctions or

Aneta J. Mieszawska was born in Lublin, Poland. She obtained her MS degree in 2002 in Environmental Protection from the Technical University of Lublin, studying "Effectiveness of Ozone on BTX-hydrocarbon Oxidation". She entered the graduate program at the University of Louisville (Louisville, KY) in the fall of 2002, where she is currently pursuing her PhD in chemistry under the guidance of Prof. F. P. Zamborini. Her research involves the synthesis, assembly, and alignment of gold nanorods and 1D nanoscale heterojunctions (Au/GaAs, Au/ CNT and CNT/GaAs) directly on surfaces and the study of their electronic and chemical-sensing properties.

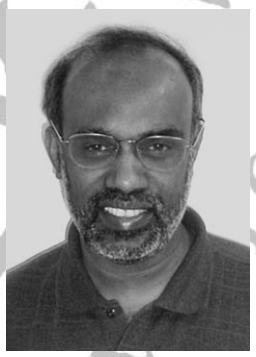

Gamini U. Sumanasekera received his BS from the University of Peradeniya (Sri Lanka) in 1980 and PhD from Indiana University (Bloomington, IN) in 1995. He then worked as a research associate at Pennsylvania State University (State College, PA) until he joined the faculty at the University of Louisville (Louisville, KY) in 2002 as an Assistant Professor in the Department of Physics. He also currently serves as an associate faculty member in the Department of Electrical and Computer Engineering and as the associate director for the Institute of Advanced Materials at the University of Louisville. His research interests include the synthesis and characterization of nanostructres, including carbon nanotubes, inorganic nanowires, and 3D interconnected porous structures. He also concentrates his research efforts on device fabrication, chemical sensors, thermoelectricity, and quantum transport.

Editorial Advisory Board Member

Romaneh Jalilian received her BSc in physics from Shahid Beheshti University (Tehran, Iran) in 2000 and MS in physics at the University of Louisville (Louisville, KY) in 2004. The focus of her MS research was nanomaterials synthesis and design of vacuum systems for nanostructure growth. She received the Manuel B. Schwartz Award for outstanding graduate student in May 2004. She is currently a PhD candidate in the Department of Electrical Engineering at the University of Louisville under the supervision of Prof. G. U. Sumanasekera. The topic of her dissertation is "Novel Properties of Semiconducting Nanowires, Superlattices & Heterojunctions". Her research interest is in the synthesis and characterization of semiconducting nanowires and heterojunction nanostructures. She recently extended her skills on nanodevice fabrication for the electrical and optical characterization of nanostructures.

Francis P. Zamborini received a BA in chemistry from Carthage College (Kenosha, WI) in 1993 and a PhD in chemistry from Texas A&M University (College Station, TX) in 1998. Under the direction of Prof. R. M. Crooks, his doctoral research focused on the use of self-assembled monolayers for corrosion passivation and nanolithography as studied by scanning probe microscopy, electrochemistry, and surface spectroscopy. He studied under Prof. R. W. Murray at the University of North Carolina (Chapel Hill, NC) as a postdoctoral research associate from 1998–2001, focusing on assembly, electron transport, and chemical-sensing properties of gold nanoparticles. He joined the faculty at the University of Louisville in 2001, where he is currently an Assistant Professor and member of the ElectroOptics Research Institute and Nanotechnology Center. His research interests are in the synthesis, assembly, and chemical-sensing properties of metal nanoparticles and 1D nanostructures.

NANO MICRO small

Schottky diodes. Another highly desirable property of 1D nanoscale heterojunctions, which may be the most important (especially for electronics), is that lattice mismatches are often avoided when forming junctions between two different materials having substantially different lattice constants. With single-crystalline bulk materials, junctions formed between materials with substantially different lattice constants are subject to large misfit dislocations, which is detrimental to the electronic performance of devices comprised of such heterojunctions. Nanowire 1D geometries, however, offer the promise of creating junctions between highly mismatched materials without suffering from these dislocations. Matthews and Blakeslee[48] recently described a critical thickness model for misfit dislocations formed in planar heterostructures, which predicts instability in a nanowire heterojunction above a critical radius. The model shows that it is possible to create perfect, dislocation-free heterojunctions from nanowires below the critical radius, even from materials with a large lattice-mismatch. Therefore, one of the greatest benefits of nanowire heterojunctions is that misfit dislocations are nonexistent below the critical radius of the nanowire (depending on the lattice mismatch). Importantly, this allows the formation of defect-free heterojunctions from materials not possible in a larger 2D geometry, which may lead to novel properties, enhanced functionality, and higher performance of electronic devices.

In Sections 2–5 of this Review, we discuss various methods for synthesizing or fabricating 1D heterojunctions. Various approaches used to synthesize single-component 1D nanostructures are commonly used to synthesize 1D heterojunctions, but with slight variations in the experimental procedure. We broadly define a 1D heterojunction in this review as a 1D nanostructure comprised of more than one material with a well-defined interface between the different materials, where both materials in the junction have a 1D anisotropic structure. This does not include junctions between nanoparticles and 1D nanostructures, such as ZnS nanoparticles deposited on carbon nanotubes[49] or quantum dots deposited on semiconductor NWs.[50] The main synthetic categories fitting our definition include vapor-phase methods, solution-phase methods, template-based synthesis, and other methods. Other methods include synthesis in supercritical fluids, lithography, assembly, solid–solid reactions, and electrospinning. Some of the methods involve a combination of two or more methods. These will be classified under the method that dominates the formation of the heterojunction. The various approaches lead to: a) SC–SC, b) SC–M, c) M–M, d) C–C, e) C–M, and f) C–SC heterojunctions, and junctions containing polymers. The C may be in the form of carbon nanotubes, amorphous carbon, or diamond. The different heterojunctions can also be classified by the nature of the junction. Scheme 1 shows some of the more common junctions, including segmented (also called superlattices or end-to-end), core/shell (also called core/sheath or coaxial), 90° or angled cross sections (or T-junctions), hyperbranched, or other multibranched ("nanobrushes") heterojunctions. The type of junction plays an important role in the measured property or application and is sometimes limited by the synthetic method or the material.

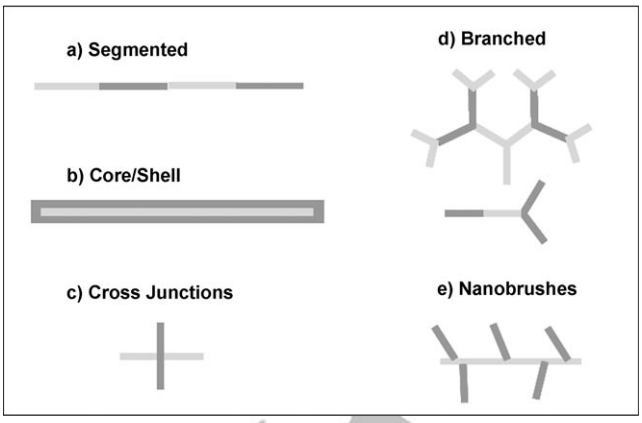

Scheme 1. Different types of nanoscale 1D heterojunctions.

For example, template-based methods are limited to forming segmented or core/shell heterojunctions.

In Section 6 we summarize the field of 1D nanoscale heterojunctions with general conclusions, limitations, future outlook, and challenges. It is important to note that this Review does not include 1D heterojunctions formed with molecules. There have been some exciting developments in the growing field of molecular electronics and molecular wires with work published on 1D heterojunctions including molecules. For example, M–molecule–M junctions were formed by combining electrochemical deposition, self-assembly, and electroless deposition in hard templates.[51] However, this Review will not cover these types of examples. We also do not cover all of the numerous examples of polymers and, for the most part, do not include examples of junctions defined by differences in structure or morphology within the same material. For example, Zhou et al. synthesized ZnO nanoplate–nanorod junctions[52] and Mather et al. synthesized crystalline Ge/nanocrystalline Ge core/shell structures[53] that fit this description. We do cite some important examples of heterojunctions in CNTs and inorganic NWs formed by doping various segments[54–59] or assembling cross junctions of metallic and semiconducting CNTs.[60] This Review does not include detailed information about all of the exciting properties and applications of 1D heterojunctions because the focus is on the synthesis and fabrication. Finally, we would like to state that we have truly done our best to include all of the work in this fast-growing field and apologize for any important examples of heterojunctions that we may have overlooked.

2. Vapor-Phase Methods

2.1. Vapor–Liquid–Solid Growth and Catalyst-Supported Techniques

2.1.1. Segmented and Branched Heterojunctions

2.1.1.1. Alternating Flow of Precursors

The vapor–liquid–solid (VLS) growth mechanism is commonly used for forming 1D NWs of elemental, III–V,

and II–VI semiconductors as well as metal oxides. There are several good reviews on the synthesis of 1D NWs by VLS and other vapor-phase growth mechanisms.[1,5,6,9,10] VLS growth can occur during different types of deposition methods, including pulsed laser deposition (PLD), chemical vapor deposition (CVD), metal–organic vapor-phase epitaxy (MOVPE), and chemical beam epitaxy (CBE), for example. For VLS growth to occur, the substrate must contain a bound metal catalyst, which is typically a noble metal (i.e., gold or silver) or other type of transition metal (i.e., nickel or iron). The growth process is held at elevated temperature, usually 500–1200 °C, where the metal particle melts, forms a liquid-phase droplet, and alloys with reactant vapors. Reactant vapors concentrate preferentially on the catalyst droplet and, with an increasing amount of reactants in the system, the alloy becomes supersaturated, which leads to nucleation and anisotropic crystallization of a NW that retains the diameter of the catalyst/reactant droplet. For single-component NWs, this process occurs with just one type of precursor molecule or the appropriate combination of precursors to form single-crystalline III–V or II–VI semiconductors. To form segmented or core/shell 1D SC/SC heterojunction NWs, two (or more) different types of precursors are introduced to the chamber in sequential fashion or all together at once as discussed in this Section and Section 2.1.1.2, respectively.

Yang and co-workers recently synthesized Si/SiGe segmented NW heterojunctions grown by the VLS mechanism where precursors were introduced in an alternating fashion.[61] The experimental setup and VLS growth process is shown schematically in Figure 1A and B, respectively. Experimentally, the reaction chamber contains a silicon substrate with Au nanoparticles (catalyst) deposited on it. The apparatus is set up to introduce reactant vapors into the chamber by laser ablation of solid targets, as shown for Ge, or by the supply of the vapor-phase precursors $SiCl_4$ and H_2, as shown for Si. The growth process of the segmented Si/SiGe NW is depicted in Figure 1B, occurring via four main steps: 1) formation of the metal/reactant alloy from the reactant vapor Si(Ge) and the surface-bound metallic Au catalyst (i.e., Au reacting with Si(Ge) to form the AuSi(Ge) alloy), 2) catalytic surface nucleation of the reactant Si(Ge), 3) axial growth of the Si or SiGe segment of the NW, and 4) continuation of the process to form a NW with alternating Si and SiGe segments. The $SiCl_4$ vapor is constantly flowing through the chamber and laser ablation of Ge is turned on and off to form SiGe at various segments (laser on) of the wire with the other parts of the NW consisting of Si only (laser off). The length of the individual Si/SiGe NW segments corresponds to the duration of the laser pulses and time between pulses.

Figure 1C shows a scanning transmission electron microscopy (STEM) image that clearly reveals the different Si and SiGe segments of two representative NWs.[61] The ≈100-nm-diameter NWs grew from a substrate containg a 20-nm-thick Au catalyst layer at the temperature range of 850–950 °C. The NW diameter depends on temperature and the thickness of the catalyst layer, where a lower temperature and thinner Au layer favors smaller diameter NWs. The high-resolution transmission electron microscopy (HRTEM) image in Figure 1D shows that the NW is highly crystalline and grows along the (111) direction, as confirmed by selected-area electron diffraction (SAED) with the zone axis along the [110] direction.[61] Gösele and co-workers synthesized Si/Ge NW superlattices by molecular beam epitaxy (MBE) at lower temperatures (525 and 545 °C) to grow the NWs on a Au-coated Si(111) substrate, where Ge segments grew during interuption of the Si source.[62]

Lieber and co-workers also synthesized superlattice nanostructures using laser-assisted growth. They formed GaAs/GaP segments on the same NW by laser ablation of GaAs and GaP solids, respectively.[63] The NWs were ≈20 nm in diameter with a length of ≈3 μm. Au nanoparticles on silicon served as a nucleation site, and segments were formed by switching between targets. Figure 2A shows a TEM image (top left) of a crystalline GaAs/GaP NW, showing that it is difficult to distinguish between the two segments. The other three images in Figure 2A show elemental mapping of the NW. The boundary between the two segments in the NW is clearly observed by the labeled P and As segments. As expected, the Ga component of the NW is evenly distributed throughout the length since it is present in both segments. These NW heterostructures exhibit interesting photoluminescent behavior and may be useful for nanoscale electronics. Lieber's group also employed local heating of a substrate to fabricate modulation-doped Si

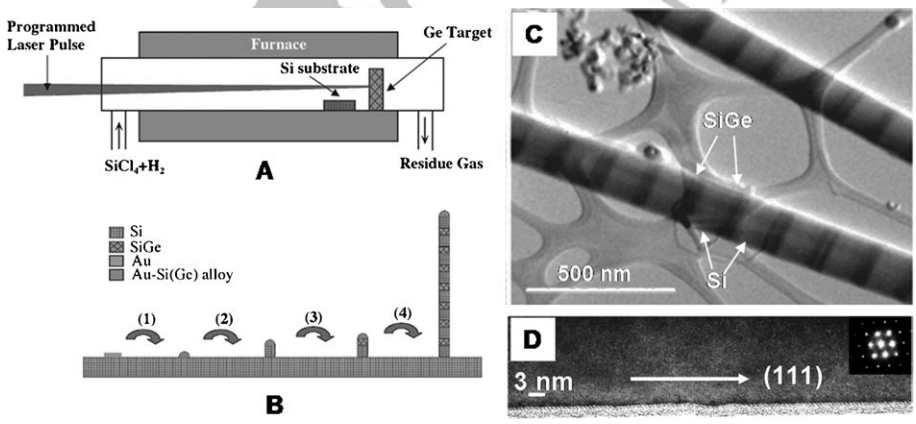

Figure 1. VLS synthesis of Si/SiGe segmented (superlattice) NWs. A) Scheme of the growth chamber and experimental setup. B) Steps of the VLS process: 1) formation of the metal/reactant alloy, 2) catalytic surface nucleation of the reactant, 3) axial growth of the Si (laser off) and SiGe segments (laser on), and 4) continuation of the process to form the Si/SiGe superlattice. C) STEM image of the Si/SiGe segments of the NW. D) HRTEM image of the same NW with a SAED pattern. Reprinted with permission from Ref. [61]. Copyright 2002, American Chemical Society.

small NANO MICRO

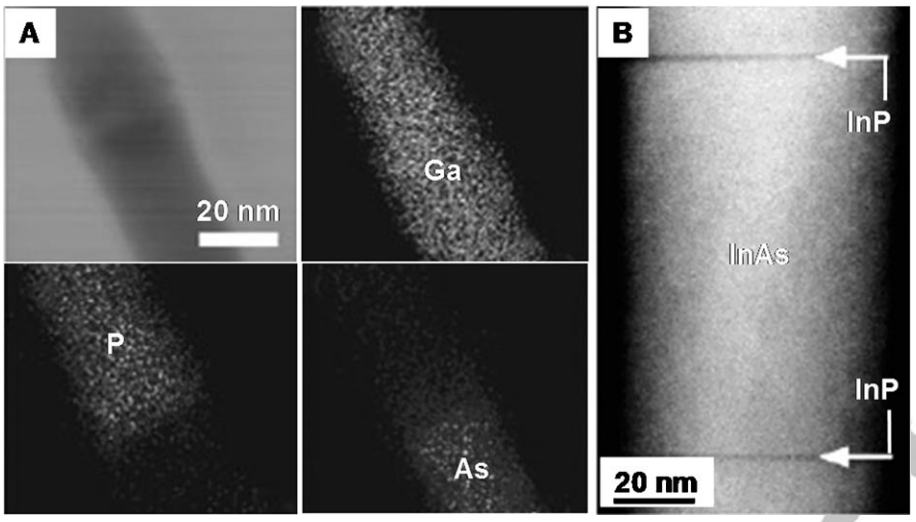

Figure 2. A) TEM image of a GaAs/GaP superlattice NW with elemental mapping of Ga, P, and As as labeled. B) STEM image of an InAs/InP segmented NW. A) Reproduced with permission from Ref. [63]. B) Reprinted with permission from Ref. [65]. Copyright 2004, American Chemical Society.

NWs by controlling the flow of silane in H_2 gas and switching between different vapor concentrations of the phosphine dopant.[58] They produced n and n^+ regions of segmented Si NWs. They also synthesized p-type-Si/intrinsic-Si/n-type-Si segmented NWs by VLS growth on 20 nm Au catalyst particles.[64] They formed p-Si in the presence of diborane, i-Si without any dopant, and n-Si in the presence of phosphine. Individual NWs behaved as avalanche photodetectors. Tutuc et al. similarly fabricated p–n junctions within a Ge nanowire, where a boron source was used as a dopant to form p-type segments of the VLS grown NWs.[59]

Samuelson and co-workers introduced precursors during the synthesis of segmented or superlattice NWs as metal-organic species, either in CBE or MOVPE processes.[65–76] Typical precursors contain trimethylindium, *t*-butylarsine, and *t*-butylphosphine as the In, As, and P source, respectively. They demonstrated sequential growth from a Au catalyst where a change in source material defines the segments forming the heterojunctions in the NWs. Epitaxial growth occurs on the surface of a (111)B InAs or (111) Si substrate. Since crystallographic growth of the NWs follows the arrangement of the substrate atoms, the NWs were predicted to grow either in the [111] or [001] direction with hexagonal or square cross sections, respectively. They also studied the electron-transport characteristics and photoconductive properties of the heterojunctions. Figure 2B shows a TEM image of the InP/InAs NW, where 100-nm-long InAs segments are inserted between small InP segments.[65] Samuelson and co-workers also reported the synthesis of GaAsP/GaP,[72,73] InAs/GaAs,[75] and InAs/InAsP[70,74,76] segmented NWs. Similarly, Verheijen et al. synthesized GaP/GaAs segmented NWs by MOVPE on a SiO_2 substrate.[77]

Su et al. used an alternating flow of precursors, which interestingly led to the fabrication of branched core/shell GaN/AlN heterojunctions instead of superlattices.[78] MCM-41 molecular sieves served as a template and In as a catalyst. Alternating the introduction of trimethylaluminum (TMAl) and the precursors for GaN NW growth led to the formation of GaN/AlN core/shell structures with AlN branches. The branched segments consisted mainly of AlN with In at the branch tips. The use of molecular sieves as a template gave a uniform 30–40 nm diameter for the GaN core, preventing coalescence of the In catalyst.

2.1.1.2. VLS combined with VLS (Two-Stage VLS)

Various processes can be combined with the VLS growth method to form heterojunctions. These usually lead to branched junctions, but there are examples of segmented or end-to-end junctions as well. In the following examples, VLS has been combined with VLS in a two-stage VLS process.

Two-stage VLS usually leads to the growth of branched heterojunctions, often termed "nanotrees" or "nanobrushes". The synthesis occurs by three steps (or two stages). The first step is the standard VLS growth of a NW (stage 1). The second step is attachment of an appropriate catalyst to the NW. The third step (stage 2) is the VLS growth of a second NW, which grows as a branch from the catalyst particles attached to the first NW. The number of branches of the second type of NW depends on the number of catalyst particles attached to the first NW. Figure 3A shows GaN/InN nanobrushes grown by a two-stage VLS procedure. Lan et al. synthesized the GaN NW backbone first and then coated the GaN NWs with a Au layer to serve as a catalyst for the VLS growth of InN NRs in the second stage.[79] $InMe_3$ and ammonia served as precursors for the high-temperature InN NW synthesis. The diameter of InN NRs ranged between 30–40 nm with lengths up to a few micrometers. Figure 3B shows a HRTEM image of the nano-heterojunction, confirming epitaxial growth of InN NRs on GaN NWs at the interface. The inset of Figure 3B is the SAED pattern showing the [100] zone axis for both GaN NWs and InN NRs.[79]

Samuelson and co-workers described a similar procedure for the two-stage growth of GaAsP branches on GaP, as shown in Figure 3C.[80] The first step involves the synthesis of GaP NWs by MOVPE on a GaP (111)B substrate using 40–70 nm Au aerosol particles as a catalyst and $GaMe_3$ and PH_3 as NW precursors. For branching, smaller Au aerosol particles (10–40 nm) were deposited onto the GaP trunks and GaAsP segments were formed from the GaP nanotrees, adding AsH_3 as a precursor. The GaAsP branches were $\approx$40 nm in diameter and up to several hundreds of nanometers long formed, on several-micrometer-long GaP trunks. The energy dispersive X-ray analysis (EDX) on various

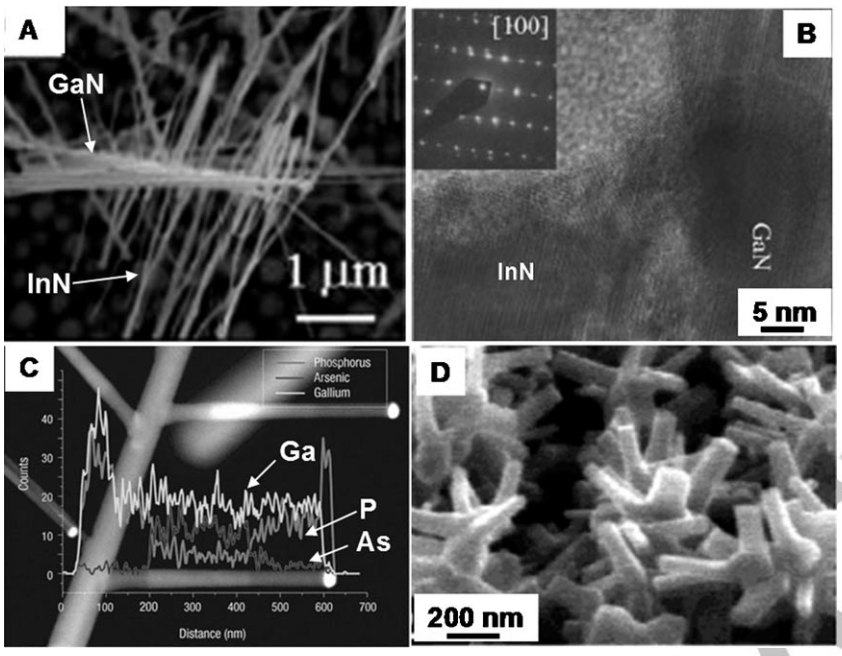

Figure 3. A) FESEM image of InN/GaN nanobrushes. B) HRTEM image of the heterojunction between InN and GaN in the nanobrushes. C) STEM image of branched GaP/GaAsP NWs with EDX elemental tracking of As, Ga, and P along a branch. D) SEM image of ZnO NRs synthesized on a CNT support. A, B) Reproduced with permission from Ref. [79]. C) Reproduced with permission from Ref. [80]. D) Reprinted with permission from Ref. [81]. Copyright 2004, American Chemical Society.

parts of the "nanotrees" shows that the As component is present only in the branches grown during the second stage. This method produces heterojunctions with high control over the density of branches either by controlling the amount of catalyst particles deposited on the first NW or the number of branching levels. This group also grew InP branches on GaP trunks.■■reference [80] as well?■■

Bae et al. synthesized various branched heterojunctions of ZnO NRs on different materials.[81] They used thermal CVD to grow ZnO NRs onto presynthesized CNTs, GaN, GaP, SiC, and core/shell SiC/C 1D nanostructures grown also by CVD on a solid substrate with appropriate catalysts. ZnO NRs grew by the VLS mechanism from powder mixtures containing Zn with Ga or In serving as the catalyst. The substrate containing the presynthesized 1D nanostructures was placed into the same boat with Zn and Ga or In precursors and growth of ZnO NRs occurred at 500 °C. They also introduced oxygen for ZnO formation. Figure 3 D shows branched heterojunctions of ZnO NRs grown on CNTs.[81] The CNT backbone is completely coated with the ZnO NRs and difficult to observe in the image. The diameter of the ZnO NRs was 80 nm and the length 300 nm.

2.1.1.3. VLS combined with Other Methods

The VLS method has also been combined with carbon-nanotube synthesis, chemical assembly, and thermal methods to form interesting heterojunctions. Carbon nanotubes (CNTs) are promising 1D materials for future applications in nanoelectronics and other nanoscale devices as they can be metallic or semiconducting, depending on their chirality, and they are mechanically very strong. For these reasons, carbon has been commonly incorporated into 1D heterojunctions as shown in the example for ZnO/CNT heterojunctions above. Similarly, in the following examples, the attachment of catalyst particles to presynthesized CNTs and subsequent growth of NWs on the catalyst by the VLS mechanism leads to the formation of CNT/SC heterojunctions. For example, Lieber and coworkers mounted MWCNTs synthesized by arc-discharge at the end of a Pt–Ir scanning tunneling microscopy (STM) tip, and formed a heterojunction with a Si NW, as shown in Figure 4 A.[82] The FESEM image shows the STM tip on the left side coated with multiple CNTs. Au electrochemically deposited onto the end of the extended nanotube served as a catalyst for the VLS growth of the Si NW. The inset in Figure 4 A is a TEM image of the junction formed, confirming that the Si NW originates from the CNT. Lazareck et al. similarly synthesized a MWCNT/ZnO heterojunction.[83,84] They synthesized MWCNTs inside an aluminum oxide porous template terminated with carboxylic acid groups through H_2SO_4/HNO_3 acid treatment. They attached amine-functionalized oligonucleotides onto the carboxylic acid groups of the CNTs through amide coupling. Next, they attached Au nanoparticles coated with the complementary oligonucleotides to the CNTs through DNA hybridization. The Au particles served as a catalyst for subsequent VLS growth of ZnO NWs to form end-to-end CNT/ZnO heterojuctions as shown in Figure 4 B.[84]

Our group recently synthesized SWCNT/GaAs NW heterojunctions directly on surfaces using a similar procedure.[85] We immobilized presynthesized SWCNTs onto amine-functionalized Si/SiO_x surfaces through strong chemical SWCNT–amine interactions. Next, we attached hexanethiolate-coated gold-monolayer-protected clusters (Au MPCs) onto the CNTs by simply immersing the substrate containing CNTs into a toluene solution of the Au MPCs. Au MPCs are 1–2-nm-diameter clusters of Au containing a monolayer shell of hexanethiolates around the Au core, which renders the clusters stable and soluble in nonpolar solvents. They selectively bind to the CNTs through hydrophobic interactions. The Au MPCs served as a catalyst for subsequent VLS growth of GaAs NWs onto the SWCNTs to produce a SWCNT/GaAs NW t-shaped heterojunction, as shown in the SEM image of Figure 4 C, where the darker features correspond to bundles of SWCNTs and the bright

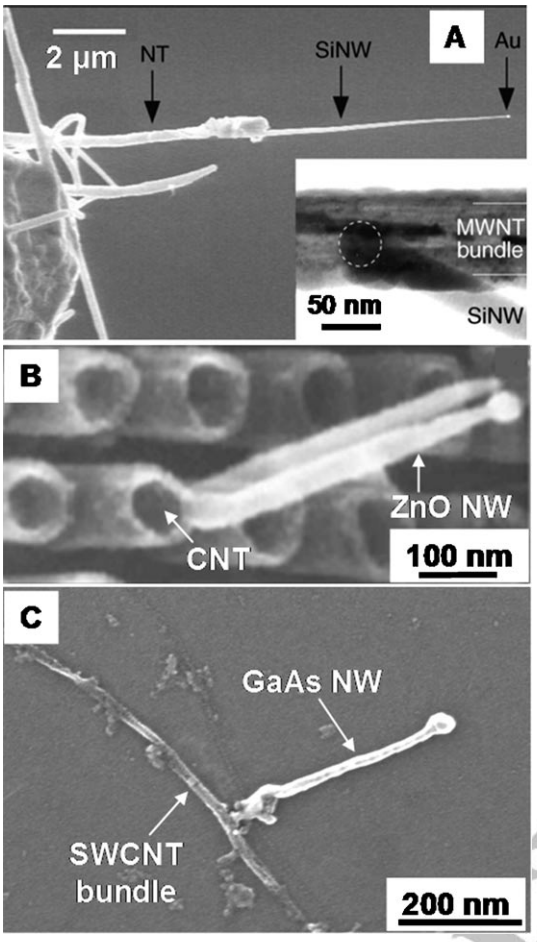

Figure 4. A) FESEM image of a CNT/Si NW end-to-end heterojunction formed on a Pt–Ir STM tip from a Au catalyst. B) SEM image of a CNT/ZnO heterojunction. C) SEM images of SWCNT/GaAs 1D heterojunctions. A) Reproduced with permission from Ref. [82], and B) reproduced with permission from Ref. [84].

features correspond to GaAs NWs. Most of the structures were branched because the Au MPCs tended to stick to the sidewall of the SWCNTs as opposed to the ends, as was the case in the studies of Lieber and co-workers[82] and Lazareck and co-workers.[83,84]

A thermal vapor deposition method was employed by Xie's group to form In_2O_3-beaded SnO_2 NWs.[86] With temperature modulation, SnO_2 NWs formed first followed by deposition of In droplets on the NWs. The substrate was a Si wafer containing a thin Au layer. A mixed powder of In_2O_3 and graphite was placed in one boat while the SnO powder was in the second boat. The temperature of the furnace was kept at 600 °C for 30 min and then raised to 900 °C for 20 min.

Kohno and Takeda described the synthesis of a segmented heterojunction by combining VLS growth with a thermal process.[87] They fabricated silicon/silicide/oxide NWs from Si nanochains grown by the VLS method, which served as a substrate for subsequent incorporation of metal into the structure. They simultaneously heated the Si nanochains with copper metal at 700 °C for 10 min. The Cu fused into the center of the Si nanochains to form Cu–silicide structures along the length of the Si nanochains.

2.1.1.4. All Precursors Introduced Together

The examples discussed up to this point include those where heterojunctions formed by alternating the precursors during VLS growth, using two-stage VLS growth, or by combining VLS growth with another method, such as the synthesis of CNTs. There are a few examples where segmented or superlattice heterojunctions form when all precursor materials are mixed together in one step. The thermal evaporation of solid powders containing all components of the NW can generate heterojunctions in one step. For example, Park and co-workers simultaneously heated ZnO, In, and Sn powders in a mixture, which resulted in the synthesis of Sn-doped $In_2O_3/(ZnO)_4$ superlattice NWs on a Si surface containing Au nanoparticles as a catalyst.[88] In Figure 5, the high-voltage (HV) TEM clearly shows the ≈2 nm Zn-O segments repeating periodically and separated by the shorter (<1 nm) In-O layers. These segments formed naturally during synthesis without purposely switching between precursors as in previous examples. Similarly, Hou and coworkers heated a solid powder mixture of ZnO, In_2O_3, and Co_2O_3 to produce ZnO/In NW superlattices by VLS growth on a Au-coated Si/SiO_2 substrate.[89]

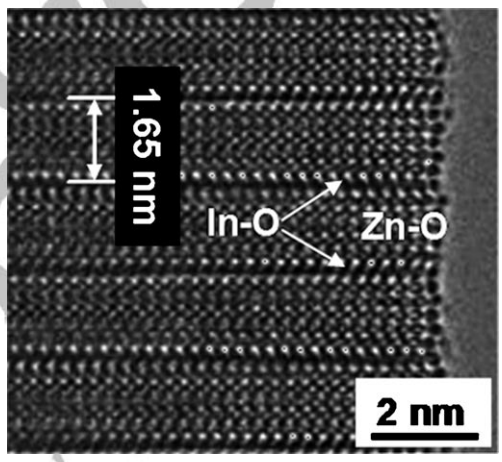

Figure 5. HV-TEM image of $In_2O_3/(ZnO)_4$ segmented NWs. Reprinted with permission from Ref. [88]. Copyright 2005, American Chemical Society.

2.1.2. Core/Shell Heterojunctions

1D core/shell heterojunctions have also been synthesized by growing a core NW by VLS growth and then using other methods to produce a shell comprised of a different material. This can occur in the same reaction chamber as the VLS process or by removing the VLS-grown NWs from the reaction chamber and reacting them further under completely different conditions and environments. Alternatively, the core/shell structure can form by mixing all the reactant pre-

cursors together in a one-step reaction. We describe these different approaches in the following sections.

2.1.2.1. Alternating Precursors and Other Multistep Processes

In order to create core/shell 1D heterojunctions within the same reaction chamber, it is necessary to achieve control over axial and radial growth of the NW. The NW core is synthesized from one material first by the VLS process, where the reaction conditions are such that axial growth occurs via reactant activation at the catalyst site and not on the nanowire surface. Next, radial growth of a second material is "turned on" by altering the growth kinetics through variations in pressure, flow rate, temperature, reactant species, or background gases. These conditions favor homogeneous vapor-phase deposition of the second material on the nanowire surface of the first material, which leads to the formation of a core/shell heterojunction. As switching of the reactant gases during axial growth leads to the synthesis of segmented or superlattice NWs (Section 2.1.1), switching the reactant gas and changing the mode to radial growth can be employed to grow core/shell and even core/multishell 1D nanostructures.

Lieber and co-workers synthesized core/shell NWs in order to fabricate a novel nanoscale field-effect transistor (FET) device.[90] In one example, an intrinsic silicon (i-Si) core and p-type Si shell (p-Si) were fabricated by altering the axial and radial growth modes during CVD. Following the VLS i-Si core synthesis, a coaxial shell formed with diborane added as a p-type dopant, which also promotes shell growth by lowering the decomposition temperature of the silane precursor molecule. The core diameter was $\approx$19 nm, consistent with the size of the 20 nm Au catalyst used, and the thickness of the shell strongly depended on the synthesis time. Thermal treatment led to shell crystallinity. The same procedure was used to fabricate Ge/Si core/shell NWs, which are shown in the TEM images of Figure 6A and B.[90] The initially amorphous p-Si shell again becomes crystalline after thermal annealing. Other examples of core/shell or core/multishell structures fabricated by the Lieber group include Ge/Si,[91,92] n-GaN/$In_xGa_{1-x}N$/GaN/p-AlGaN/p-GaN,[93] n-GaN/InGaN/p-GaN,[94] GaN/AlN/AlGaN,[95] and p- or n-Ge/i-Ge[96] NWs, where again modulation of the temperature and reactants led to the formation of the outer shells. These nanostructures are promising materials for nanoscale electronics and photonics. Similarly, Samuelson and co-workers synthesized GaAs/$Ga_xIn_{1-x}P$ core/shell NWs by formation of a GaAs core at 450 °C followed by growth of a $Ga_xIn_{1-x}P$ shell at 600 °C.[97] They also synthesized GaAs/AlInP core/shell NWs and studied phase segregation and photoluminescence.[98] Lee and co-workers used a similar two-step CVD process to fabricate GaN/MnGaN[99] or GaP/Ga_2O_3[100] heterojunctions and Wu and co-workers used a two-stage MOCVD process to form Ga_2O_3/TiO_2[101] or Ga_2O_3/ZnO[102] core/shell NWs. Zhang et al. synthesized core/multishell NWs of Ge/Si/Al_2O_3/Al by several steps involving VLS growth of single-crystal Ge NWs followed by Si and nitride passivation by CVD, Al_2O_3 deposition by ALD, and sputter deposition of Al.[103] These NWs were utilized in the construction of Ge NW surround-gate field-effect transistors.

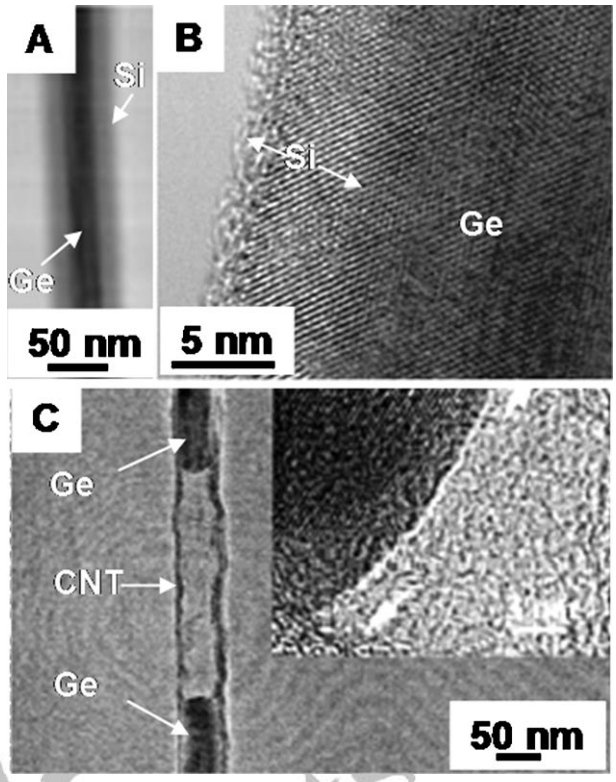

Figure 6. A) Bright-field image of a Ge/Si core/shell NW. B) HRTEM image of the Ge/Si NW after annealing. C) TEM image of Ge NWs encapsulated within a CNT. The inset is the HRTEM image of the NW and nanotube junction. A, B) Reproduced with permission from Ref. [90], and C) reproduced with permission from Ref. [106].

Lin et al. synthesized GaP/GaN and GaN/GaP core/shell NWs using the VLS mechanism for the core synthesis and the vapor–solid (VS) process for the shell formation.[104] The GaP core was prepared on the Si wafer using an Fe catalyst, and subsequently placed in a furnace at 950 °C under ammonia gas flow to form the GaN shell. For GaN/GaP NWs, the VLS-grown GaN cores were coated with a GaP shell after heating at 1000 °C in the presence of gallium, gallium oxide, and red phosphor precursors.

Carbon materials are commonly used as a shell material for core/shell heterojunctions as well. For example, Wu and Yang reported the synthesis of 10–100-nm-diameter Ge NWs by VLS growth, which were then coated with carbon by pyrolysis of organic molecules.[105,106] They studied Ge NW melting/recrystallization, forming the Ge/CNT core/shell structures shown in Figure 6C. The TEM image shows two Ge NWs inside the CNT separated by a 150–200 nm gap as a result of the NW breaking during the thermal processing. Chen et al. used a similar approach to fabricate GaN/CNT core/shell NWs by CVD of methane for the CNT coating,[107] and Yin et al. synthesized VLS-grown InP NWs from an In catalyst that was coated with layers of carbon by a VS process.[108]

NANO MICRO small

Zhou and co-workers grew thin shells ($\approx$10 nm) of Fe_3O_4 on the outside of MgO NWs formed by the VLS mechanism.[109,110] They used pulsed laser deposition (PLD) of Fe_3O_4 powder with growth speeds close to 2–3 Å min^{-1} after laser ablation. The same group also synthesized MgO/$LaCaMnO_3$, MgO/$LaSrMnO_3$,[111] MgO/$YBa_2Cu_3O_{6.66}$, MgO/$La_{0.67}Ca_{0.33}MnO_3$, and MgO/$PbZr_{0.58}Ti_{0.42}O_3$[112] core/shell heterostructures by combining VLS core growth and PLD shell deposition. Bell and co-workers used the same VLS/PLD method to fabricate p-Si/n-CdS core/shell heterojunctions.[113] Boron doped p-Si NW cores were grown on an oxidized silicon substrate with the assistance of Au catalysts under the flow of SiH_4 and B_2H_6 precursors. As prepared p-Si NWs were coated immediately with an n-CdS shell using a PLD system.

Gösele and co-workers employed atomic layer deposition (ALD) to produce uniform Al_2O_3 shells surrounding VLS-grown ZnO cores.[114] The ZnO NWs were synthesized from zinc vapor after carbothermal reduction of ZnO powder precursor at 910 °C. The usual thickness of the NWs ranged between 10–30 nm, and the length reached up to 20 μm. The shell was synthesized in the ALD chamber from $Al(CH_3)_3$ and H_2O precursors as sources of aluminum and oxygen, respectively. In this example the shell thickness is directly proportional to the number of precursor/purge cycles, as opposed to growth time. After a total number of 65 cycles, the Al_2O_3 shell thickness was 10.0 ± 0.3 nm. The same group used thermal oxidation of Si NWs under O_2 flow to form Si/SiO_x core/shell structures with an oscillating diameter of the oxide shell.[115] The first step involved growth of Si NWs on a Si(110) substrate (coated with an 8 nm Au layer) from a SiO precursor at an evaporation temperature of 1050 °C. Once the NW growth was complete the oxide layer formed on the Si NWs was removed by chemical etching in HF solution. Subsequent high-temperature treatment at 1000 °C with an O_2 flow led to the formation of an oscillating SiO_2 shell on the Si NW cores. The average NW diameter ranged from 60 to 90 nm and the length was on the order of micrometers.

2.1.2.2. All Precursors Introduced Together

Most methods for forming 1D core/shell heterojunctions by VLS require a second step to produce a shell over the VLS-grown core wire. However, there are VLS methods where all the precursors for the core and the shell are introduced to the growth chamber at the same time. This one-step VLS process is used to produce the core and shell simultaneously, which occurs due to differences in the reactivity of the core and shell material. An excellent example is the work of Hsu and Lu for the fabrication of CdS/ZnS core/shell heterojunctions.[116] They fed CdS ($Cd(S_2CN(C_3H_7)_2)_2$ denoted as Cd33) and ZnS ($[Zn(S_2CNBu_2)_2]_2$ denoted as Zn44) precursors into the system simultaneously. Cd33 decomposes at the catalyst first since it is of higher reactivity than Zn44, leading to growth of the CdS core via the VLS mechanism. The CdS core subsequently serves as a catalyst for thermal decomposition of Zn44, resulting in the core/shell heterojunctions. Hsu et al. used a similar procedure, introducing all precursors in a single step, to synthesize CdS/ZnS and $Cd_{1-x}Zn_xS$/ZnS coaxial heterojunctions.[117] Heo et al. synthesized ZnO/(Mg,Zn)O radial NWs spontaneously, where the core grows by the VLS mechanism and the composition is determined by bulk solid solubility.[118,119] The (Mg, Zn)O shell grows as a heteroepitaxial layer. Jang et al. used a one-step thermal CVD reaction of GaP, B_2O_3, and NH_3 to synthesize GaN/BN core/shell nanocables.[120] Gwo and co-workers fabricated In/GaN core/shell NWs on a substrate containing Au catalyst by a single evaporation step.[121] Lee and co-workers synthesized Ge/SiO_x coaxial nanocables by an oxide-assisted self-catalyzed VLS process.[122] A reaction occurs within the droplet of GeO_4/SiO_2 to form the SiO_x shell while the core consists of Ge. Other examples of single-step syntheses include core/shell heterojunctions of GaN/BN NRs,[123] linear or helical SiC/SiO_x NWs,[124–126] ZnS/SiO_2 NWs (ZnS wrapped in high-density SiO_2),[127] and GaP/C and GaP/SiO_x/C nanocables.[128]

Seo et al. synthesized GaN NWs coated with boron carbonitride (BCN) layers when Ga, Ga_2O_3, CNTs, B_2O_3, and NH_3 precursors were introduced into the reaction chamber at the same time.[129] The high-temperature processing led to the formation of the Ga core that grew by the VLS mechanism on the Fe catalyst, coated with BCN layers. Wang et al. fabricated Cu/SiO_{2-x} NWs by encapsulating Cu nanoparticles inside the SiO_{2-x} NW.[130] The procedure involved simultaneous heating of the precursor powder mixture of SiO and CuO. Under the presence of H_2 in the atmosphere the environment is suitable for reducing the CuO to Cu particles and formation of SiO_{2-x} NW/Cu NP heterostructures. Wu et al. reported a VLS process to form B NWs on a substrate containing Au catalyst.[131] The diameter ranged from 30 to 500 nm and the length reached hundreds of micrometers. Evaporation of SiO_x during B NW growth led to bead-like B/SiO_x heterojunctions. The VLS growth mechanism was also proposed for the core in SiC/BN or Si_3N_4/BN core/shell NWs synthesized by Tang and co-workers.[132,133] The heterostructures were synthesized on Ni-supported highly ordered pyrolytic graphite (HOPG) and Ni–BN substrates from B and SiO_2 precursors either under the flow of nitrogen and argon for HOPG or ammonia and argon for the BN substrate. Zhou et al. synthesized β-SiC/SiO_x by a one-step procedure.[134,135] A tablet of silicon and graphite powders was reacted with atomic hydrogen activated at 2200 °C, leading to the formation of SiH_x and CH_x precursors. The β-SiC NWs formed by the VLS process where metallic particle impurities served as the catalyst. The SiC NWs were coated with an amorphous $\approx$1–2-nm-thick SiO_x shell.

2.2. Vapor–Solid (VS) and Catalyst-Free Growth Mechanisms

There are a large number of reports of heterojunctions synthesized without using any catalyst to promote the growth of nanostructures. The growth mechanism is often classified as a vapor–solid (VS) process, but usually is not well understood. We will review heterojunctions formed by the VS method and other growth procedures not requiring a

catalyst in the next sections. The sections are divided by the structures formed, including segmented, core/shell, or branched heterojunctions. We also divided the sections into those using an alternating flow of precursors or reactions conditions, those using a combination of techniques, and those where all of the reactants are combined together. It is important to note that even in examples where all of the reactants are combined, multiple reaction steps may occur to form the heterojunction.

2.2.1. **Segmented Heterojunctions**

2.2.1.1. Alternating Flow of Precursors

Chung and co-workers fabricated segmented GaN nanowire p–n junctions via hydride vapor-phase epitaxy (HVPE) using an alternating flow of precursors to form the different segments.[136] A GaCl precursor was produced via the reaction of HCl gas and Ga metal and mixed with NH_3 to grow GaN at 478 °C. The n-type segment of the NW forms during the nitrogen flow while the p-doped region grows by introducing Cp_2Mg to the growth chamber. The ≈3-μm-long p–n GaN NWs are promising for use as diodes in electronic and photonic devices.

2.2.1.2. All Precursors Combined Together

Golberg and co-workers used thermal evaporation of a mixture of precursor powders to fabricate Ga/ZnS segmented nanowires encapsulated within a silica tube, as shown in Figure 7.[137] A mixture of ZnS, Ga_2O_3, and SiO powders

Figure 7. TEM image of a Ga/ZnS segmented NW within a silica shell. Reproduced with permission from Ref. [137].

was heated at 1400–1500 °C. Even though all of the precursors are mixed together, they proposed two stages of growth, where silica tubes formed first by oxide-assisted growth and served as templates for the following NW heterojunction synthesis. An increase in temperature allows for the deposition of Ga/ZnS solution inside the tube, and after supersaturation, ZnS precipitates to form a separate segment of the NW. The typical diameter of the Ga/ZnS heterojunction ranges between 150–250 nm and the thickness of the silica tube is 4–8 nm. Other heterojunctions synthesized by the same group include ZnS-sheathed Zn/Cd NWs formed in a one-step thermal process.[138] Rapid heating of a ZnS and CdS powder mixture to 1200 °C led to the formation of 30–70-nm-diameter Zn/Cd segmented NWs encapsulated with a few-nanometers-thick ZnS shell on the walls of the quartz tube. The same group also used thermal evaporation of a solid mixture of In and SiO precursors to prepare In/Si segemented NWs sheathed with amorphous silica.[139] The Si NWs sheathed with silica grow by oxide-assisted growth, while silica nanotubes grow in the opposite direction at the junction between the Si NWs and In droplets. Vapor-phase In is drawn into the silica nanotubes and condenses to form the final In/Si segmented junctions sheathed with amorphous silica. Wang et al. synthesized bundles or brushlike arrays of Si/SiO_x nanostructures formed by pyrolysis of a Si and SiO_x powder mixture.[140]

2.2.2. **Core/Shell Heterojunctions**

2.2.2.1. Alternating Reaction Precursors or Conditions

Fukui and co-workers synthesized various core/shell heterojunctions by selective-area (SA)-MOVPE, where the precursors were introduced in an alternating fashion.[141–144] For example, they synthesized GaAs/AlGaAs[143,144] hexagonal pillars and InP/InAs[142] core/shell structures in this manner. In the case of InP/InAs, they grew the InP core first at 635 °C from trimethylindium (TMI) and tertiarybutylphosphine (TBP) precursors followed by growth of the shell from TMI and AsH_3 precursors at 400 °C. They used a similar method to prepare InP/InAs/InP core/multishell heterojunctions on a hexagonally patterned surface.[141] In this case they formed the InP/InAs core/shell structure as previously described and then added another InP shell by controlling the growth temperature (600 °C) as well as the partial pressure of the TBP precursor. Figure 8A shows an SEM image of the highly aligned core/multishell NW arrays.[141] The shape of the pattern from the substrate was transferred to the grown nanostructures, which have a hexagonal cross section as shown for the individual NW in Figure 8B. Additionally, this image reveals the composition of the NW with well-defined regions of the InP core and InAs/InP shells. The length of this core/multishell heterostructure was 2.5 μm and the diameter of the InP core was 70 nm, while the thickness of the InAs and InP shell was 5 nm and 30 nm, respectively. Yi and co-workers also used MOVPE and alternating reaction conditions to fabricate ZnO/$Mg_{0.2}Zn_{0.8}O$[145,146] and ZnO/GaN[147] core/shell structures.

Zhan and co-workers heated a powder mixture of SiO and ZnS or SiO and ZnSe to 1300 °C for 1 h and then to 1600 °C or 1500 °C for 1.5 h to form 60–120-nm-diameter Si/ZnS biaxial and ZnS/Si/ZnS triaxial NWs or 40–90-nm-diameter Si/ZnSe biaxial NWs through a two-stage thermal-evaporation process.[148] The NWs were several micrometers in length. Chen and co-workers used a two-step procedure to form ZnO/$ZnGa_2O_4$ core/shell heterojunctions.[149] The ZnO NWs, formed by a thermal vapor deposition process, served as templates for the shell deposition. The Ga_2O_3 and graphite powders (shell precursors) were placed in a zone of the furnace held at 1000 °C, while the ZnO NWs were placed downstream. The deposition temperature was 600–900 °C. Similarly, Hu et al. synthesized ZnS/Si core/shell NWs.[150] They synthesized ZnS NWs first by heating ZnS

NANO MICRO small

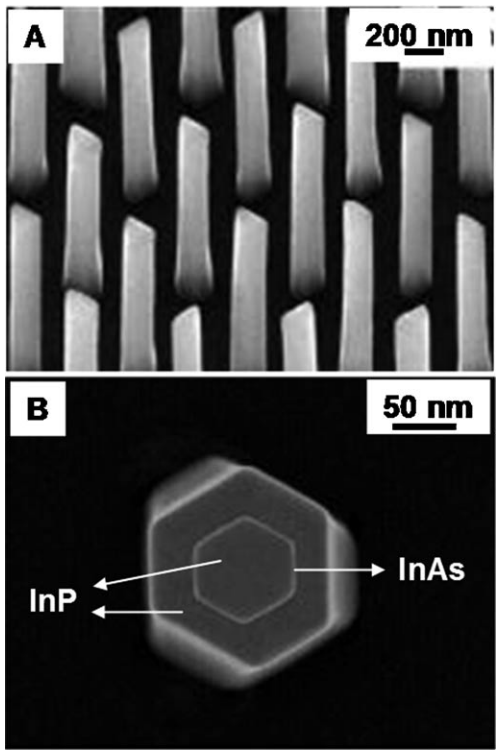

Figure 8. A) SEM image of aligned InP/InAs/InP core/shell/shell NWs. B) SEM image of the cross section of an InP/InAs/InP NW showing hexagonal shape and composition. Reprinted with permission from Ref. [141]. Copyright 2006, American Institute of Physics.

powder at 1200 °C and used these NWs as a template for the growth of the Si shell, which formed after heating SiO powder at 1450 °C for 1 h. Zhu et al. reported ZnS nanostructures coated with a BN layer.[151] The ZnS twinned-crystal whiskers were prepared first by heating the ZnS powder at 1200 °C under N_2, and then reheated again with B/N/O vapors under N_2/NH_3 flow. Zheng and co-workers synthesized tetrapod ZnO NRs coated with a SnO_2 sheath by a two-step procedure involving the initial formation of ZnO nanostructures through heating of a zinc powder at 800 °C, and subsequent reheating to 770 °C with the introduction of a SnH_4/N_2 mixture to form the final ZnO/SnO_2 core/shell heterojunctions.[152]

Yin et al. reported the synthesis of several-micrometer-long cubic aluminum nitride/boron nitride (c-AlN/BN) coaxial nanotubes by the VS method.[153] The $AlCl_3$ and B/N/O precursors were heated in the furnace under Ar flow. When the temperature reached 950 °C, they introduced a flow of NH_3/N_2 only and raised the temperature to 1200 °C for 1.2 h. The temperature was then increased further to 1600 °C. AlN nanotubes grow first at the lower temperature followed by the BN shell, which forms at higher temperatures. The outer diameter of the heterojunctions was ≈50 nm with a wall thickness of about 15 nm and a BN coating of 2–3 nm. Golberg and co-workers synthesized ZnS or Si/SiO_2 NWs sheathed with BN coatings.[154] For the latter, SiO precursors were placed above B/N/O precursors. Heating at 1200 °C led to the formation of Si/SiO_2 NWs and changing to 1600 °C and a flow of N_2/NH_3 led to growth of the BN coating. ZnS/BN core/shell NWs were prepared similarly. Alternatively, the Si/SiO_2 or ZnS NWs were prepared first and then subsequently coated with BN. More recently, the same group synthesized BN nanosheets protruding form Si_3N_4 NWs by placing a BN crucible containing Si powder above a crucible containing the B/N/O precursor and B_2O_3 powder in a graphite susceptor, which was heated at 1500 °C in N_2 and 1750 °C in N_2/NH_3 to form the Si_3N_4 NWs and BN sheets, respectively.[155]

Golberg and co-workers used a VS route in a CVD system to produce Mg_2Zn_{11}/MgO beltlike nanocables by heating Mg and ZnO powders.[156] The ZnO and Mg powders were heated to temperatures of 1300–1400 °C and 800–900 °C, respectively. The Mg_2Zn_{11}/MgO nanocables were collected from the graphite surface inside the furnace. The cables were typically 30–150 nm wide and tens of micrometers in length. Another example is the synthesis of Zn/ZnO core/shell heterostructures by thermal reduction of ZnO with H_2 to form the Zn core and thermal annealing to form the ZnO shell.[157]

2.2.2.2. All Precursors Mixed Together

Li and co-workers used thermal evaporation to fabricate ZnSe nanopeas filled inside SiO_2 nanotubes by a one-step thermochemical method.[158] Two separate mixtures of precursor powders containing Se with Zn and Si with SiO_2 were placed in the furnace and heated to 1300 °C for 2 h under Ar flow. The products were collected on a Si wafer. The core/shell structure was ≈80 nm in diameter and tens of micrometers in length. The nanotube wall was about 20–25 nm thick and ZnSe-formed nanodots or short rods were observed inside the nanotube■■sentence ok?■■. Hsu et al. synthesized $ZnO/ZnGa_2O_4$ NWs by heating the precursor mixture of Zn metal and Ga powder at 600 °C for 1 h.[159]

Peng and co-workers synthesized core/shell structures from precursors placed in different temperature zones.[160] In this example, they synthesized CdSe-filled silica nanotubes by loading Si and SiO_2 powders in the center of a furnace, with Cd and Se precursors upstream and the collection substrate downstream. The furnace was set to 1200 °C, which caused the Si and SiO_2 powders to be at 1200 °C, the Cd and Se to be at 900 °C, and the substrate (where CdSe/silica heterostructrues were collected) at 1100 °C. In another example, Hu et al. synthesized partially Ga-filled Ga_2O_3/ZnO core/shell coaxial nanotubes by simultaneous heating Ga_2O_3 and ZnO precursors at 1350 °C for 2 h.[161] The core/shell nanostructures were tens of micrometers long and 150 nm in diameter with a shell-wall thickness of 40 nm and an inner core of ≈80 nm. Uemura and co-workers fabricated InS/SiO_2 core/shell NWs 30–200 nm in diameter and tens of micrometers in length by a one-step physical vapor-deposition process.[162] InS and silicon powders were heated to 900–1000 °C for 1 h and the product collected from the wall of the alumina crucible. Teo et al. prepared Si/SiO_2 core/shell NWs on a zeolite template where the diameter of the Si core varied between 1–5 nm and the SiO_2 shell was about 20–40-nm thick.[163] The SiO powder was used as a precursor

and heated gradually to 1250 °C and held at this temperature for 1 h. The product was collected from the zeolite substrate. During this procedure they also fabricated silicon nanotubes filled with amorphous silica and biaxial silicon/silica NWs. Wang et al. synthesized ZnSe/Si bi-coaxial NWs that were 80–100 nm in diameter and tens of micrometers long by thermal evaporation of a ZnSe powder at 1250 °C for 2 h under Ar/H_2 flow (5 % H_2).[164] Li and Wang reported a single-step thermal evaporation to form single-crystalline Si/CdSe nanocables.[165] The CdSe was heated to 1200 °C for 2 h and the product collected at a silicon wafer coated with a thin oxide layer.

Thermal evaporation of a $MoSi_2$ precursor led to the formation of ≈100-nm-diameter Si/SiO_x core/shell NWs, which were several micrometer long.[166] Li and Jiao produced Au/Si junctions in Si/SiO_x core/shell NWs by filling Au into the voids between the Si core and the SiO_x shell.[167] Smashed Si wafers were used as precursors and alumina (0001) with a thin Au film as a substrate. Subsequently, the furnace was heated at 1300 °C for 2–4 h under an Ar/H_2 flow (10 % H_2).

Other examples include CaF_2/a-C and MgF_2/a-C core/shell NWs (a-C = amorphous carbon) reported by Chiu and co-workers.[168] The precursors, which include CaC_2 and Mg_2N_3, were reacted with C_6F_6 at elevated temperatures to produce CaC_2/a-C and Mg_2F_2/a-C, respectively. Wang and co-workers synthesized Zn/ZnO core/shell nanobelts and nanotubes by evaporating ZnO powder at 1350 °C and introducing an Ar flow for 30 min.[169,170] The products were collected at a silicon substrate placed in the 200–400 °C temperature region. Kang and co-workers fabricated Zn/$ZnSiO_4$ nanocables by vapor-phase oxidation of Zn powder.[171] The Zn powder was heated up to 1100 °C at a rate of 15 °C min^{-1} under N_2 flow and the product collected at a Si substrate. The nanocables were ≈100 nm in diameter with a ≈25-nm-thick shell.

2.2.2.3. Combined Techniques

Catalyst-free vapor methods can be combined with other methods to grow various heterojunctions. Solution-based systems are commonly used as the second technique. Jiang et al. used this setup to prepare FeCoNi/SiO_x core/shell NWs.[172] First, SiO_x NWs were synthesized by heating a mixture of Si and SiO_2 powder and collecting the product on an Al_2O_3 substrate. Then, the Al_2O_3 substrate containing SiO_x NWs was placed in a solution of FeCoNi vitriol. Continued growth of SiO_x on the Al_2O_3 substrate led to NWs with a crystalline metallic FeCoNi alloy core (≈20 nm in diameter) surrounded by a double-layer amorphous SiO_x shell. The typical diameter of these heterojunctions was about 20 nm for the FeCoNi core, 50 nm for the inner shell, and 90 nm for the outer SiO_x shell layer. Similarly, a combination of vapor and solution techniques was employed by Fan and co-workers to fabricate ZnO/ZnS core/shell NWs.[173] ZnO NWs were initially synthesized by a vapor-phase transport process and then coated with ZnS by solution self-assembly. The first solution contained Na_2S and the second contained $Zn(NO_3)_2$ where the NWs were soaked for 2 h at 60 °C. The ZnO/ZnS heterojunctions were ≈100 nm in diameter and ≈3 μm long. Zheng and co-workers fabricated Se/Ag_2Se nanocables;[174] they modified Se NRs, synthesized via laser ablation of a Se powder, by immersing them in a $AgNO_3$ solution. The diameter of the Se/Ag_2Se nanocables was ≈20 nm for the core and ≈33 nm for the shell. Zettl and co-workers formed KI/BN, KCl/BN, and KBr/BN core/shell heterostructures by filling in BN nanotubes (formed by substitution of C atoms in a boron oxide/nitrogen vapor phase reaction) with potassium halide crystals from solution by capillary action.[175] Yang et al. described another example of combining noncatalyst vapor methods with solution methods in the formation of Cu_2S/X core/shell NW heterojunctions (X = nanoparticles of CdS, Au, or polypyrrole).[176] Cu_2S NW arrays were fabricated first by subjecting a Cu foil to a flow of O_2 and H_2S for 10 h. The Cu_2S NWs were subsequently coated chemically with nanoparticles of CdS, Au, or polypyrrole. The Cu_2S NWs were 60–100 nm thick and several micrometers long, while the sheath was 20–50 nm thick.

2.2.3. Branched Heterojunctions

There are not many reports of branched heterojunctions by non-catalyst methods. One example is the saw-like nanostructures synthesized by Shen et al. in a two-step VS growth process, where a ZnO nanobelt was synthesized first and ZnS NWs were grown on the nanobelts.[177] Zn and SnS powders were placed in two different zones of the furnace and heated to 550 °C in 20 min. Subsequently the temperature of the SnS precursor was up to 1100 °C while the Zn powder was held at 550 °C for 30 min. This resulted in the formation of an interesting saw-shape morphology as shown in Figure 9. The surface of the ZnO nanobelt remains chemically active to facilitate the formation of ZnS NWs during the second step of the synthesis. Typically the diameter of the saw was about 100 nm and the length reached hundreds of micrometers.

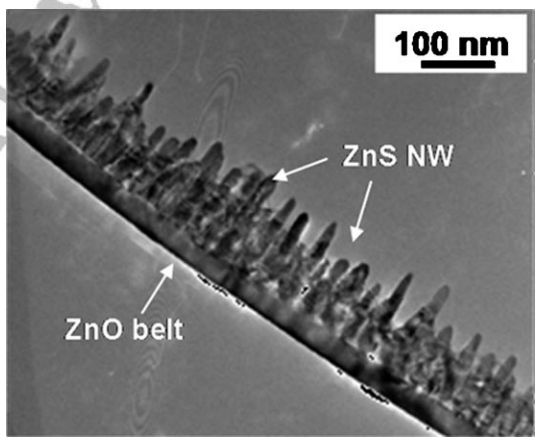

Figure 9. TEM image of a sawlike heterojunciton of ZnS NWs grown on a ZnO belt. Reprinted with permission from Ref. [177]. Copyright 2006, American Chemical Society.

NANO MICRO small

2.3. Carbon-Containing Heterojunctions

We have already described heterojunctions containing carbon involving VLS growth where 1) a NW is synthesized by VLS and then a carbon shell is deposited onto it to form a core/shell heterojunction or 2) a CNT is first synthesized and a NW grown from a catalyst bound to the CNT by VLS to form a segmented or branched heterojunction. In this section, we describe other types of segmented or core/shell heterojunctions containing carbon species such as CNTs, SiC, CN_x, amorphous carbon, or diamond synthesized mostly by multi-step procedures.

2.3.1. Segmented Heterojunctions

Golberg and co-workers prepared segmented SiC/CNT nanochains after thermal treatment of SiC/SiO_2/CNT core/shell nanocables.[178] Thermal evaporation of SiO and Fe powders under a CH_4 atmosphere led to the formation of SiC/SiO_2/CNT nanocables with diameters between 20–50 nm and lengths of several micrometers. High-temperature annealing in vacuum transformed the nanocables into SiC/CNT end-to-end nanochains. Wu and co-workers reported the synthesis of segmented CN_x/CNT heterojunctions by CVD through pyrolysis of a mixture of ferrocene and melamine.[179,180] Similarly, Hu et al. fabricated CN_x/C nanotube junctions by pyrolysis of iron phthalocyanine, where C segments were obtained with an H_2 flow only and CN_x with an NH_3 carrier gas.[181] The diameter ranged between 30–60 nm and the length reached tens of micrometers. Ma and Wang synthesized segmented heterojunctions between CN_x nanotubes and CNTs by a two-step microwave plasma-assisted CVD process using an Fe catalyst, where N_2/CH_4 and H_2/CH_4 gaseous mixtures formed the CN_x and CNTs, respectively.[182] Cassel et al. prepared end-to-end junctions consisting of vertical connections between two MWCNTs by a two-step process.[183] In the first step, they grew vertically aligned CNTs and embedded them into an SiO_2 matrix. In the second step, they electroplated Ni on the end of the first CNTs and grew the second segment of CNTs by a plasma-enhanced CVD process. Multiple segments could be formed by repeating the procedure. The first generation of CNTs was about 50 nm in diameter and the second was also $\approx$50 nm at the junction point but became thinner towards the end. The average length was about 1 μm. Also, Liu et al. synthesized CNT/ZnO heterojunction arrays by pyrolysis of C_2H_2 on a zinc foil at 850 °C under combined Ar and H_2 flow passed through a water bubbler.[184] Zn served as the source of ZnO and catalyst for CNT growth by the tip-growth mechanism while the water enhanced CNT growth and promoted ZnO formation. Post-synthesis annealing of the sample under Ar passed through the water bubbler led to increased growth of the ZnO structures formed at the tip of the CNTs.[184] The flow rate of Ar during synthesis controlled the formation of ZnO nanoparticles or ZnO nanorods, with the latter occurring at higher flow rates.

2.3.2. Core/Shell Heterojunctions

The synthesis of core/shell heterojunctions with carbon usually involves either 1) filling a carbon nanotube with some material, 2) coating a carbon nanotube with some material, or 3) coating a 1D material with a carbon shell. There are also examples of carbon-containing materials in the core or shell by various methods. In the first example, Chan et al. fabricated multi-walled carbon nanotubes (MWCNTs) filled with Pd using a microwave plasma-enhanced CVD system in a two-step process.[185] A Pd film was activated by a H_2 plasma and then methane and H_2 were introduced into the reaction chamber, resulting in core/shell Pd-filled CNTs with some void spaces between the Pd regions.

Examples of the second procedure include heterojunctions of MWCNT/maghemite composites made by Zhang and co-workers.[186] MWCNTs, made by catalytic decomposition of methane, were coated with iron oxides using high-temperature decomposition of ferrocene. Also, Strongin and co-workers synthesized MWCNTs or BNTs by arc-discharge and a CNT substitution reaction, respectively, and coated them with amorphous Ge that crystallized at elevated temperature to form MWCNT/Ge and BNT/Ge core/shell structures.[187] The thickness of the Ge coating was typically 4 nm for CNTs and 2 nm for BNTs. Duan and co-workers reported CNT/SiO_x core/shell structures where CVD-grown MWCNTs on a silicon wafer were used as substrates.[188] The sample was loaded into a PECVD chamber and heated to 700 °C in the presence of hydrogen. Zhang and Dai synthesized SWCNT/M (where M = Au, Pd, Fe, Al, and Pb) by using CVD to grow suspended SWCNTs over holes on a TEM grid and depositing the appropriate metal on the tubes by electron-beam evaporation.[189] The procedure requires deposition of a 1 nm titanium layer on the SWCNTs for forming continuous metal wires.

Carbon also serves as a coating material by various methods. For example, Cao et al. formed Au NWs coated with an amorphous carbon shell using a plasma-assisted method.[190] They coated template-synthesized Au NWs dispersed in a radio-frequency Ar plasma with a C shell using isopropanol as a carbon source. Sun et al. used a hydrogen plasma to transform CNTs into diamond NRs.[191] The final product consisted of diamond NRs coated with an amorphous carbon sheath. The typical diameter of the diamond NRs ranged between 4–8 nm and their length reached several hundreds of nanometers. Golberg and co-workers fabricated C/AlN/C coaxial nanotubes via substitution and carbonitridation processes where the C atoms of CNTs were replaced by AlN components.[192] The MWCNTs were mixed with Al_2O_3 powder and heated at 1600 °C for 1 h under Ar flow and another hour under NH_3 flow. The product consisted of AlN nanotubes with inner and outer layers coated with carbon. The thickness of the carbon coating was 2–2.5 nm, the tube-wall thickness was about 13 nm, and the total diameter ranged between 50–55 nm. Chen et al. used a CVD system to remove Si from SiC whiskers and fabricate SiC/C core/shell heterojunctions.[193] SiC whiskers were heated to an appropriate temperature before introducing the Cl_2:H_2 extraction mixture.

There are a few other examples of heterojunctions involving carbon-containing materials in the core, such as SiC/BN[194] and SiC/SiO_x[195] heterojunctions. In the former, SiC/BN core/shell structures were synthesized by mixing Si and In_2O_3 in a BN crucible and heating to 1600 °C in the presence of CH_4 gas. The 30–60-nm-thick SiC core was coated with 8–15-nm-thick BN nanotubes in this single-step process. Interestingly, a 10–15 nm gap existed between the core and the sheath. The decomposition of SiO■■SiO_2?■■ onto MWCNT templates resulted in the formation of biaxial SiC/SiO_x NWs as reported by Sun et al.[195] Wang et al. synthesized the same SiC/SiO_x biaxial NWs by reacting amorphous SiO ■■SiO_2?■■with carbon/graphite at 1500 °C.[196]

3. Solution-Phase Methods

3.1. Chemical Methods

In this section we describe chemical methods in the solution phase or methods combining solution-phase synthesis with some other technique, such as CNT synthesis or VLS growth. The chemical methods may involve the crystallization of solution-phase precursors through spontaneous oxidation/reduction or other chemical reactions either at room temperature or elevated temperatures. This usually occurs in the presence of a stabilizing ligand, polymer, or surfactant. Some of the examples in this section involve chemical formation of a thin film from the solution phase onto a 1D nanostructure synthesized in solution or by some other technique.

3.1.1. Branched and Segmented Heterojunctions

3.1.1.1. Alternating Solution Precursors

Alivisatos and co-workers chemically synthesized segemented and branched heterojunctions containing CdSe, CdS, or CdTe in the solution phase using Cd oxide complexed with alkylphosphonic acids as a cation precursor and Se, S, or Te dissolved in a tri(*n*-alkylphosphine) as anion precursors.[197] They synthesized CdS/CdSe segmented rods, CdS/CdTe branched rods, CdSe/CdTe branched rods, CdSe/CdTe segmented tetrapods, or CdSe/CdTe branched tetrapods as illustrated in Scheme 2. The procedure involves growth of a NR or tetrahedral particle of either CdS or CdSe for the first generation. Growth of the second-generation material (CdSe or CdTe) onto the first-generation NR or tetrahedral particle leads to four different possible heterostructures. The NRs and arms of the tetrahedral particle may simply extend in length to form a second segment of material when the precursor anion is switched during synthesis. This corresponds to the synthesis of segmented rods and segmented tetrapods as shown in Scheme 2. Alternatively, if the second precursor anion is introduced at supersaturation, branching of the first-generation structure occurs to produce the branched rod and branched tetrapod structures in Scheme 2. These four possible heterojunctions can

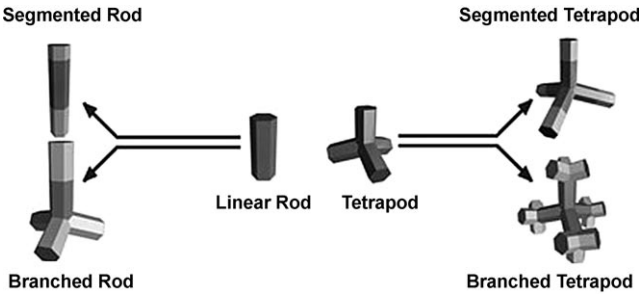

Scheme 2. Solution method for forming nanoscale segmented or branched NRs and tetrapods containing CdS, CdSe, and CdTe segments. Reprinted with permission from Ref. [197].

be synthesized either by 1) using an excess of Cd in the first generation and then just simply switching the precursor anion from the first to the second generation of growth, or 2) by synthesizing the first-generation structure, isolating it, and then growing the second generation in a separate reaction solution. Using precursors with different surface energies promotes end growth to form segmented structures instead of core/shell structures. At supersaturation, branching occurs by nucleation in the zinc blende phase, whereas a low concentration of precursor favors linear anisotropic growth of the wurtzite stucture.[197] Figure 10 shows a TEM

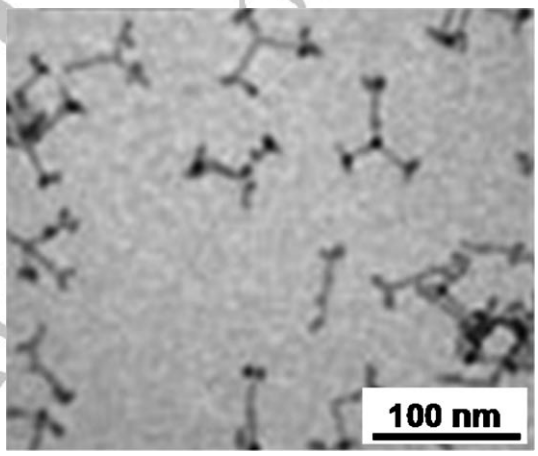

Figure 10. TEM image of CdSe tetrapods branched with CdTe segments. Reproduced with permission from Ref. [197].

image of a CdSe/CdTe branched tetrapod synthesized in this manner by Alivisatos and co-workers.[197] The diameter of the CdSe tetrapods and CdTe extensions was ≈3 nm and the arms were tens of nanometers in length. Peng et al. also fabricated CdSe/CdTe branched tetrapods, where CdSe rods were used as a starting material and subsequently branched with CdTe.[198] The length of the CdSe rods was 49.76 ± 9.51 nm and the diameter 6.36 ± 0.93 nm. After branching with CdTe the diameter remains largely unchanged but the length of the arms increased to 86.35 ± 9.22 nm.[198]

Yang and Zeng chemically synthesized various heterojunctions, including $TiO_2/H_2Ti_5O_{11}·H_2O$, $ZnO/H_2Ti_5O_{11}·H_2O$, $ZnO/TiO_2/H_2Ti_5O_{11}·H_2O$, and ZnO/TiO_2.[199] The step-by-

NANO MICRO small

step reaction of TiO_2/$H_2Ti_5O_{11}{\cdot}H_2O$ nanobelts formed in the first stage led to the formation of different flowerlike, fishbone-like, or multipode nanostructures on the surface of the nanobelts.

3.1.1.2. Combination of Methods

Our group recently reported the synthesis of branched heterojunctions by combining SWCNT synthesis and assembly with the chemical synthesis of 1D Au NRs by seed-mediated growth. The seed-mediated growth of Au and Ag NRs or NWs was recently developed by Murphy and co-workers[15,16] and also studied by the groups of El-Sayed[14] and Mulvaney,[8] ourselves,[85,200–203] and others.[204–206] In general, the synthesis of Au NRs occurs by adding presynthesized 3–5 nm gold-nanoparticle (Au NP) seeds into a solution containing cetyltrimethylammonium bromide (CTAB), $AuCl_4^-$ ions, and ascorbic acid. This leads to the anisotropic growth of Au nanoparticles into NRs or NWs by electroless deposition of Au onto the seed particles. The seed/$AuCl_4^-$ ratio controls the aspect ratio of the NRs and NWs. The yield of 1D structures is usually about 10%, but this has been improved synthetically or the NRs/NWs are purified to prepare samples >90% pure. It is believed that preferential blocking of certain crystal planes of the Au NP seeds by CTAB promotes the anisotropic growth of nanorods[206–209] and preferential growth on the NR ends due to enhanced electric fields may also play a role.[8]

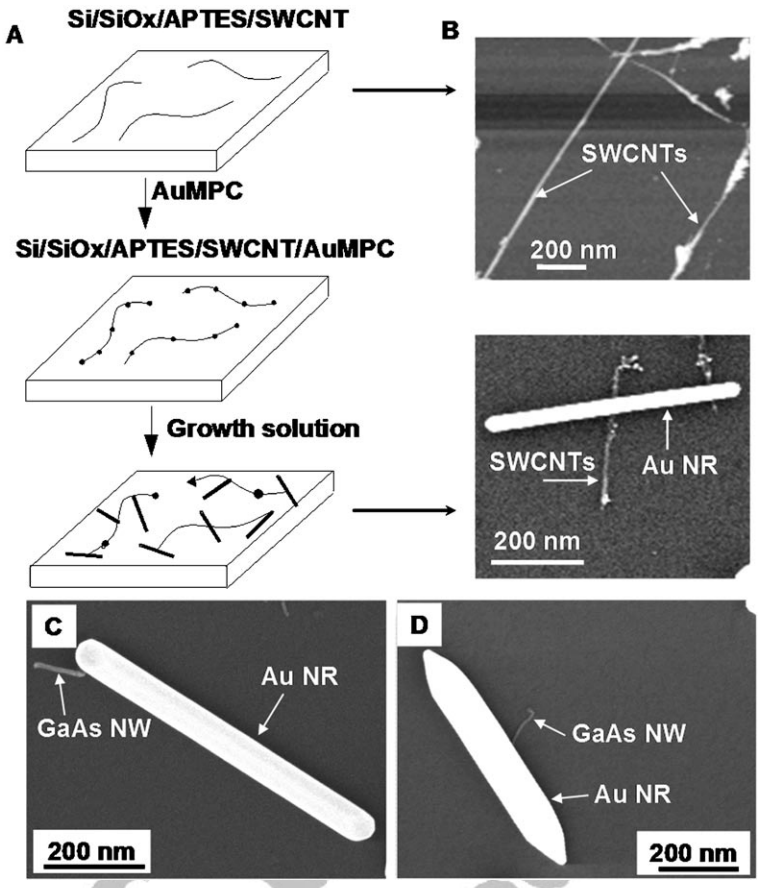

Figure 11. Seeded growth of Au NRs on SWCNTs: A) Schematic of the experimental procedure. B) AFM image of SWCNTs on a Si/SiO_x surface only, and SEM image after growth of Au NRs on SWCNTs. C, D) SEM micrographs of GaAs NW/Au NR heterojunctions. A, B) Reprinted with permission from Ref. [85].

We synthesized SWCNT/Au NR heterojunctions directly on Si/SiO_x surfaces by the seed-mediated growth of Au NRs from Au nanoparticles seeds attached to surface-bound SWCNTs.[85] A scheme of the procedure along with the corresponding SEM images are displayed in Figure 11 A and B. In the first step, SWCNTs were deposited onto an amine-functionalized Si/SiO_x substrate based on the well-known affinity of CNTs for NH_2 groups. The second step required depositon of Au seed particles selectively onto the SWCNTs. Immersion of the substrate into a solution of hexanthiolate-coated Au-monolayer-protected clusters (MPCs), which are hydrophobic and soluble in toluene, led to selective deposition of Au MPCs onto the SWCNTs.[85] SEM imaging and UV/Vis spectroscopy confirmed the selective deposition, which is presumably through hydrophobic interactions. The seed-mediated growth of the Au MPCs bound to SWCNTs on the surface led to the formation of SWCNT/Au NR heterojunctions assembled on surfaces. Figure 11 B shows an AFM image of SWCNT bundles immobilized on the Si/SiO_x substrate (top image), and an SEM image of a heterojunction formed between two bundles of SWCNTs and one Au NR (bottom image). The SWCNTs were typically several micrometers in length while the Au NRs were 600–900 nm in length.

Our group also synthesized GaAs/Au NR heterojunctions by combining VLS growth of GaAs NWs and seed-mediated growth of Au NRs on surfaces. In this case, citrate-stabilized Au nanoparticles bound to the thiol groups of a Si/SiO_x surface modified with mercaptopropyltrimethoxysilane served as catalysts for the CVD growth of GaAs NWs by the VLS process directly on the surface. The Au catalyst remains at the end of the synthesized GaAs NWs, which we used as seeds for the subsequent growth of Au NRs by seed-mediated growth. This procedure led to the formation of GaAs/Au NR branched heterojunctions assembled directly on the surface. Figure 11 C and D show SEM images of the heterojunctions.

3.1.2. **Core/Shell Heterojunctions**

3.1.2.1. Solution Phase Only

Chemical solution-based methods are common for synthesizing core/shell structures containing semiconductors, metals, carbon, or polymers. The synthesis can occur by introducing all precursors at once in one step, by alternating the precursors in the solution, or by synthesizing the core chemically and then transferring it to a new solution for the shell. We will describe these different situations below.

There are only a few examples of one-step procedures. For example, Li et al. used a polymerization/carbonization process to prepare C/ZnSe core/sheath heterojunctions.[210] The products were obtained in a one-step reaction from an aqueous solution containing $ZnCl_2$, ammonia, glucose, and SeO_2. Stirring and heating up to 160 °C led to the formation of C/ZnSe heterostructures. In this example the glucose precursor served as both the carbon source and the reducing agent, while the ammonia sustained the alkaline environment and acted as a soft template. Huang and co-workers synthesized Ag/TiO_2 core/shell NWs from tetrabutyl titanate (TBT) and $AgNO_3$ in ethylene glycol.[211] In this one-step method the samples were heated up to 240 °C or 270 °C for 14 h giving products with a smooth or rough surface, respectively. The diameter of the NWs was ≈40 nm for the core and ≈35 nm for the shell. Leung and co-workers synthesized Fe/Fe_2O_3FeO or Fe/FeCOOHFeO core/shell NRs by a technique involving electrodeposition on H-terminated Si, with the composition controlled by precursor concentration.[212] This technique is a one-step process where Fe is electrodeposited from an $FeCl_3$ precursor in $NaClO_4$ electrolyte. As reported, the nanorod-like shape was obtained at a 10 mM concentration of $FeCl_3$.[212] A closer examination of the sample revealed a 130 nm × 25 nm core/shell NR structure, with Fe comprising the core and FeOOH/FeO the shell.

For semiconductor/semiconductor core/shell heterojunctions, the synthesis usually occurs in strongly coordinating solvents from metalorganic precursors using alternating precursors or by synthesizing the core first and then the shell in another solution. For example, Weller and co-workers[213,214] synthesized a CdSe/CdS core/shell NR by first synthesizing the CdSe core in a mixture of hexadecylamine (HDA), tri-*n*-octylphosphine oxide (TOPO), and tri-*n*-octylphosphine (TOP) using dimethylcadmium and tri-*n*-phosphine selenide as precursors and then growing a CdS shell from a TOP solution containing dimethylcadmium and bis(trimethylsilyl-sulfide) precursors. The diameter of the CdSe cores was typically between 3–6 nm and the length was controlled by the concentration of the shell precursor. Other groups used similar procedures that employ coordinating solvent mixtures as well. Alivisatos and co-workers,[215] Lomascolo and co-workers,[216] and Rosenthal and co-workers[217] reported the synthesis of CdSe/(CdS/ZnS) core/shell NRs. A double shell of CdS/ZnS formed on the surface of CdSe NRs, with the CdS shell growing closer to the core due to a smaller lattice mismatch between the two materials. As reported by Alivisatos and co-workers, the diameter of the NRs were 3.3 nm, 6.0 nm, and 7.3 nm for a thin, medium, and thick shell, respectively.[215] The groups of Wang[218] and Banin[219] fabricated CdSe/ZnS core/shell NRs. The average length of the core/shell NWs with the shell thickness of 1.7 monolayers (ML) was 24.3 nm and diameter was 4.2 nm, for 3.5 ML the length was 24.5 nm and diameter 4.9 nm. Weiss and co-workers synthesized the same nanostructure coated with a phytochelatin-related peptide.[220] The TOPO-coated core/shell NRs were redissolved in pyridine and mixed with the peptide solution. Subsequent surfactant exchange was facilitated by addition of tetramethylammonium hydroxide, which enabled binding of the peptides to the NR surface. Zhang and co-workers synthesized CdS/CdSe core/shell NWs, where the CdSe sheath formed around CdS by a substitution process with selenium.[221] For CdSe formation the CdS NWs were suspended with selenium in TBP and reacted for 24 h at 100 °C. The typical diameter was 7.7 nm for the core and 0.75 nm for the shell.

Core/shell 1D metal/silica and metal/metal nanostructures have been synthesized using the seed-mediated growth approach described previously. Hunyadi and Murphy synthesized Ag/silica nanopeapods by synthesizing Ag NWs by seed-mediated growth, coating the NWs chemically with silica, and finally reacting them with aqueous ammonia, which partially dissolves the Ag, creating a silica shell filled with a "pea-like" Ag material.[222] The thickness of the silica shell was controlled synthetically and varied between 9 and 150 nm. Similarly, the length of the Ag "peas" depended strongly on the reaction parameters, ranging from 35–240 nm. Chang and co-workers synthesized Au NRs first by seed-mediated growth and then chemically deposited an a Ag shell to form bimetallic core/shell NRs or Ag and Hg to synthesize trimetallic Au/Ag–Hg core/shell structures.[223–225] The pH of the solution, concentration of the metal ions, and presence of the CTAB surfactant during the second stage of growth determines the shape of the final core/shell structures. They observed dumbbell-shaped structures, as shown in Figure 12, as well as boat-shaped structures.[225] Depending on the pH of the solution, the fabricated NRs had differ-

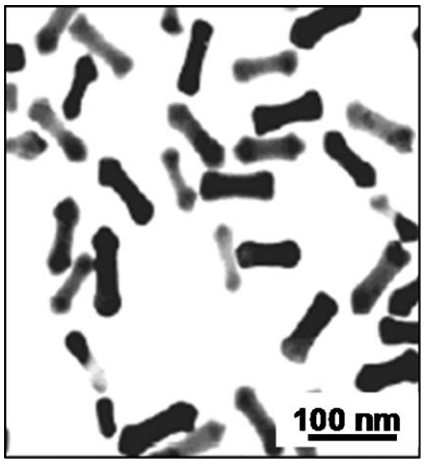

Figure 12. TEM image of dumbbell-shaped Au/Ag core/shell NRs. Reprinted with permission from Ref. [225]. Copyright 2004, American Chemical Society.

NANO MICRO small

ent ARs. For trimetallic NRs the AR was 3.39, 2.89, and 4.10 for a pH of 8.0, 9.5, and 10.5, respectively. The AR for bimetallic NRs was 4.10, 2.72, and 1.90 for the same pH values. A similar procedure was used by Liu and Guyot-Sionnest to fabricate Au/Ag core/shell NRs.[226] Yang and co-workers electrochemically synthesized Au NRs and used them as seeds to fabricate Au/Ag and Au/Pd core/shell NRs by growing the shell from a solution containing surfactant, mild reducing agent, and silver or palladium ionic precursors.[227] The resulting core/shell NRs were about 25 nm in diameter and 50–60 nm in length.

Sun and Xia synthesized AuAg/PdAg core/shell heterostructures using Ag NWs synthesized by the polyol process as sacrificial templates.[228] Galvanic replacement of Ag from the NWs with Au by immersing the NWs into a solution of $HAuCl_4$ led to the formation of Au/Ag nanotubes in the first step. Next, after electrolessly plating more Ag onto the Au/Ag nanotubes by suspending the nanotubes into a solution of L-ascorbic acid and adding $AgNO_3$ dropwise, the nanotubes were immersed into $Pd(NO_3)_2$ solution to form the outer Pd/Ag alloy shell. This led to the formation of double-walled nanotubes containing Au/Ag on the inside, and Pd/Ag tubes on the outside. The average diameter of the double-walled nanotubes was about 100 nm.

Tsuji et al.[229] and Ah et al.[230] reported the synthesis of Au NRs coated with Ag shells by combining the polyol method with microwave heating or by reaction of Au NRs with $AgCl_4^{3-}$ ions in NH_2OH solution, respectively. In the latter report, the average diameter of the Au/Ag NRs was 22.5–25.0 nm and the length varied between 56.5 and 58.0 nm. Wen and Yang synthesized Cu_2S NWs by surfactant-assisted growth in solution and coated the NWs with an Au shell.[231] This occurred by depositing Au from $HAuCl_4$ solution onto Cu_2S NWs that were synthesized on a copper substrate by a redox reaction, where the NWs served as the cathode and the copper surface as the anode. The Cu_2S core was typically 60 nm in diameter and the Au shell was $\approx$20 nm thick. Wang and co-workers prepared Bi_2S_3 NRs by a solution-based polyol method, and subsequently coated the as-synthesized NRs with silica by dispersing the NRs in a solution of the shell precursor, which was comprised of tetraethoxysilane (TEOS) and ammonia catalyst.[232] The Bi_2S_3 NRs were 150–180 nm in diameter and hundreds of nanometers in length. The thickness of the silica coating was 30–40 nm.

3.1.2.2. Combined Procedures

The above examples demonstrate chemical methods for the chemical synthesis of both the core and shell. Other methods utilize solution methods combined with another technique for the synthesis of core/shell heterojunctions. The solution-based system can be employed for the synthesis of the shell or for synthesis of the core. As an example of solution shell synthesis, Cao et al. first synthesized TiO_2 NWs and CNTs by a hydrothermal method and direct-current arc discharge, respectively. They synthesized TiO_2/CdS[233] and CNT/CdS[234] heterojunctions by suspending the core wires in solution and coating the surfaces chemically with CdS via KBH_4 reduction of S powder and $CdCl_2$ in dried THF. Typically the NWs were micrometers in length with a TiO_2 core $\approx$60 nm in diameter and a CdS shell $\approx$15 nm thick. Colorado and Barron deposited a $\approx$25 nm layer of silica onto vapor-phase-synthesized 3–6-nm-diameter SWNTs using a basic sodium silicate solution.[235] Han and Zettl chemically coated SWCNTs made by laser ablation with a 5-nm layer of SnO_2 by stirring in the Sn precursor solution.[236] Dai and co-workers deposited Pt and Au onto presynthesized single-walled carbon nanotubes by spontaneous reduction from aqueous solutions.[237]

As an example of solution-based core synthesis, Woggon et al. synthesized CdSe NRs and CdSe/ZnS core/shell NRs chemically in solution and then coated them with an epitaxial layer of ZnSe using vapor-phase MBE.[238,239] The NRs were typically 6.7 ± 0.5 nm in diameter and 34.7 ± 0.5 nm long. Gajbhiye and Bhattacharyya formed ε-Fe_3N/GaN core/shell NWs by wet-chemical procedures combined with a nitridation process.[240] In this example, Fe/Ga citrate fibers were formed first during the evaporation of citrate gel and transformed to Fe/Ga oxide in air atmosphere. Next, the nitridation of Fe/Ga oxide NWs in NH_3 gas produced ε-Fe_3N/GaN heterostructures that were typically 30 nm in diameter and $\approx$1 μm in length.

3.1.2.3. Polymer-Containing Structures

Various heterojunctions of chemically synthesized 1D nanostructures containing polymer materials have been reported. In most cases, the polymer material is used as a shell to coat metals, semiconductors, or carbon 1D nanostructures. The polymer coating may be deposited as a shell after synthesis of the core structures or the entire core/shell structure may form in a one-pot reaction. Huang et al. described a one-pot self-assembly process, where chlorauric acid reacted with aniline monomers in the presence of D-camphor-10-sulfonic acid (CSA) as a dopant/surfactant formed Au/PANI-CSA nanocables.[241] The dimensions depend on the synthetic conditions, and for a 7:1 molar ratio of aniline to chlorauric acid the diameter of the nanocables was 50–60 nm and length was 1–2 μm. At higher concentrations of CSA the diameter was 180 nm and the length was 1–5 μm. Li and co-workers described a one-step process used to fabricate Ag/PPY coaxial nanocables via reaction between $AgNO_3$ and pyrrole monomer.[242] Qian et al. synthesized Te/poly(vinyl alcohol) (PVA) nanocables using a different approach.[243] They formed the core/shell structures via synergistic soft–hard template effects between Te^{4+} ions and PVA in a one-step process. The concentration of PVA influenced the diameter of the nanocables, ranging from 400 nm to 2 μm, with their lengths reaching tens of micrometers.

In a two-step process, Yang and co-workers coated Si/SiO_2 core/shell NWs with PMMA using an atom-transfer radical polymerization (ATRP) process.[244] The (Si/SiO_2)/PMMA core/shell NWs are shown in Figure 13. The average diameter of the Si/SiO_2 NWs increased from $\approx$65 nm to $\approx$122 nm after the PMMA coating. In another example, Kim and Song pregrew Au NRs as seeds for the polymeri-

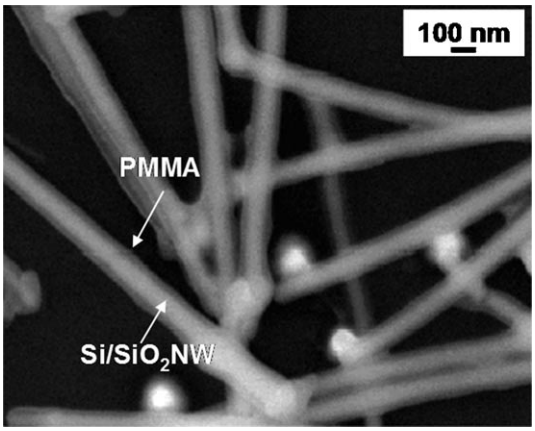

Figure 13. SEM image of PMMA-coated Si/SiO_2 NWs. Reprinted with permission from Ref. [244]. Copyright 2005, American Chemical Society.

zation of PPY shells.[245] Caruso's group coated Ni NRs with alternating layers of poly(diallyldimethylammonium chloride) (PDADMAC) and poly(sodium-4-styrenesulfonate) (PSS) polymers using layer-by-layer deposition and electrostatic attraction.[246] The Ni NRs had diameters of 65 ± 15 nm, and lengths of 1.5 ± 0.25 μm. The eight-layer polymer shell was ≈8 nm thick. Kroto and co-workers used an in situ atom-transfer radical polymerization process to form poly(*N*-isopropylacrylamide) (PNIPAAm) shells around MWCNTs.[247] Yu et al. formed MWCNT/PANI core/shell heterojunctions by inverse microemulsion polymerization.[248] They controlled the polymer thickness on the nanotube surface by reaction time and the diameter of the heterojunction increased from 60 nm after 12 h to 80–100 nm after 24 h reaction time. Liu et al. described the synthesis of CNTs with polymer shells, where MWCNTs formed by catalytic CVD were coated with a PMMA layer by a radical grafting polymerization processing of methyl methacrylate.[249]

3.2. Soft Templating

Soft templating involves the use of organic or biological molecules that self-assemble into nanoarchitectures as soft templates for the synthesis of inorganic materials. For example, Stupp and co-workers utilized "dendron rodcoils" (DRCs), which form helical nanoribbons in ethyl methacrylate/2-ethylhexyl methacrylate (EMA/EHMA) gels.[250] CdS/DRC helical heterostructures formed from $CdNO_3$ and H_2S precursors, where the CdS helix grew onto the DRC backbone. The helical structures were 35–100 nm wide with lengths reaching about 2 μm. Each coil of the periodical structure repeated every 40–50 nm.

Gazit and co-workers formed metal–insulator–metal (Ag–peptide–Au) coaxial nanocables from soft biological templates.[251] A peptide that self-assembled into nanotubes served as the template and insulator. They filled the inside of the nanotubes with silver by incorporating Ag^+ ions into the tubes and then reducing them to silver metal. Attachment of gold nanoparticles to the outer walls of the peptide backbone through a thiol-terminated peptide linker and subsequent reduction of gold ions onto the peptide-bound gold nanoparticles led to the formation of the Ag/peptide/Au metal–insulator–metal trilayered heterojunctions. They were able to obtain a 20-nm-thick continuous film of Au on the surface of the peptide nanotubes.

3.3. Sonochemistry

Sonochemistry involves acoustic cavitation as a driving force for reactions to occur in solution. During this process, bubbles formed in the liquid phase grow and collapse implosively, producing local heating of about 5000 °C, pressures close to 500 atm, and high cooling rates ($\approx 10^7$ K s^{-1}).[252] Many reactions may take place under these conditions (oxidation, reduction, dissolution, etc.).

Gao and Wang used sonochemical methods to decorate SnO_2 nanobelts with a sheath of CdS nanoparticles forming core/shell nanobelts/nanoparticles[253] and to fabricate ZnO/CdS core/shell NR/nanoparticle junctions.[254] SnO_2 nanobelts prepared previously by a thermal evaporation process were mixed with cadmium chloride and thiourea in deionized water. Subsequent sonication led to SnO_2/CdS heterostructure formation. The SnO_2 nanobelts were 30–200 nm wide, 10–50 nm thick, hundreds of micrometers long, and coated with ≈10–20 nm CdS nanoparticles. Similarly, ZnO NRs synthesized by the oxidation of ZnO/Zn particles at 920 °C were suspended in deionized water with the same shell-forming precursors, producing ZnO/CdS heterostructures after sonication. Typically, the ZnO NRs were 20–40 nm in diameter and a few micrometers long. The CdS nanoparticles coating the ZnO NRs ranged from 8.5 nm up to 20–50 nm in diameter after agglomeration. Qiu et al. fabricated striped Bi_2Se_3 NWs composed of orthorhombic and hexagonal phases produced by pulsed ultrasound, where ultrasonication accompanied the passing of current through the cell.[255] The average phase length was about 30 nm for 29.2-nm-thick NWs with an AR of ≈13.2. Yan and co-workers deposited SnO_2 nanorods on α-Fe_2O_3 nanotubes by ultrasonication of the nanotubes in a reverse micelle solution with the addition of $Sn(OH)_6^{2-}$ ions.[256] The nanorods grew preferentially along the [101] direction, forming angled architectures with the length controlled by the reaction time. The NRs were about 70 nm long following a reaction time of about 6 h. Zhang et al. used reverse micelles and ultrasound to fabricate Ag/polystyrene (PS) core/shell NRs.[257] Metal particles formed in a reverse micelle solution subsequently grew into Ag NRs when treated with ultrasound. Finally, a 0.5 h ultrasound treatment of a solution containing the polymer precursors and CO_2 led to 30 nm average diameter Ag NRs coated with a 5-nm-thick PS layer and a length of 200 ± 40 nm. The diameter remained constant with increasing sonication time while the length increased to 390 ± 30 nm.

Xia and co-workers combined sonochemistry with other techniques to produce interesting heterojunctions. They ultrasonically synthesized trigonal Se NRs, which were subse-

NANO MICRO small

quently heated in a solution containing appropriate precursors to grow $RuSe_2$ or $Pd_{17}Se_{15}$ shells on the Se NW cores.[258] The Se NR templates were 10–100 nm in diameter and the length could reach ≈100 μm. The $RuSe_2$ shell thickness was 2–4 nm. They also grew overlayers of CdSe onto sonochemically prepared Se NWs by treatment of the as-prepared NWs in a Cd^{2+}-containing solution.[259] Stirring at 100 °C led to the formation of a 5–10-nm-thick CdSe wall on the NW core.

3.4. Other Solution Systems

Zhu and co-workers demonstrated an interesting method for fabricating p–n junctions in Si NWs.[260] Si p–n wafers prepared in a UHV CVD system by n-type silicon film deposition (9 μm thick) on p-type Si wafers were used as precursors. Selective etching at 50 °C in HF solution with the addition of $AgNO_3$ formed p–n Si NW arrays arranged parallel to each other with the length depending on etching time. Typically, the Si NWs were single-crystalline with diameters ranging from 30 to 200 nm and lengths of 10–20 μm.

Fang et al. used the solution–liquid–solid–solid (SLSS) method to fabricate Sn-filled $In(OH)_3$ nanotubes.[261] This is a single-step procedure where the liquid part of an In–Sn droplet serves as a catalyst and source of precursors to the nanostructure at the same time. In foil, Sn foil, and NaOH served as precursors, and were heated at 180 °C for 30 h. Slow dissolution of Sn in the In droplet forms an alloy that during precipitation divides into a solid Sn core and solid $In(OH)_3$ shell under oxidizing conditions. Also, depending on the In precursor concentration, the nanotubes may have an open or closed end. The diameter of the Sn/$In(OH)_3$ NWs was ≈70 nm for the core and ≈10–20 nm for the shell. NWs with nonuniform diameters were also present, where the thicker part was about 220 nm with a 50-nm-thick shell, which gradually decreased to 80 nm with a 20-nm-thick shell.

4. Template-Directed Synthesis

In the early 1990s, Martin and co-workers pioneered the use of hard templates in the synthesis of metal and polymer tubules, rods, and wires by electrochemical or electroless deposition in porous membranes followed by dissolution of the membrane.[262,263] The commercially available membranes, usually polycarbonate or alumina, contain a controlled density of well-defined, uniform pores with diameters ranging from 15 nm to 1.2 μm. The diameter of the resulting nanostructures formed inside these templates is determined by the pore diameter and the length is determined by the membrane thickness, which are both variable. Therefore, the final AR of the 1D structures is easily controlled by these two parameters. Since these early studies on one-component materials, many groups have utilized the same approach to fabricate 1D nanostructures that are comprised of multiple components containing heterojunctions. NWs, NRs, and NTs containing M–M, M–SC, M–C, or M–P junctions have been formed by sequential deposition of the metal, semiconductor, carbon, or polymer in the pores of the membranes. The 1D structures usually contain segmented heterojunctions, however, strategies exist for fabricating core/shell or coaxial heterojunctions as well. It is important to note that Hurst et al. recently published an excellent review on the preparation of multisegmented 1D nanorods by hard-template methods.[4] We will review these template-based methods for forming heterojunctions in the following sections, categorizing the examples into electrochemical, electrochemical combined with other methods, methods involving electrophoretic deposition, and non-electrochemical methods. The sections are further divided into segemented and core/shell heterojunctions.

4.1. Electrochemical Deposition in Templates

4.1.1. Segmented Heterojunctions

The general procedure for electrochemical deposition of segmented structures is outlined in Scheme 3. The first step is to evaporate metal on the backside of a polycarbonate or alumina membrane template. It is best to use a metal that is easy to dissolve later, such as Cu or Ag, but Au has also been used. Next, some Cu or Ag may be electrochemically deposited to fill in the pores slightly before depositing the materials of interest (Step 2). Step 3 is to electrochemically

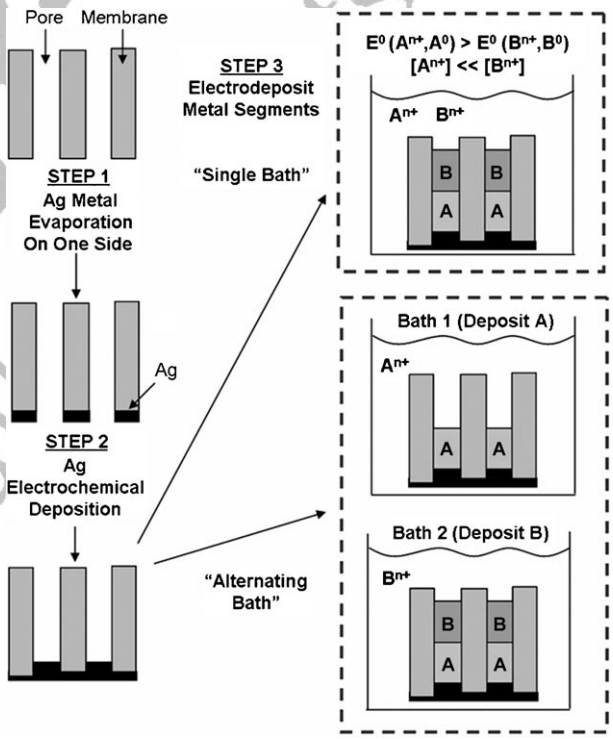

Scheme 3. Schematic illustration of the procedure for forming segmented metal NRs and NWs electrochemically in hard templates by the single-bath or alternating-bath procedure.

deposit the different segments of the NW with the materials of interest. The segments are most commonly metals, however, semiconductors and polymers may also be electrochemically deposited into the pores. There are two main ways to perform Step 3. The first is by using a single plating bath containing the precursors of all of the materials to be deposited. This strategy has been utilized mainly for depositing different segments of metal from their corresponding ions. As shown in Scheme 3, in the case of two metals with different reduction potentials, the more noble metal (A) can be selectively deposited at a potential that is more positive than the reduction potential of the second metal (B). The potential is then poised more negative to deposit the second metal. However, at a more negative potential both of the metals will codeposit. The concentration of the second metal in the plating solution is made much higher than the more noble first metal ($[B^{n+}] \gg [A^{n+}]$) in order to minimize the amount of noble metal deposited during deposition of the second metal. The second strategy for Step 3 in Scheme 3 is by simply depositing material from one plating bath and then switching to a new plating bath containing a different material of interest to form different segments. This takes more time since it involves switching plating solutions, but it avoids having a small contamination of the more noble metal when the second metal is deposited.

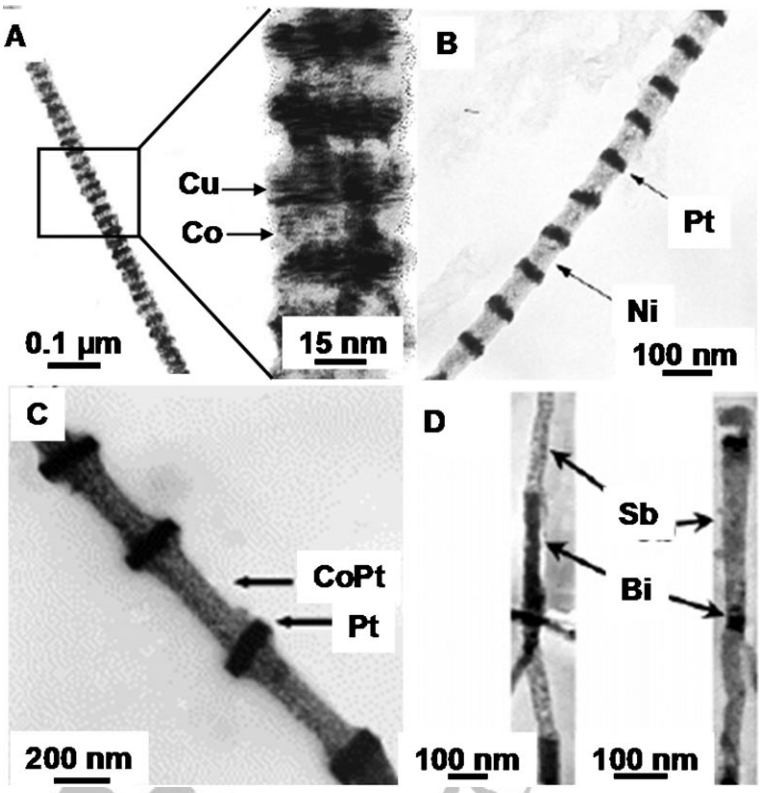

Figure 14. TEM images of segmented NWs prepared electrochemically in a single bath. A) A Co/Cu segmented NW made in a polycarbonate membrane. B) A Ni/Pt superlattice prepared in an AAO template. C) A CoPt/Pt segmented NW from AAO. D) A Bi/Sb segmented NW made in AAO. A) reprinted with permission from Ref. [264]. Copyright 1994, American Institute of Physics; B, D) reprinted with permission from Refs. [279] and [285], respectively. Copyright 2005, American Chemical Society; C) reprinted from Ref. [283]. Copyright 2004, with permission from Elsevier.

One of the earliest examples of multicomponent template-synthesized nanowires is the work of Piraux et al., who synthesized Co/Cu segmented wires by electrochemical deposition in the pores of polycarbonate for studies of giant magnetoresistance (GMR) using a single plating bath.[264] The polycarbonate pores ranged from 10 to 50 nm in diameter. The first step in the synthesis was the evaporation of a thin film of copper on one side of the membrane, which served as the working electrode. Then, Co/Cu multilayered nanowires were deposited by electrochemical deposition from a single sulfate-plating bath containing both Cu^{2+} ions (10^{-3} M) and Co^{2+} ions (0.5 M). The electrochemical potential was pulsed between −0.2 V and −0.9 V, where Cu and Co were deposited, respectively. At −0.2 V, only Cu deposits because the potential is not sufficiently negative to reduce Co. At −0.9 V, Co and Cu both deposit, but only trace amounts of Cu deposits due to the much lower concentration in the plating bath. Figure 14 A shows a TEM image of a wire formed by this procedure. The Co (light bands) and Cu (dark bands) segments are clearly observable in the image. The NW is about 40 nm in diameter and each segment of Co and Cu are about 10 nm thick, which is controlled by the charge passed during the pulsed deposition at the two different potentials. The same group reported other work on the GMR of Co/Cu[265,266] and NiFe/Cu[267] segemented NWs using a similar approach. The single-bath approach is crucial for the synthesis of these superlattice NWs with multiple small segments within one NW since switching between plating baths would be a long and tedious approach.

Following this early work, other groups synthesized different types of segmented magnetic wires using a similar single-bath, pulsed-deposition approach. For example, Searson and co-workers synthesized Co/Cu[268] and Ni/Cu[269–271] for studies of GMR and other magnetic properties. They also synthesized Pt/Ni/Pt wires for magnetic assembly, but it was not clear if this was achieved using a single plating bath or alternating solutions.[272] Schwarzacher and co-workers synthesized Co-Ni-Cu/Cu[273–275] and NiCu/Cu[276] NWs and

studied GMR and remanant magnetization of the nanostructures. Bai and co-workers fabricated Ni/Cu particles[277] from Ni/Cu segmented nanowires and prepared arrays of Ni/Cu[278] and Ni/Pt[279] segmented wires with enhanced coercivity and high remanence ratio. A TEM image of a 50-nm-diameter Ni/Pt nanowire is shown in Figure 14B. Other examples of single-plating-bath approaches include the fabrication of Ni/Cu,[280] Au/Co,[281] Co/Cu,[282] CoPt/Pt,[283] and Ni/CuSn/Ni[284] segmented NWs for studies of magnetic properties, spin valves, and magnetic manipulation. Figure 14C shows an example of a bamboo-shaped CoPt/Pt nanowire resulting from thinner 300-nm-long segments of CoPt compared to the thicker 20-nm-long Pt segments, which is thought to occur by partial etching of Co in the acidic electrolyte solution.[283] Finally, Xue et al. synthesized segmented Bi/Sb superlattice nanowires by electrodeposition in anodic alumina templates from a single ethanol plating bath.[285] Figure 14D shows a TEM image of two of the four different kinds of structures synthesized.[285] Blondel et al. prepared Co/Cu segmented NWs by single-bath and alternating-bath techniques and compared the magnetoresistance of the prepared structures.[286]

Several groups have also used alternating plating solutions (Scheme 3) to synthesize NWs with various electrochemically deposited metal, semiconducting, or polymer segments. One of the early examples is the work of Natan, Mallouk, and co-workers, who synthesized striped Au/Pt nanorods inside an alumina template by evaporating Ag on the backside of the membrane, electrochemically depositing a small amount of Ag inside the pores, and finally electrochemically depositing segments of Au and Pt sequentially from separate commercially available plating solutions.[287] The Ag and alumina membrane were then dissolved to release the striped Au/Pt nanorods, which were suspended in solution. The different chemistry of Au and Pt allowed for selective assembly of different molecules on the two segments. Following this work, Natan and co-workers synthesized various striped nanorods in alumina templates, which they refer to as metallic barcodes.[42,288–291] Au/Ag rods are the most common, but they have also demonstrated rods containing Pd, Pt, Ni, Cu, and Co by sequential deposition in alumina templates using alternating plating baths of the individual metal. The rod diameters are generally 200–300 nm with lengths of 4–10 μm. The different metal segments are distinguishable optically by their different reflectivity. Changing the lengths of the segments and the metal leads to a variety of different patterns (barcodes). The metallic barcodes can be used to detect biological molecules based on bioassay chemistry and optical detection.[42] Figure 15 A and B shows the optical image and SEM image of a striped Au/Ag nanorod, respectively.[288] The segments are observable in both images. The five Au segments are constant at 550 nm in length and the variable Ag segments are 60, 110, 170, and 240 nm in length from bottom to top.[288] The Ag segments appear brighter in the optical image due to its higher reflectivity. Note that in these examples of alternating plating baths, there are generally fewer and longer segments compared to the single-bath NWs, partially due to the inconvenience of switching baths and the fact that superlattices were not required for this application. Keating and co-workers also synthesized Au/Ag metal barcodes and those containing other metals such as Co, Cu, Ni, Pt, and Pd.[292–294] These studies were aimed at understanding their reflectivity,[292] fluorescence,[292] stability,[293] and issues related to DNA-hybridization efficiency.[294]

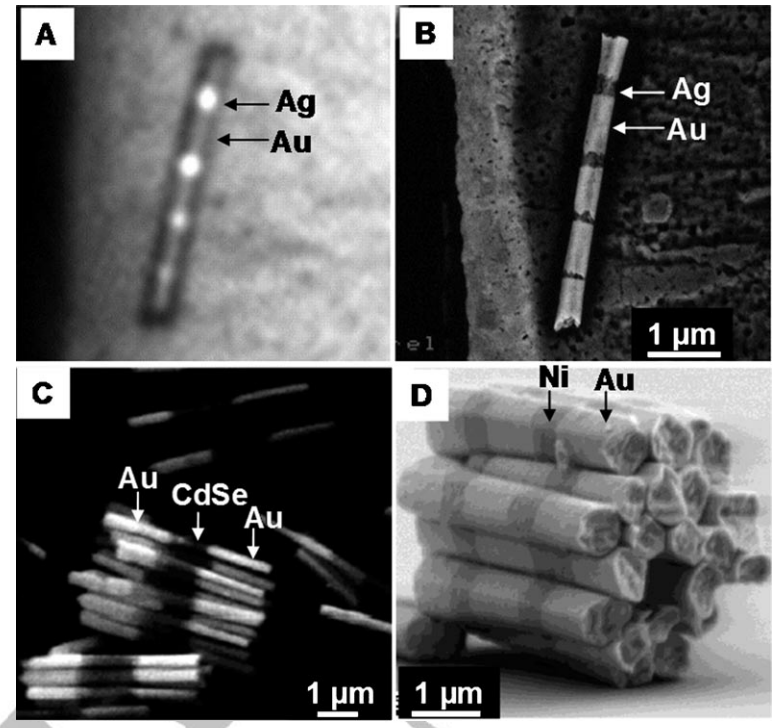

Figure 15. A) Optical image of an Au–Ag striped nanorod with corresponding FE-SEM image of the same heterostructure in (B). C) SEM image of Au/CdSe/Au nanowires synthesized in a polycarbonate membrane. D) SEM image of a Au/Ni nanowire bundle with ferromagnetic attraction. A, B) are from Ref. [288], reprinted with permission from AAAS. C) Reprinted with permission from Ref. [295]. Copyright 2002, American Chemical Society. D) Reprinted with permission from Ref. [300]. Copyright 2003, American Chemical Society.

Mallouk and co-workers synthesized Au/CdSe/Au and Ni/CdSe/Ni segmented NWs by alternating the electrochemical deposition in polycarbonate membranes using commer-

cially available plating solutions for the Au and Ni segments and an acid solution of $CdSO_4 + SeO_2$ for deposition of the semiconducting CdSe segment.[295] The SEM image in Figure 15C shows the Au/CdSe/Au wires, where the Au ends appear brighter. These metal–semiconductor–metal junctions exhibit interesting photoconductive behavior. They also synthesized Au/Sn/Au NWs[296] in polycarbonate for studies of interdiffusion and both Pt/Au[297] and Pt/Ni/Au/Ni/Au[298] wires for studies on their motor properties driven by the formation of oxygen at the Pt segments due to catalytic decomposition of hydrogen peroxide. Fournier-Bidoz et al. synthesized Au/Ni NRs from alumina templates and attached the rods to a silicon surface through the Au ends.[299] The catalytic decomposition of hydrogen peroxide to form oxygen at the unattached Ni ends led to a constant circular movement of the rods, behaving as self-propelled nanorotors.[299]

Whitesides and co-workers used the alternating deposition method to form Ni/Au[300] and CoNi/Au[301] segmented rods that were 400 nm and 80 nm in diameter, respectively, and a few micrometers in length. Ni/Au rods formed three-dimensional assemblies, as shown in Figure 15D, based on their magnetic interactions,[300] and CoNi/Au rods trapped magnetic Fe_2O_3 nanoparticles at the interface between segments due to the high magnetic-field gradients generated at the ferromagnetic (CoNi)/diamagnetic (Au) heterojunctions.[301] Meyer and co-workers synthesized Au/Ni segmented NWs in alumina templates that were typically 200–350 nm in diameter and 10–20 μm in length and studied selective functionalization,[302] protein adsorption,[303] and magnetic trapping.[304] Hangarter and Myung synthesized Ni/Au/Ni and Ni/Bi/Ni segmented NWs and demonstrated alignment in magnetic fields.[305] They deposited Au segments from a commercial plating solution and Ni and Bi from $Ni(H_2NSO_3)_2$ and $Bi(NO_3)_3$ or $BiCl_2$ solutions, accordingly, in an alumina template to form wires that were 100–200 nm in diameter and 10–20 μm in length. Xue et al. synthesized Ni/Fe multisegmented nanowires by electrodeposition in alumina from alternating solutions and studied their coercivity mechanism.[306] Zhou and co-workers synthesized Pt/Ni,[45,307] Pt/Ru,[45,308] and Pt/RuNi[45] NRs in alumina templates that were typically ≈200 nm in diameter and 1–2 μm long. They studied the important electrocatalytic properties of these materials in methanol electrooxidation as a function of composition and different segment configurations.[45,307,308]

Searson and co-workers synthesized two-component Au/Ni NRs in alumina templates by alternating electrochemical deposition for applications in gene delivery,[43] self-assembly,[309] and vaccination.[310] They also synthesized and assembled three-component Au/Pt/Au[47] and Au/Ni/Au[311,312] NRs in an end-to-end fashion by selectively functionalizing the shorter Au segments with biotin and connecting the NRs through biotin-avidin linkages. Mirkin and co-workers synthesized Au/Ni/Au NRs in alumina templates for biomolecular separations, utilizing the specific chemistry of the different metal segments and ferromagnetic properties of Ni for magnetic removal from solution.[44,313] They also studied the self-assembly properties of two-segment Au/polypyrrole (Ppy) and three-segment Au/Ppy/Au synthesized by electrochemical deposition in alumina templates.[46] Au is deposited as usual and the Ppy segments are deposited by electrochemical oxidative polymerization of pyrrole. These rods self-assembled into interesting two- and three-dimensional structures as shown in Figure 16 A.[46] Similarily, this group

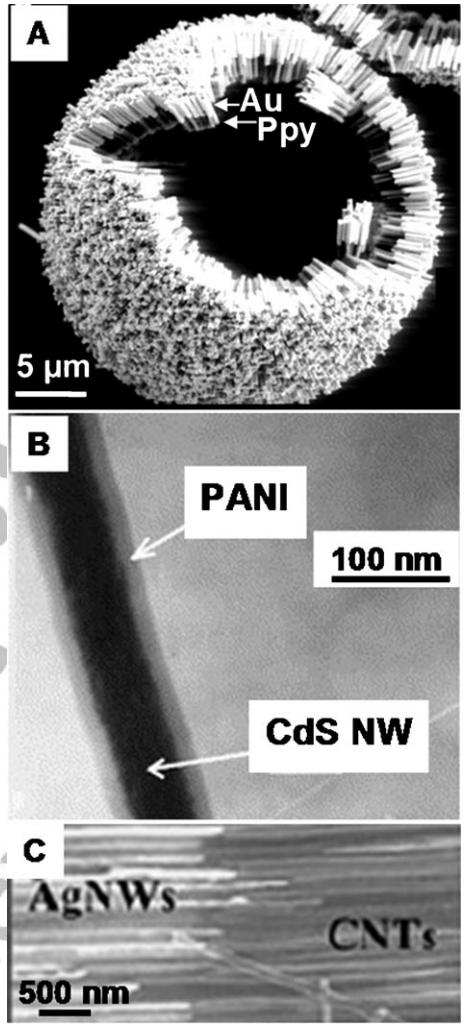

Figure 16. A) SEM image of assembled Au–Ppy segmented NRs. B) TEM image of a PANI shell around a CdS NW. C) SEM image of AgNW/CNT segmented heterojunctions. A) Reprinted from Ref. [46] with permission from AAAS. B) Reprinted from Ref. [316]. Copyright 2005, with permission from Elsevier. C) Reproduced with permission from Ref. [317].

synthesized Au/Ppy/Au and Au/Ppy/Cd/Au segmented nanorods and studied their behavior as nanoresistors and diodes.[314] Ag or Cd, CdSe, or polyaniline could alternatively be used for the metal, semiconductor, or polymer segments, respectively. Whitesides and co-workers synthesized Au/polyaniline (PANI) segmented 1D nanostructures by depositing Au and PANI sequentially in anodic aluminum oxide (AAO), but also deposited a self-assembled monolayer (SAM) of *p*-mercaptoaniline on the Au before PANI deposition to improve adhesion between layers.[315]

4.1.2. Core/Shell Heterojunctions

The work of Xi et al. represents an example of a core/shell heterojunction prepared by an electrochemical deposition method from alternating solutions in hard templates.[316] The group synthesized a CdS/PANI core/shell coaxial nanocable inside an AAO membrane. The diameters of the CdS core and PANI tube were about 50 nm and 90 nm, respectively. The procedure involved sputtering a conductive layer of Au on the AAO membrane to serve as the working electrode. Next, they electrochemically deposited the PANI nanotube by cycling between -0.2 and $+0.7$ V versus a standard calomel electrode (SCE) at $100\,mV\,s^{-1}$ for 400 cycles in a solution of 1 M $HClO_4$ + 0.5 M aniline. Finally, they filled in the hollow interior of the PANI nanotubes by electrochemically depositing CdS from a solution of 0.055 M $CdCl_2$ and 0.19 M sulfur. They studied the photoluminescent properties of the coaxial nanocables. Figure 16B shows a TEM image of the CdS/PANI core/sheath structure where the PANI shell and CdS core are easily distinguished.[316] Whitesides and co-workers synthesized PANI/Au core/shell nanotubes by electrochemically polymerizing PANI first in an AAO membrane and then electrochemically depositing Au under high-pH conditions, which leads to deposition of Au on the outside of the PANI instead of inside the PANI tube because PANI is insulating and the membrane pore widens by dissolution at high pH. The Au-shell coverage is controlled by deposition time.[315]

4.2. Combination of Electrochemical and Chemical Processes in Templates

4.2.1. Segmented Heterojunctions.

There are several examples of segmented NRs and NWs containing heterojunctions synthesized by combining electrochemical deposition in hard templates with some other chemical procedure, such as chemical vapor deposition (CVD), layer-by-layer assembly, electroless deposition, thermal heating, chemical anodization, and chemical assembly. For example, Zhu and co-workers combined electrochemical deposition with CVD to form various M–SC and M–CNT 1D end-to-end heterojunctions.[317–321] Specifically, they synthesized Ni/CNT,[318–320] Ag/Si,[319–321] Pt_6Si/Si,[319,321] Ag/amorphous-CNT,[317,319] and Ni/MWCNT/amorphous-CNT[318] heterojunctions by first depositing the Ni, Ag, or Pt segments in AAO templates from common plating solutions and then depositing CNT and Si segments on the tips of the metal by CVD through the decomposition of ethylene or the reaction of $SiCl_4$ with H_2, respectively. Diameters ranged between 30 and 100 nm and lengths between 7 and 90 μm and importantly the authors used AFM and microfabricated electrodes to study the interesting electron-transport characteristics of the 1D heterojunctions. Figure 16C shows an example of Ag/amorphous-CNT heterojunctions prepared by this method.[317] Mallouk and co-workers synthesized films of ZnO-PANI, TiO_2-PANI, or TiO_2-polystyrenesulfonate (PSS) sandwiched between Au, Ag, or Pt segments.[322,323] The films of semiconductor particles and PANI or PSS were deposited through electrostatic interactions using layer-by-layer assembly while the metal segments were deposited electrochemically in polycarbonate or alumina membranes. The M/(ZnO-PANI)/M, M/(TiO_2-PANI)/M, and M/(TiO_2-PSS)/M junctions exhibit interesting electronic properties. Mock et al. synthesized Ag/Au, Au/Ag/Au, and Ag/Au/Ni segmented NWs that were 30 nm in diameter and ≈7 μm in length in polycarbonate membranes and studied their light-scattering properties.[324] The Au and Ni segments were deposited electrochemically in a similar manner to previous studies, but the Ag segments were deposited with an electroless-plating bath since they found that the electrochemical Ag plating bath tended to dissolve the PC membrane. Tresback et al. synthesized Au/SnO_2/Au and Au/NiO/Au segmented heterojunction NWs by electrochemically depositing Au/Sn/Au and Au/Ni/Au metal segments and then thermally oxidizing the Sn segment to SnO_2 and the Ni segment to NiO by a two-step and one-step heat treatment, respectively.[325] These metal–oxide–metal heterojunction nanowires (≈60 nm in diameter and 2 μm in length) have potential applications in nanoelectronics and chemical sensing. Sokolov et al. described the synthesis of Ni/NiO/Co NWs by electrochemical deposition of Ni, chemical anodization of Ni in a pH 8.4 solution of Na_3BO_3 and $H_2B_4O_7$, and finally electrochemical deposition of Co from a nonaqueous plating bath to avoid dissolution of the oxide.[326] They formed the ≈80-nm-diameter and 6-μm-long segmented wires in polyester track-etch membranes and performed magnetotransport studies. Li and Wiley synthesized structured Au tips in alumina templates from multicomponent NWs using combined chemical and electrochemical methods.[327] Filling of the templates involved glue coating, Ni electrochemical deposition, Ni chemical oxidation, and Au electrochemical deposition. Dissolution of the Ni, glue, and template resulted in single-component structured Au tips that were formed from the Au/NiO heterostructured materials.

Lee et al. demonstrated the synthesis of multisegmented nanotubes, as opposed to all of the examples described up to this point of segmented or core/shell nanorods, through the combination of chemical and electrochemical methods.[328] The chemical process involved the deposition of Ag nanoparticles onto the inner walls of the AAO membrane used in the study by sequential immersion into aqueous solutions of $SnCl_2$ followed by $AgNO_3$. This cycle, usually repeated about six times, results in the deposition of metallic Ag nanoparticles on the AAO walls by chemical reduction of Ag^I with surface-bound Sn^{II} ions. With Ag particles chemically attached to the inner walls of the template, metals subsequently deposited electrochemically into the pores; using the standard methodology, they preferentially grow along the membrane walls to form NTs as opposed to the usual uniform deposition throughout the pore to form NRs■■Please check this last sentence. It did not seem to make sense originally; now the text makes sense, but may have lost its original meaning■■. Deposition of continuous tubes depended greatly on the deposition rate; slow rates ($<0.4\,mA\,cm^{-2}$) led to solid nanorods and fast rates (>

3.0 mA cm^{-2}) led to highly porous, mechanically unstable nanotubes. An intermediate rate of current density (2.2 to 2.5 mA cm^{-2}) was optimal for smooth, continuous nanotubes.[328] This method led to the formation of Au/Ni/Au/Ni/Au segmented nanotubes with some Ag nanoparticle impurities. Ag, Pt, Pd, Fe, Co, and Ni could also be incorporated into the segments to prepare various barcoded nanotubes. SEM images of the Au/Ni segmented nanotubes are displayed in Figure 17 with the segments labeled appropriately.[328]

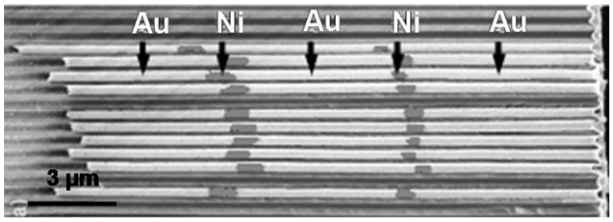

Figure 17. SEM image of Au/Ni segmented nanotubes synthesized in an AAO membrane. Reproduced with permission from Ref. [328].

4.2.2. Core/Shell Heterojunctions

Core/shell structures have also been synthesized in hard templates by combining electrochemical and chemical procedures. This usually occurs by either 1) synthesizing NRs or NWs in the pores of the membrane electrochemically first and then chemically functionalizing the NR with a shell, or 2) chemically functionalizing the inner walls of the membrane to form a nanotube and then electrochemically filling in the nanotube. We will describe examples of both approaches below.

Using the first approach, Kolmakov et al. synthesized Sn/SnO or Sn/SnO_2 core/shell NWs by electrochemically depositing Sn in the pores of an AAO membrane, releasing the wires by dissolution of the template, and then thermally oxidizing the Sn to form the oxide shell.[329] The Sn core was formed by ac electrodeposition from a solution of $SnCl_2$ at pH 1 and the formation of the oxide shell was controlled kinetically, revealing several different phases. The diameters of the NWs ranged from 30 to 50 nm and the lengths were ≈50 μm and, importantly, the oxidation procedure resulted in preservation of the NW structure. These wires have potential sensing and optoelectronic applications. Chatterjee et al. synthesized Au/Au_2S core/shell NRs of ≈100 nm in diameter and 1 μm in length by a combined electrochemical and chemical process in the pores of a polycarbonate membrane.[330] They first deposited Au electrochemically from a tetrachloroauric acid solution, then dissolved the polycarbonate membrane in chloroform, and finally coated the rods with Au_2S by chemically treating them with thiourea and a few drops of ammonia solution at 343 K. Wang et al. electrochemically deposited Zn into polycarbonate or AAO membranes from a $ZnCl_2$ solution at different potentials and temperatures.[331] The wires were 40 to 100 nm in diameter and several micrometers in length. The structure could be single-crystal, nanocrystalline, or polycrystalline comprised of Zn, ZnO, or Zn and ZnO composites, depending on the preparation. Under one set of conditions (low temperature and low reduction potential), pure Zn wires formed but were oxidized after removal from the template to form core/shell Zn/ZnO structures.[331] Under another set of conditions (high temperature and high reduction potential), wires with alternating segments of Zn and ZnO formed.

The next two examples are of segmented NWs that have been chemically coated to form segmented and core/shell wires. For example, Qin et al. synthesized ≈360-nm-diameter, 2–5-μm-long segmented Au/Ag and Au/Ni NWs electrochemically in alumina templates that were subsequently removed from the template, dispersed onto a substrate, and coated with Au/Ti or SiO_2 by thermal evaporation or plasma-enhanced CVD, respectively.[332] Sonication removed the wires from the substrate, which had a structure of segmented metal wires partially coated by a Au/Ti or SiO_2 shell. The shell served as a backbone to stabilize the Au segments following a post-etching treatment of the Ag or Ni segments to form nanometer gaps whose dimensions depended upon the length of the sacrificial Ag and Ni segments.[332] They deposited a mixture of polyethylene oxide and polypyrrole into one of the gaps using dip-pen nanolithography and characterized the electronic properties of the Au/polymer/Au heterojunction. Similarly, Sioss et al. combined electrochemical and chemical processes to form segmented nanowires containing Au, Ag, and Ni coated with a SiO_2 shell that was 60 to 100 nm in diameter and a few micrometers in length.[333] They electrochemically deposited Au, Ag, and Ni into porous alumina templates with the Ni between the more noble Au and Ag segments. After releasing the wires from the template, treatment in a solution of tetraethylorthosilane and NH_4OH led to a SiO_2 shell that coated the entire surface. The Ni segments were chemically etched in H_2SO_4 to form various chains of Au, Ag, and alternating Au–Ag particles, whose optical properties depend on the metal, size of segments, and spacing.[333]

Mallouk and co-workers demonstrated examples of both of the above-described approaches to form core/shell NWs.[322] In the first approach, they synthesized metal NRs in the pores of a membrane template and then functionalized the metal with a shell containing a film of semiconductor particles and polyelectrolyte. The film was prepared by alternating layer-by-layer deposition of ZnO or TiO_2 colloids with polystyrene sulfonate (PSS) to form a ZnO–PSS or TiO_2–PSS shell held together electrostatically. The overall structure is a metal/$(ZnO–PSS)_n$ZnO or metal/$(TiO_2–PSS)_n TiO_2$ core/shell material, where n represents the number of shell layers.[322] Mallouk's group also formed core/shell NWs using the second approach, where the walls of the membrane were coated first followed by electrochemical deposition.[322,334–336] In one example, they synthesized tubes of TiO_2–PSS or ZnO–PSS by layer-by-layer deposition on the membrane walls. Next, they electrochemically deposited Au or Ag to form Au(Ag)/TiO_2–PSS or Au(Ag)/ZnO–PSS core/shell 1D structures.[322] In another example, the membrane walls were coated chemically with SiO_2 by surface sol–gel deposition involving repetitive adsorption and

NANO MICRO small

hydrolysis of $SiCl_4$.[334,336] In this case, they electrochemically deposited Au, Au-CdS-Au, or Au-CdSe-Au, leading to the formation of Au/SiO_2[336] or $(Au\text{-}CdS(Se)\text{-}Au)/SiO_2$[334] core/shell 1D structures. The wires usually had diameters of 40 to 300 nm and lengths on the order of 10 μm. Figure 18 shows

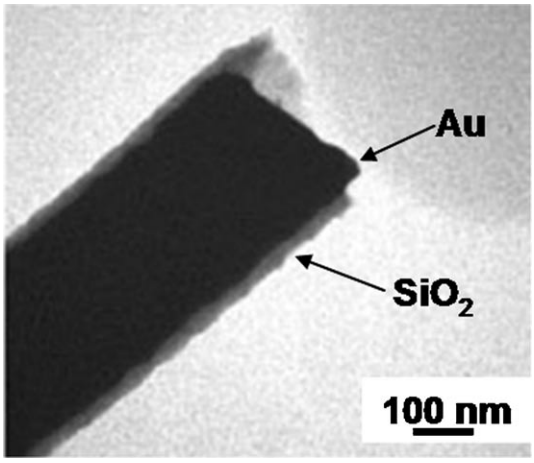

Figure 18. TEM image of a Au nanowire sheathed by a SiO_2 nanotube. Reproduced with permission from Ref. [336].

a TEM image of a Au/SiO_2 NW prepared by this method.[336] The Mallouk group also fabricated on-wire p–n heterojunction diodes using both methods on the same nanostructure.[335] In this case, TiO_2–$W_{12}O_{41}$ films were deposited on the inner walls of the AAO membrane by alternating immersion in aqueous $(NH_4)_{10}W_{12}O_{41}$ and TiO_2 solutions. Subsequent electrochemical deposition of Au led to the formation of $Au/(TiO_2–W_{12}O_{41})$ core/shell wires by method 2. These wires were then further functionalized chemically (method 1) using layer-by-layer assembly of polyaniline (PANI) and oxidized single-walled carbon nanotubes ($SWCNT_{ox}$) to form a final structure of $Au/(TiO_2–W_{12}O_{41})_3/(PANI\text{-}SWCNT_{ox})_3PANI$.[335] The various structures studied by Mallouk and co-workers are important for the fabrication of nanoscale transistors, diodes, and other electronic functions.

Cepak et al. synthesized conductor/insulator/conductor and insulator/conductor/insulator composites in an alumina membrane by method 2.[337] In this case, they sequentially deposited Au and poly(2,6-dimethylphenol) (PPO) chemically on the inner walls of the membrane to form the two outer shells and then electrochemically polymerized Ppy down the middle to form the final Ppy/PPO/Au core/shell/shell structure. A similar approach with different chemistry led to the formation of an Au/polyacrylonitrile/C core/shell/shell nanostructure. Ku et al. used a similar method to synthesize Te/Au core/shell nanocables.[338] Au was deposited as a tube along the walls of the membrane by electroless deposition and Te was deposited electrochemically (slowly) to fill in the core of the nanocable. Wu et al. combined a chemical and electrochemical process to form very interesting mesostructured arrays that have somewhat of a coaxial structure.[339] They first filled the pores of an alumina template with mesostructured silica using a sol–gel dip-coating procedure involving triblock polymers containing poly(ethylene oxide) and poly(propylene oxide) to direct the interesting multilayer-stacked donuts and single- or double-helical structures observed. Subsequent electrochemical deposition of Ag, Ni, or Cu_2O into pores containing mesostructured silica also led to 1D metals with these interesting structures.

4.3. Methods Involving Electrophoretic Deposition in Hard Templates

Cao and co-workers developed a method for forming $Ni/V_2O_5{\cdot}nH_2O$ core/shell NRs by a two-step electrochemical/electrophoretic deposition method and studied their Li^+-intercalation properties.[340–342] In the first step, they formed Ni NRs by electrochemical deposition into track-etch polycarbonate membranes with diameters of 200 nm and lengths of 10 μm. Attachment to a titanium plate before dissolution of the polycarbonate in methylene chloride led to free standing Ni NRs. Subsequent electrophoretic deposition of $V_2O_5{\cdot}nH_2O$ from a sol solution prepared from V_2O_5 powder dissolved in 30% H_2O_2 led to freestanding $Ni/V_2O_5{\cdot}nH_2O$ core/shell NRs.

Limmer et al. synthesized SiO_2/Au or TiO_2/Au core/shell NRs in polycarbonate templates by first forming SiO_2 or TiO_2 NRs in the template by sol–gel electrophoresis, then removing the membrane by heat treatment and attaching Au particles to the NRs chemically by using aminopropytrimethoxysilane (APTMS), and finally reducing $HAuCl_4$ onto the attached Au particles to form the Au shell.[343]

4.4. Non-Electrochemical Deposition Methods in Hard Templates

There are a few examples of non-electrochemical deposition methods in templates to form 1D heterojunctions. The first example combines a chemical method with CVD. Cepak et al. deposited Au chemically by electroless deposition on the walls of a polyester template, released the Au tubules, and then coated them with TiS_2 by CVD to form Au/TiS_2 core/shell tubules.[337] The next two examples are vapor-phase growth methods; Liu et al. synthesized ZnO nanowires with intramolecular end-to-end p–n junctions in AAO membranes.[344] ZnO and graphite powders were used as the source material and growth occurred in a tube furnace at 4 Pa and 900 °C. In order to form the p–n junction, a boron dopant was added to the source material during the first part of the growth process and then removed for the second step of the growth. Lu et al. used an all-CVD growth process to form Si/CNT core/sheath 1D NWs in an alumina template (Figure 19).[345] The template was placed in the CVD reactor at 700 °C under a flow of H_2 and Ar. They introduced acetylene to the reaction chamber first for 1 h to form the CNTs and then switched the flow to SiH_4 for 1 h to form the Si component. Open-ended CNTs form along

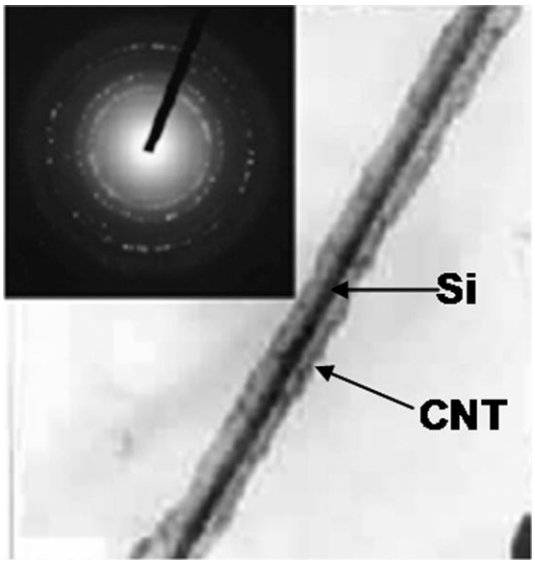

Figure 19. TEM images of a Si NW coated with a CNT (inset is a SAED pattern of the Si NW). Reprinted with permission from Ref. [345] with kind permission from Springer Science and Business Media.

the walls of the membrane in the first step and Si NWs fill in the hollow interior of the CNTs to form the core/sheath structure shown in Figure 19.[345]

Son et al. used an all-chemical process to form Fe_3O_4/silica core/shell heterostructures with potential applications in bioseparations and drug delivery.[346] First, they chemically formed silica nanotubes by surface sol–gel deposition on the walls of porous alumina, using the methods developed by Martin and Mallouk's groups. Then, they filled in the silica nanotubes with Fe_3O_4 nanoparticles by dip-coating in a solution containing $FeCl_3$ and $FeCl_2$ and immersing in a solution of NH_4OH.

5. Other Methods

5.1. Growth in Supercritical Fluids

Supercritical fluids (SF) have characteristics of both liquids and gases. For example, SFs are able to solubilize many reagents (like liquids), but they also have the characteristics of gases, such as low viscosity, high diffusivity, and no surface tension. These qualities allow for high penetration of SFs into hollow structures with very small diameters or difficult-to-reach regions, such as CNTs. Accordingly, Wai and co-workers filled MWCNTs with metals in a SF medium.[347] The presence of MWCNTs in supercritical CO_2 together with the metal-chelate precursor $M(hfa)_2{\cdot}H_2O$ (hfa = hexafluoroacetylacetonate; M = Pd, Ni, Cu) resulted in rapid filling of the hollow cores of the nanotubes. The NWs sheathed with the MWCNTs were 7–9 nm in diameter and as long as 200 nm. Fu et al. also used a SF environment for coating Ga_2O_3 nanoribbons with a Eu_2O_3 sheath.[348] The Ga_2O_3 nanoribbons reacted with europium(III) nitrate hexahydrate ethanol solution in supercritical CO_2, resulting in a Ga_2O_3 core with crystalline Eu_2O_3 multisheaths. The thickness of the shell depended on the europium precursor concentration; for a 10 wt% soution the shell was 7.0–8.0 nm, but when the concentration was halved the shell thickness decreased to 4.0–5.0 nm.

5.2. Lithography

5.2.1. Electrochemical Dip-Pen Nanolithography (E-DPN)

Liu and co-workers fabricated GaN/Ga_2O_3 NW heterojunctions by E-DPN, which involves performing local electrochemical reactions on a GaN NW underneath an atomic force microscopy (AFM) tip.[349] The NWs were typically ≈100 nm in diameter and several micrometers in length. Figure 20 A illustrates the experimental setup where a KOH-coated silicon AFM tip is placed over a surface-bound n-type GaN NW. Under a humid atmosphere, a layer of condensed water exists between the AFM tip and the surface. Applying a voltage between the tip and surface creates a localized electrochemical cell, leading to site-selective oxidation of the GaN NW under the AFM tip to form segments of Ga_2O_3. Figure 20 B shows an AFM image of the fabricated GaN/Ga_2O_3 heterojunctions created by applying a voltage of 5, 7, and 10 V to the surface. The applied voltage and the amount of current passed controls the amount of GaN oxidized.

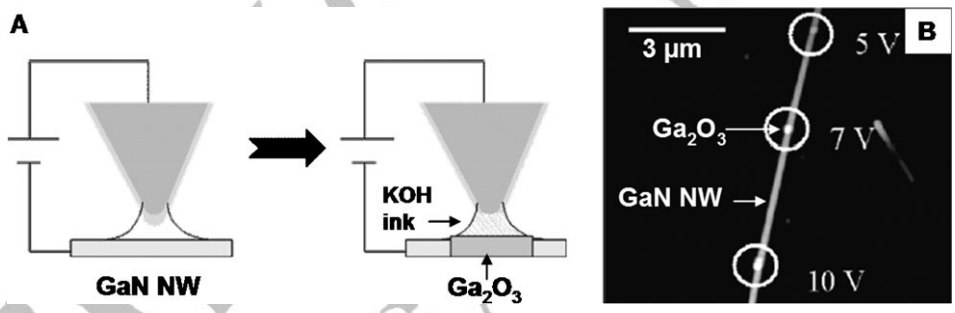

Figure 20. A) AFM-based E-DPN experimental procedure. B) GaN/Ga_2O_3 NW heterojunction fabricated using E-DPN. Reprinted with permission from Ref. [349]. Copyright 2004, American Chemical Society.

5.2.2. Electron-Beam Lithography

Dai and co-workers fabricated p–n–p junctions in an initially p-type SWCNT by selectively doping the middle part of the nanotube.[54] To fabricate the heterojunction, they coated the entire nanotube with a 340-nm-thick layer of polymethylmethacrylate (PMMA) resist and opened a window in the center part by e-beam lithography. Subse-

small NANO MICRO

quent doping of the exposed part of the nanotube with potassium formed an n-type section of the SWCNT between two p-type PMMA-coated sections. This group similarly used modulated chemical doping to fabricate intramolecular p–n junctions within a SWCNT.[55,56] In this case, they coated one half of the nanotube with a PMMA layer to retain the p-type character and then exposed the other half to potassium for n-doping. Avouris and co-workers used a similar approach to fabricate an intramolecular p–n SWCNT 1D heterojunction.[57] Similar to Dai and co-workers, they used e-beam lithography to expose one half of a PMMA-coated p-type SWCNT followed by potassium doping of the unprotected area to the form the n-type part of the nanotube. Lieber's group used e-beam lithography to fabricate CdS NWs with segments of PMMA.[350] The NWs were placed on a 200-nm-thick PMMA layer on the Si substrate, then coated again with a 200-nm-thick PMMA layer, and openings in the coating were defined lithographically.

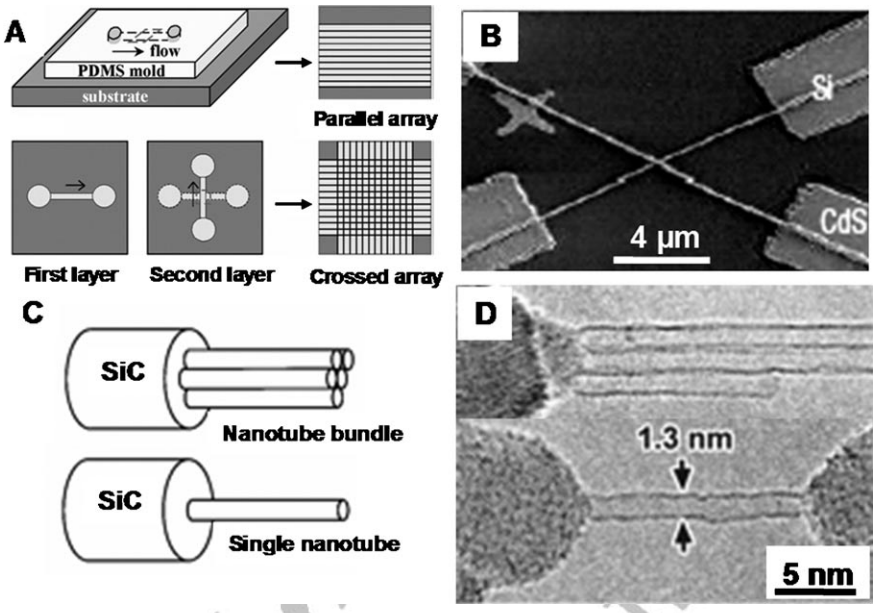

Figure 21. A) Schematic representation of the microfluidic flow system used for assembling NWs. B) SEM image of the Si/CdS NW crossed junction formed using microfluidic flow in a PDMS mold. C) Illustration of the possible SiC/CNT junctions formed using a solid–solid reaction. D) TEM image of a SiC/CNT heterojunction formed by a solid–solid reaction. A) originates from Ref. [352] and C, D) are from Ref. [358]; reprinted with permission from AAAS. B) Reproduced with permission from Ref. [40].

5.2.3. Photolithography

Wu et al. fabricated striped metal–semiconductor nanowire heterostructures containing NiSi and Si segments.[351] They synthesized the Si NWs first by the VLS method and then used photolithography to form the NiSi segments. The method involved deposition of a photoresist on the surface of the Si NWs and exposure of the as-prepared substrate to UV light through a striped mask. Polymer development, evaporation of Ni, and lift-off of the polymer led to the segmented Si/NiSi heterojunctions. The heterojunctions were 22.8 ± 3.4 nm in diameter and tens of micrometers long, with ≈1-μm-long segments.

5.3. Assembly of Heterojunctions on Surfaces

Most of the junctions discussed up to this point were created directly by synthesis or after lithography. Lieber and co-workers synthesized two different types of NWs and then used post-synthesis assembly to form heterojunctions between the two different NWs.[352] Specifically, they synthesized semiconducting NWs by vapor methods, suspended the NWs in organic solvents, and subsequently transferred the NWs to a surface by fluid-directed assembly. The two different wires were assembled sequentially in a crossed junction. The fluidic assembly involves the formation of channels for microfluidic flow by placing an appropriately patterned PDMS mold onto a flat surface. The procedure is illustrated in Figure 21 A.[352] Typical microfluidic channels were 50–500 μm wide and 6–20 mm long. A solution containing a suspension of the first NW flows through the channel and deposits with its alignment in the direction of the channel. The second NW deposits in the same manner, but after rotating the flow direction by ≈90°. They formed various crossed heterojunctions, including n-CdS/p-Si,[40] p-Si/n-Si,[353,354] and n-GaN/p-Si NWs.[39,41,355,356] Figure 21 B shows an SEM image of a crossed Si/CdS heterojunction with electrical contacts to the wires.[40] These junctions have interesting electronic and electrooptical properties. Payne and co-workers also fabricated crossed n-CdS/p-Si nanowires similarly.[357] McEuen and co-workers synthesized SWCNTs by laser ablation, dispersed the nanotubes in solution, and assembled them on a substrate from solution.[60] After rinsing, they observed random locations on the substrate where metal/semiconductor SWCNTs were arranged in crossed heterojunctions.

5.4. Solid–Solid Reactions

Zhang et al. reported the formation of heterojunctions between single-walled carbon nanotubes (SWCNTs) and carbide materials using a controlled solid–solid reaction:

C (nanotubes) + M (solid) → MC (solid)

where M can be either Si or a transition metal.[358] First, the nanotube is deposited on the solid substrate and the sample is heated in ultrahigh vacuum or an inert atmosphere. Once a sufficient temperature of 800 °C is reached, the formation of carbide occurs initially at the C/M interface. Continuous diffusion of M to the C/M interface supplies the material for conversion of SWCNTs to the carbide at a later stage of the reaction. Figure 21C illustrates SWCNTs linked to crystalline SiC rods. Figure 21D clearly shows the interface between the SiC and the SWCNTs. The first example shows a scheme of five nanotubes in a bundle connected to the carbide, along with a corresponding TEM image, and the second example shows only one SWCNT of 1.3 nm diameter forming the heterojunction with SiC. Controlling the interface area is extremely important since the number of interfacial atoms at the junction can drastically change the behavior of the heterojunction. This fabrication method is highly controlled and can be applied to single-walled as well as multi-walled carbon nanotubes.

Ag nanowires were also coated with an amorphous silica shell in another example of a solid–solid reaction.[359] A single-step reaction between the mixture of the two solids ($AgNO_3$ and $(Me_3Si)_4Si$ under low pressure) led to the formation of Ag/Si core/shell NWs. The Ag NWs were about 10–20 nm in diameter and surrounded by a 1–3-nm-thick shell.

Yong and co-workers used the solid–liquid–solid (SLS) process to synthesize SiC/SiO_x core/shell NWs.[360] NiO particles on a Si surface served as a catalyst where carbothermal reduction of WO_3 by C produced the CO/CO_2 necessary for NW growth. Under these conditions, Si supplied from bulk Si forms a Si-Ni-O alloy with the NiO catalyst particles, which results in the 1D growth of Si/SiO_x or SiC/SiO_x core/shell NWs in the absence and presence of WO_3/C, respectively. They classified the growth as SLS instead of a VLS mechanism since there were no vapor precursors. Figure 22 shows a TEM image of the SiC/SiO_x core/shell

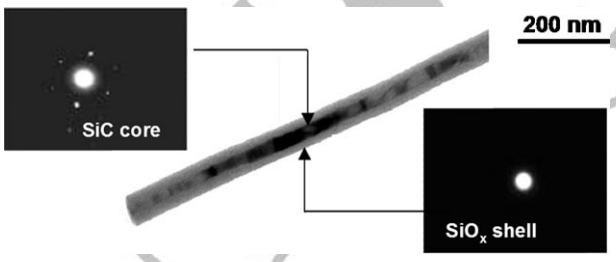

Figure 22. TEM image of a SiC/SiO_x core/shell nanowire with the corresponding SAED patterns for the crystalline core and amorphous shell. Reproduced from Ref. [360].

heterojunction.[360] The SAED pattern shows that an amorphous SiO_x shell surrounds a crystalline SiC core. The diameter of the core was typically between 20–50 nm, the shell was 40–60 nm thick, and lengths were in the micrometer range.

5.5. Electrospinning

Xia and co-workers used an electrospinning technique combined with a calcination process to fabricate V_2O_5 nanorods on TiO_2 nanofibers.[361] Electrospinning of a precursor mixture of Ti(O*i*Pr)$_4$, VO(O*i*Pr)$_3$ with acetic acid, poly(vinylpyrrolidone) (PVP), hexadecyltimethylammonuim bromide (HTAB), and 2-propanol produced smooth nanofibers of V_2O_5/TiO_2 or $V_2O_5/TiO_2/Ta_2O_5$ when TaO(O*i*Pr)$_3$ was added to the solution. Subsequent calcinations of the fibers at 475 °C over various durations led to branched heterojunctions with NR-shaped structures protruding from the surface of the nanofibers. They identified these as V_2O_5 NRs, which were single-crystalline with lengths ranging from 100–150 nm after 1 h of calcination. Figure 23 shows a SEM

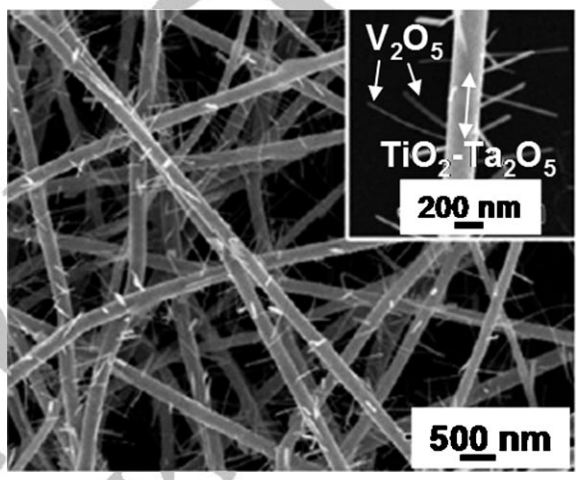

Figure 23. SEM image of V_2O_5 NRs grown on $V_2O_5/TiO_2/Ta_2O_5$ electrospun nanofibers. Reprinted with permission from Ref. [361]. Copyright 2006, American Chemical Society.

image of the heterojunctions of V_2O_5 NRs on electrospun $V_2O_5/TiO_2/Ta_2O_3$ nanofibers calcinated for 6 h. The size of the NRs depended on the nanofiber composition and calcination temperature. The NRs formed in 475 °C over a 1 h reaction time were 15 nm by 25 nm in rectangular cross section and about 100–150 nm in length.

6. Summary and Future Directions

In summary, we have described a wide range of methods for producing different types of one-dimensional nanoscale heterojunctions, including vapor, solution, template, lithographic, solid–solid, electrospinning, and assembly methods. The 1D heterojunctions are formed from combinations of various materials (metals, semiconductors, carbon, and polymers), where the properties depend on the composition, size, and structure of the nanomaterial. The type of material and type of junction is often dictated by the synthetic method. As discussed, though, most methods can be used to form a variety of segmented, core/shell, branched, or cross junctions with a variety of materials.

NANO MICRO small

The study of 1D nanoscale heterojunctions is rapidly growing because of the numerous potential applications for these multicomponent stuctures. It has already been demonstrated that many of the 1D heterojunctions synthesized/fabricated to date are useful for applications in nanoelectronics, photonics, sensing, catalysis, and separations. For example, sophisticated light-emitting diodes (LEDs),[93] and diode logic devices[362] have been realized by crossing p- and n-type nanowires or using lithography-assisted selection of distinct p- and n-type regions within a nanotube.[363] However, compared to the progress in the synthesis of homogeneous 1D nanowire and nanotube systems, the synthesis of 1D heterojunctions with well-defined interfaces has lingered far behind. Many applications require nanowires that possess built-in interfaces. For example, radial interfaces can function as p–n junctions, while longitudinal interfaces are useful as dielectric mirrors or for scattering phonons in thermoelectric nanowires. Another type of basic nanowire heterostructure envisioned in the future is the bilayer nanowire, in which two nanowires can be joined in a side-by-side configuration.

Future developments will rely on improved synthetic methods and novel fabrication processes to better control the dimensions, composition, structure, and interface of 1D heterojunctions as well as the yield and uniformity. It will also be crucial to develop better characterization methods to fully understand the nature of the junction at the atomic level. Equally important is the development of tools for studying the fundamental properties of individual or collective ensembles of heterojunction materials in order to relate these properties to their detailed structure and compare experimentally measured properties to theoretical models. It is critical for researchers to devise simple and reproducible strategies for assembling, orienting, and integrating 1D heterojunctions into functional devices. Reliable control of the interfaces in nano-heterostructures are critical in the assembly of electronic and optoelectronic devices. For example, the performance of organic photovoltaics is severely limited by poor exciton dissociation and charge transport due in part to high rates of exciton recombination and low charge mobilities in polymers. This challenge can be partially overcome through the use of blended and layered heterojunctions composed of polymer/SWNT heterostructures. Such morphologies offer multiple-exciton dissociation sites and separate charge pathways, thus limiting exciton recombination. Low-resistance ohmic contacts in nanostructures are crucial for the optimum performance of optoelectronic devices and can significantly impact the performance limitations of a device. Heterojunctions consisting of metallic single-walled carbon nanotubes have the potential to function as interconnects in hierarchical nanoscale networks with reduced specific contact resistance. Research in these areas will continue to grow in the coming years at a fast rate as researchers pursue the important goal of utilizing these fascinating building blocks for technological applications.

Acknowledgements

A.J.M. and F.P.Z. gratefully acknowledge the National Science Foundation (CHE-0518561) and the donors of the American Chemical Society Petroleum Research Fund for support of this research. We also acknowledge Dr. Robert Cohn from the Department of Electrical and Computer Engineering at the University of Louisville for allowing access to the scanning electron microscope that was used for obtaining images of the synthesized 1D nanoscale heterojunctions reported by our group.

[1] Y. Xia, P. Yang, Y. Sun, Y. Wu, B. Mayers, B. Gates, Y. Yin, F. Kim, H. Yan, *Adv. Mater.* **2003**, *15*, 353.
[2] Y. Huang, C. M. Lieber, *Pure Appl. Chem.* **2004**, *76*, 2051.
[3] J. C. Hulteen, C. R. Martin, *J. Mater. Chem.* **1997**, *7*, 1075.
[4] S. J. Hurst, E. K. Payne, L. Qin, C. A. Mirkin, *Angew. Chem.* **2006**, *118*, 2738; *Angew. Chem. Int. Ed.* **2006**, *45*, 2672.
[5] L. J. Lauhon, M. S. Gudiksen, C. M. Lieber, *Philos. Trans. R. Soc. London Ser. A* **2004**, *362*, 1247.
[6] M. Law, J. Goldberger, P. Yang, *Annu. Rev. Mater. Res.* **2004**, *34*, 83.
[7] J. G. Lu, P. Chang, Z. Fan, *Mater. Sci. Eng. R* **2006**, *52*, 49.
[8] J. Perez-Juste, I. Pastoriza-Santos, L. Liz-Marzan, P. Mulvaney, *Coord. Chem. Rev.* **2005**, *249*, 1870.
[9] C. N. R. Rao, F. L. Deepak, G. Gundiah, A. Govindaraj, *Prog. Solid State Chem.* **2003**, *31*, 5.
[10] L. Samuelson, *Mater. Res. Materials Today* **2003**, *6*, 22.
[11] L. Samuelson, C. Thelander, M. T. Bjork, M. Borgstrom, K. Deppert, K. A. Dick, A. E. Hansen, T. Martensson, N. Panev, A. I. Persson, W. Seifert, N. Skold, M. W. Larsson, L. R. Wallenberg, *Phys. E* **2004**, *25*, 313.
[12] Y. Xiong, B. T. Mayers, Y. Xia, *Chem. Commun.* **2005**, 5013.
[13] F. Wang, A. Dong, J. Sun, R. Tang, H. Yu, W. E. Buhro, *Inorg. Chem.* **2006**, *45*, 7511.
[14] M. A. El-Sayed, *Acc. Chem. Res.* **2001**, *34*, 257.
[15] N. R. Jana, L. Gearheart, C. J. Murphy, *J. Phys. Chem. B* **2001**, *105*, 4065.
[16] N. R. Jana, L. Gearheart, C. J. Murphy, *Chem. Commun.* **2001**, 617.
[17] B. Nikoobakht, M. A. El-Sayed, *J. Phys. Chem. A* **2003**, *107*, 3372.
[18] B. Nikoobakht, J. Wang, M. A. El-Sayed, *Chem. Phys. Lett.* **2002**, *366*, 17.
[19] A. Tao, F. Kim, C. Hess, J. Goldberger, R. He, Y. Sun, Y. Xia, P. Yang, *Nano Lett.* **2003**, *3*, 1229.
[20] M. B. Mohamed, V. Volkov, S. Link, M. A. El-Sayed, *Chem. Phys. Lett.* **2000**, *317*, 517.
[21] S. A. Maier, M. L. Brongersma, P. G. Kik, S. Meltzer, A. A. G. Requicha, H. A. Atwater, *Adv. Mater.* **2001**, *13*, 1501.
[22] S. A. Maier, P. G. Kik, H. A. Atwater, S. Meltzer, E. Harel, B. E. Koel, A. A. G. Requicha, *Nat. Mater.* **2003**, *2*, 229.
[23] X. Duan, C. Niu, V. Sahi, J. Chen, J. W. Parce, S. Empedocles, J. L. Goldman, *Nature* **2003**, *425*, 274.
[24] B. Polyakov, B. Daly, J. Prikulis, V. Lisauskas, B. Vengalis, M. A. Morris, J. D. Holmes, D. Erts, *Adv. Mater.* **2006**, *18*, 1812.
[25] Y. Jiang, W. J. Zhang, J. S. Jie, X. M. Meng, J. A. Zapien, S.-T. Lee, *Adv. Mater.* **2006**, *18*, 1527.
[26] F. Favier, E. C. Walter, M. P. Zach, T. Benter, R. M. Penner, *Science* **2001**, *293*, 2227.
[27] J. Li, H. T. Ng, A. Cassell, W. Fan, H. Chen, Q. Ye, J. Koehne, J. Han, M. Meyyappan, *Nano Lett.* **2003**, *3*, 597.
[28] B. J. Hinds, N. Chopra, T. Rantell, R. Andrews, V. Gavalas, L. G. Bachas, *Science* **2004**, *303*, 62.

[29] H. W. C. Postma, T. Teepen, Z. Yao, M. Grifoni, C. Dekker, *Science* **2001**, *293*, 76.
[30] R. Martel, T. Schmidt, H. R. Shea, T. Hertel, P. Avouris, *Appl. Phys. Lett.* **1998**, *73*, 2447.
[31] Y. Cui, Z. Zhong, D. Wang, W. U. Wang, C. M. Lieber, *Nano Lett.* **2003**, *3*, 149.
[32] G. Zheng, W. Lu, S. Jin, C. M. Lieber, *Adv. Mater.* **2004**, *16*, 1890.
[33] Y. Cui, Q. Wei, H.-Y. Park, C. M. Lieber, *Science* **2001**, *293*, 1289.
[34] J.-i. Hahm, C. M. Lieber, *Nano Lett.* **2004**, *4*, 51.
[35] J. Kong, H. Dai, *J. Phys. Chem. B* **2001**, *105*, 2890.
[36] J. Wang, M. S. Gudiksen, X. Duan, Y. Cui, C. M. Lieber, *Science* **2001**, *293*, 1455.
[37] X. Duan, Y. Huang, Y. Cui, J. Wang, C. M. Lieber, *Nature* **2001**, *409*, 66.
[38] A. Bogozi, O. Lam, H. He, C. Li, N. J. Tao, L. A. Nagahara, I. Amlani, R. Tsui, *J. Am. Chem. Soc.* **2001**, *123*, 4585.
[39] Y. Huang, X. Duan, Y. Cui, C. M. Lieber, *Nano Lett.* **2002**, *2*, 101.
[40] O. Hayden, R. Agarwal, C. M. Lieber, *Nat. Mater.* **2006**, *5*, 352.
[41] M. C. McAlpine, R. S. Friedman, C. M. Lieber, *Proc. IEEE* **2005**, *93*, 1357.
[42] S. G. Penn, L. He, M. J. Natan, *Curr. Opin. Chem. Biol.* **2003**, *7*, 609.
[43] A. K. Salem, P. C. Searson, K. W. Leong, *Nat. Mater.* **2003**, *2*, 668.
[44] K.-B. Lee, S. Park, C. A. Mirkin, *Angew. Chem.* **2004**, *116*, 3110; *Angew. Chem. Int. Ed.* **2004**, *43*, 3048. .
[45] F. Liu, J. Y. Lee, W. J. Zhou, *Small* **2006**, *2*, 121.
[46] S. Park, J.-H. Lim, S.-W. Chung, C. A. Mirkin, *Science* **2004**, *303*, 348.
[47] A. K. Salem, M. Chen, J. Hayden, K. W. Leong, P. C. Searson, *Nano Lett.* **2004**, *4*, 1163.
[48] J. W. Matthews, A. E. Blakeslee, *J. Cryst. Growth* **1974**, *27*, 118.
[49] L. Zhao, L. Gao, *J. Mater. Chem.* **2004**, *14*, 1001.
[50] D. G. Ramlan, S. J. May, J.-G. Zheng, J. E. Allen, B. W. Wessels, L. J. Lauhon, *Nano Lett.* **2006**, *6*, 50.
[51] J. K. N. Mbindyo, T. E. Mallouk, J. B. Mattzela, I. Kratochvilova, B. Razavi, T. N. Jackson, T. S. Mayer, *J. Am. Chem. Soc.* **2002**, *124*, 4020.
[52] J. Zhan, Y. Bando, J. Hu, D. Golberg, K. Kurashima, *Small* **2006**, *2*, 62.
[53] S. Mather, H. Shen, V. Sivakov, U. Werner, *Chem. Mater.* **2004**, *16*, 2449.
[54] J. Kong, J. Cao, H. Dai, E. Anderson, *Appl. Phys. Lett.* **2002**, *80*, 73.
[55] C. Zhou, J. Kong, E. Yenilmez, H. Dai, *Science* **2000**, *290*, 1552.
[56] A. Javey, R. Tu, D. B. Farmer, J. Guo, R. G. Gordon, H. Dai, *Nano Lett.* **2005**, *5*, 345.
[57] V. Derycke, R. Martel, J. Appenzeller, P. Avouris, *Nano Lett.* **2001**, *1*, 453.
[58] C. Yang, Z. Zhong, C. M. Lieber, *Science* **2005**, *310*, 1304.
[59] E. Tutuc, J. Appenzeller, M. C. Reuter, S. Guha, *Nano Lett.* **2006**, *6*, 2070.
[60] M. S. Fuhrer, J. Nygård, L. Shih, M. Forero, Y.-G. Yoon, M. S. C. Mazzoni, H. J. Choi, J. Ihm, S. G. Louie, A. Zettl, P. L. McEuen, *Science* **2000**, *288*, 494.
[61] Y. Wu, R. Fan, P. Yang, *Nano Lett.* **2002**, *2*, 83.
[62] N. D. Zakharov, P. Werner, G. Gerth, L. Schubert, L. Sokolov, U. Gösele, *J. Cryst. Growth* **2006**, *290*, 6.
[63] M. S. Gudiksen, L. J. Lauhon, J. Wang, D. C. Smith, C. M. Lieber, *Nature* **2002**, *415*, 617.
[64] C. Yang, C. J. Barrelet, F. Capasso, C. M. Lieber, *Nano Lett.* **2006**, *6*, 2929.
[65] M. T. Björk, C. Thelander, A. E. Hansen, L. E. Jensen, M. W. Larsson, L. R. Wallenberg, L. Samuelson, *Nano Lett.* **2004**, *4*, 1621.
[66] C. Thelander, M. T. Björk, M. W. Larsson, A. E. Hansen, L. R. Wallenberg, L. Samuelson, *Solid State Commun.* **2004**, *131*, 573.
[67] C. Thelander, H. A. Nilsson, L. E. Jensen, L. Samuelson, *Nano Lett.* **2005**, *5*, 635.
[68] M. T. Björk, B. J. Ohlsson, T. Sass, A. I. Persson, C. Thelander, M. H. Magnusson, K. Deppert, L. R. Wallenberg, L. Samuelson, *Nano Lett.* **2002**, *2*, 87.
[69] M. T. Björk, B. J. Ohlsson, T. Sass, A. I. Persson, C. Thelander, M. H. Magnusson, K. Deppert, L. R. Wallenberg, L. Samuelson, *Appl. Phys. Lett.* **2002**, *80*, 1058.
[70] A. I. Persson, M. T. Björk, S. Jeppesen, J. B. Wagner, L. R. Wallenberg, L. Samuelson, *Nano Lett.* **2006**, *6*, 403.
[71] M. T. Björk, B. J. Ohlsson, C. Thelander, A. I. Persson, K. Deppert, L. R. Wallenberg, L. Samuelson, *Appl. Phys. Lett.* **2002**, *81*, 4458.
[72] W. Seifert, M. Borgstrom, K. Deppert, K. A. Dick, J. Johansson, M. W. Larsson, T. Mårtensson, N. Skold, C. P. T. Svensson, B. A. Wacaser, L. R. Wallenberg, L. Samuelson, *J. Cryst. Growth* **2004**, *272*, 211.
[73] T. Mårtensson, C. P. T. Svensson, B. A. Wacaser, M. W. Larsson, W. Seifert, K. Deppert, A. Gustafsson, L. R. Wallenberg, L. Samuelson, *Nano Lett.* **2004**, *4*, 1987.
[74] H. Pettersson, J. Trägårdh, A. I. Persson, L. Landin, D. Hessman, L. Samuelson, *Nano Lett.* **2006**, *6*, 229.
[75] B. J. Ohlsson, M. T. Björk, A. I. Persson, C. Thelander, L. R. Wallenberg, M. H. Mangusson, K. Deppert, L. Samuelson, *Phys. E* **2002**, *13*, 1126.
[76] E. Lind, A. I. Persson, L. Samuelson, L.-E. Wernersson, *Nano Lett.* **2006**, *6*, 1842.
[77] M. A. Verheijen, G. Immink, T. de Smet, M. T. Borgstrom, E. P. A. M. Bakkers, *J. Am. Chem. Soc.* **2006**, *128*, 1353.
[78] J. Su, G. Cui, M. Gherasimova, H. Tsukamoto, J. Han, D. Ciuparu, S. Lim, L. Pfefferle, Y. He, A. V. Nurmikko, C. Broadbridge, A. Lehman, *Appl. Phys. Lett.* **2005**, *86*, 013105.
[79] Z.-H. Lan, C.-H. Liang, C.-W. Hsu, C.-T. Wu, H.-M. Lin, S. Dhara, K.-H. Chen, L.-C. Chen, C.-C. Chen, *Adv. Funct. Mater.* **2004**, *14*, 233.
[80] K. A. Dick, K. Deppert, M. W. Larsson, T. Mårtensson, W. Seifert, L. R. Wallenberg, L. Samuelson, *Nat. Mater.* **2004**, *3*, 380.
[81] S. Y. Bae, H. W. Seo, H. C. Choi, J. Park, J. Park, *J. Phys. Chem. B* **2004**, *108*, 12318.
[82] J. Hu, M. Ouyang, P. Yang, C. M. Lieber, *Nature* **1999**, *399*, 48.
[83] A. D. Lazareck, T.-F. Kuo, J. M. Xu, B. J. Taft, S. O. Kelley, S. G. Cloutier, *Appl. Phys. Lett.* **2006**, *89*, 103109.
[84] A. D. Lazareck, S. G. Cloutier, T.-F. Kuo, B. J. Taft, S. O. Kelley, J. M. Xu, *Nanotechnology* **2006**, *17*, 2661.
[85] A. J. Mieszawska, R. Jalilian, G. U. Sumanasekera, F. P. Zamborini, *J. Am. Chem. Soc.* **2005**, *127*, 10822.
[86] J. X. Wang, H. Y. Chen, Y. Gao, D. F. Liu, L. Song, Z. X. Zhang, X. W. Zhao, X. Y. Dou, S. D. Luo, W. Y. Zhou, G. Wang, S. S. Xie, *J. Cryst. Growth* **2005**, *284*, 73.
[87] H. Kohno, S. Takeda, *Appl. Phys. Lett.* **2003**, *83*, 1202.
[88] C. W. Na, S. Y. Bae, J. Park, *J. Phys. Chem. B* **2005**, *109*, 12785.
[89] J. Jie, G. Wang, X. Han, J. G. Hou, *J. Phys. Chem. B* **2004**, *108*, 17027.
[90] L. J. Lauhon, M. S. Gudiksen, D. Wang, C. M. Lieber, *Nature* **2002**, *420*, 57.
[91] J. Xiang, W. Lu, Y. Hu, Y. Wu, H. Yan, C. M. Lieber, *Nature* **2006**, *441*, 489.
[92] W. Lu, J. Xiang, B. P. Timko, Y. Wu, C. M. Lieber, *Proc. Natl. Acad. Sci. USA* **2005**, *102*, 10046.
[93] F. Qian, S. Gradečak, Y. Li, C.-Y. Wen, C. M. Lieber, *Nano Lett.* **2005**, *5*, 2287.
[94] F. Qian, Y. Li, S. Gradečak, D. Wang, C. J. Barrelet, C. M. Lieber, *Nano Lett.* **2004**, *4*, 1975.

[95] Y. Li, J. Xiang, F. Qian, S. Gradečak, Y. Wu, H. Yan, D. A. Blom, C. M. Lieber, *Nano Lett.* **2006**, *6*, 1468.
[96] A. B. Greytak, L. J. Lauhon, M. S. Gudiksen, C. M. Lieber, *Appl. Phys. Lett.* **2004**, *84*, 4176.
[97] N. Sköld, L. S. Karlsson, M. W. Larsson, M.-E. Pistol, W. Seifert, J. Trägårdh, L. Samuelson, *Nano Lett.* **2005**, *5*, 1943.
[98] N. Sköld, J. B. Wagner, G. Karlsson, T. Hernán, W. Seifert, M.-E. Pistol, L. Samuelson, *Nano Lett.* **2006**, *6*, 2743.
[99] B. Ha, H. C. Kim, S.-G. Kang, Y. H. Kim, J. Y. Lee, C. Y. Park, C. J. Lee, *Chem. Mater.* **2005**, *17*, 5398.
[100] B.-K. Kim, J.-J. Kim, J.-O. Lee, K.-j. Kong, H. J. Seo, C. J. Lee, *Phys. Rev. B* **2005**, *71*, 153313.
[101] K.-W. Chang, J.-J. Wu, *Adv. Mater.* **2005**, *17*, 241.
[102] K.-W. Chang, J.-J. Wu, *J. Phys. Chem. B* **2005**, *109*, 13572.
[103] L. Zhang, R. Tu, H. Dai, *Nano Lett.* **2006**, *6*, 2785.
[104] H.-M. Lin, Y.-L. Chen, J. Yang, Y.-C. Liu, K.-M. Yin, J.-J. Kai, F.-R. Chen, L.-C. Chen, C.-C. Chen, *Nano Lett.* **2003**, *3*, 537.
[105] Y. Wu, P. Yang, *Appl. Phys. Lett.* **2000**, *77*, 43.
[106] Y. Wu, P. Yang, *Adv. Mater.* **2001**, *13*, 520.
[107] C.-C. Chen, C.-C. Yeh, C.-H. Liang, C.-C. Lee, C.-H. Chen, M.-Y. Yu, H.-L. Liu, L. C. Chen, Y.-S. Lin, K.-J. Ma, K. H. Chen, *J. Phys. Chem. Solids* **2001**, *62*, 1577.
[108] L. W. Yin, Y. Bando, Y. C. Zhu, M. S. Li, *Appl. Phys. Lett.* **2004**, *84*, 5314.
[109] D. Zhang, Z. Liu, S. Han, C. Li, B. Lei, M. P. Stewart, J. M. Tour, C. Zhou, *Nano Lett.* **2004**, *4*, 2151.
[110] Z. Liu, D. Zhang, S. Han, C. Li, B. Lei, W. Lu, J. Fang, C. Zhou, *J. Am. Chem. Soc.* **2005**, *127*, 6.
[111] B. Lei, C. Li, D. Zhang, S. Han, C. Zhou, *J. Phys. Chem. B* **2005**, *109*, 18799.
[112] S. Han, C. Li, Z. Liu, B. Lei, D. Zhang, W. Jin, X. Liu, T. Tang, C. Zhou, *Nano Lett.* **2004**, *4*, 1241.
[113] O. Hayden, A. B. Greytak, D. C. Bell, *Adv. Mater.* **2005**, *17*, 701.
[114] H. J. Fan, M. Knez, R. Scholz, K. Nielsch, E. Pippel, D. Hesse, M. Zacharias, U. Gösele, *Nat. Mater.* **2006**, *5*, 627.
[115] F. M. Kolb, H. Hofmeister, M. Zacharias, U. Gösele, *Appl. Phys. A* **2005**, *80*, 1405.
[116] Y.-J. Hsu, S.-Y. Lu, *Chem. Commun.* **2004**, *18*, 2102.
[117] Y.-J. Hsu, S.-Y. Lu, Y.-F. Lin, *Adv. Funct. Mater.* **2005**, *15*, 1350.
[118] Y. W. Heo, M. Kaufman, K. Pruessner, K. N. Siebein, D. P. Norton, F. Ren, *Appl. Phys. A* **2005**, *80*, 263.
[119] Y. W. Heo, C. Abernathy, K. Pruessner, W. Sigmund, D. P. Norton, M. Overberg, F. Ren, M. F. Chisholm, *J. Appl. Phys.* **2004**, *96*, 3424.
[120] W. S. Jang, S. Y. Kim, J. Lee, J. Park, C. J. Park, C. J. Lee, *Chem. Phys. Lett.* **2006**, *422*, 41.
[121] X. M. Cai, Y. H. Leung, K. Y. Cheung, K. H. Tam, A. B. Djurišić, M. H. Xie, H. Y. Chen, S. Gwo, *Nanotechnology* **2006**, *17*, 2330.
[122] X.-M. Meng, J.-Q. Hu, Y. Jiang, C.-S. Lee, S.-T. Lee, *Appl. Phys. Lett.* **2003**, *83*, 2241.
[123] W.-Q. Han, A. Zettl, *Appl. Phys. Lett.* **2002**, *81*, 5051.
[124] Y. Q. Zhu, W. B. Hu, W. K. Hsu, M. Terrones, N. Grobert, J. P. Hare, H. W. Kroto, D. R. M. Walton, H. Terrones, *J. Mater. Chem.* **1999**, *9*, 3173.
[125] H.-F. Zhang, C.-M. Wang, L.-S. Wang, *Nano Lett.* **2002**, *2*, 941.
[126] D. F. Liu, S. S. Xie, X. Q. Yan, L. J. Ci, F. Shen, J. X. Wang, Z. P. Zhou, H. J. Yuan, Y. Gao, L. Song, L. F. Liu, W. Y. Zhou, G. Wang, *Chem. Phys. Lett.* **2003**, *375*, 269.
[127] G. Shen, Y. Bando, C.-C. Tang, D. Golberg, *J. Phys. Chem. B* **2006**, *110*, 7199.
[128] S. Y. Bae, H. W. Seo, H. C. Choi, D. S. Han, J. Park, *J. Phys. Chem. B* **2005**, *109*, 8496.
[129] H. W. Seo, S. Y. Bae, J. Park, H. Yang, B. Kim, *J. Phys. Chem. B* **2003**, *107*, 6739.
[130] Y. G. Wang, A. Z. Jin, Z. Zhang, *Appl. Phys. Lett.* **2002**, *81*, 4425.
[131] J. Z. Wu, S. H. Yun, A. Dibos, D.-K. Kim, M. Tidrow, *Microelectron. J.* **2003**, *34*, 463.
[132] C. Tang, Y. Bando, T. Sato, K. Kurashima, *J. Mater. Chem.* **2002**, *12*, 1910.
[133] C. Tang, Y. Bando, T. Sato, K. Kurashima, *Adv. Mater.* **2002**, *14*, 1046.
[134] X. T. Zhou, N. Wang, F. C. K. Au, H. L. Lai, H. Y. Peng, I. Bello, C. S. Lee, S. T. Lee, *Mater. Sci. Eng. A* **2000**, *286*, 119.
[135] X. T. Zhou, N. Wang, H. L. Lai, H. Y. Peng, I. Bello, N. B. Wong, C. S. Lee, S. T. Lee, *Appl. Phys. Lett.* **1999**, *74*, 3942.
[136] H.-M. Kim, T. W. Kang, K. S. Chung, *Adv. Mater.* **2003**, *15*, 567.
[137] J. Hu, Y. Bando, J. Zhan, D. Golberg, *Adv. Mater.* **2005**, *17*, 1964.
[138] G. Shen, Y. Bando, Y. Gao, D. Golberg, *J. Phys. Chem. B* **2006**, *110*, 14123.
[139] J. Zhan, Y. Bando, J. Hu, Z. Liu, L. Yin, D. Golberg, *Angew. Chem.* **2005**, *117*, 2178; *Angew. Chem. Int. Ed.* **2005**, *44*, 2140. .
[140] Z. L. Wang, R. P. Gao, J. L. Gole, J. D. Stout, *Adv. Mater.* **2000**, *12*, 1938.
[141] P. Mohan, J. Motohisa, T. Fukui, *Appl. Phys. Lett.* **2006**, *88*, 133105.
[142] P. Mohan, J. Motohisa, T. Fukui, *Appl. Phys. Lett.* **2006**, *88*, 013110.
[143] J. Motohisa, J. Takeda, M. Inari, J. Noborisaka, T. Fukui, *Physica E (Amsterdam, Neth.)* **2004**, *23*, 298.
[144] J. Noborisaka, J. Motohisa, S. Hara, T. Fukui, *Appl. Phys. Lett.* **2005**, *87*, 093109.
[145] E.-S. Jang, J. Y. Bae, J. Yoo, W. Park, D.-W. Kim, G.-C. Yi, T. Yatsui, M. Ohtsu, *Appl. Phys. Lett.* **2006**, *88*, 023102.
[146] W. Park, J. Yoo, D.-W. Kim, G.-C. Yi, M. Kim, *J. Phys. Chem. B* **2006**, *110*, 1516.
[147] S. J. An, W. Park, G.-C. Yi, Y. J. Kim, H.-B. Kang, M. Kim, *Appl. Phys. Lett.* **2004**, *84*, 3612.
[148] J. Hu, Y. Bando, Z. Liu, T. Sekiguchi, D. Golberg, J. Zhan, *J. Am. Chem. Soc.* **2003**, *125*, 11306.
[149] Y. J. Li, M. Y. Lu, C. W. Wang, K. M. Li, L. J. Chen, *Appl. Phys. Lett.* **2006**, *88*, 143102.
[150] J. Hu, Y. Bando, Z. Liu, J. Zhan, D. Golberg, T. Sekiguchi, *Angew. Chem.* **2004**, *116*, 65; *Angew. Chem. Int. Ed.* **2004**, *43*, 63.
[151] Y.-C. Zhu, Y. Bando, L.-W. Yin, *Adv. Mater.* **2004**, *16*, 331.
[152] Q. Kuang, Z.-Y. Jiang, Z.-X. Xie, S.-C. Lin, Z.-W. Lin, S.-Y. Xie, R.-B. Huang, L.-S. Zheng, *J. Am. Chem. Soc.* **2005**, *127*, 11777.
[153] L.-W. Yin, Y. Bando, Y.-C. Zhu, D. Golberg, M.-S. Li, *Adv. Mater.* **2004**, *16*, 929.
[154] Y.-C. Zhu, Y. Bando, D.-F. Xue, F.-F. Xu, D. Golberg, *J. Am. Chem. Soc.* **2003**, *125*, 14226.
[155] Y. Zhu, Y. Bando, L. Yin, D. Golberg, *Nano Lett.* **2006**, *6*, 2982.
[156] Y. B. Li, Y. Bando, D. Golberg, *Chem. Phys. Lett.* **2003**, *375*, 102.
[157] Y.-h. Wong, Q. Li, *J. Mater. Chem.* **2004**, *14*, 1413.
[158] L. Shi, Y. M. Xu, Q. Li, *Nanotechnology* **2005**, *16*, 2100.
[159] C.-L. Hsu, Y.-R. Lin, S.-J. Chang, T.-S. Lin, S.-Y. Tsai, I.-C. Chen, *Chem. Phys. Lett.* **2005**, *411*, 221.
[160] B. Geng, G. Meng, L. Zhang, G. Wang, X. Peng, *Chem. Commun.* **2003**, 2572.
[161] J. Hu, Y. Bando, Z. Liu, *Adv. Mater.* **2003**, *15*, 1000.
[162] Y. B. Li, Y. Bando, D. Golberg, Y. Uemura, *Appl. Phys. Lett.* **2003**, *83*, 3999.
[163] B. K. Teo, C. P. Li, X. H. Sun, N. B. Wong, S. T. Lee, *Inorg. Chem.* **2003**, *42*, 6723.
[164] C. Wang, J. Wang, Q. Li, G.-C. Yi, *Adv. Funct. Mater.* **2005**, *15*, 1471.
[165] Q. Li, C. Wang, *J. Am. Chem. Soc.* **2003**, *125*, 9892.
[166] C. Wu, W. Qin, G. Qin, D. Zhao, J. Zhang, W. Xu, H. Lin, *Chem. Phys. Lett.* **2003**, *378*, 368.

[167] Q. Li, Y. Jiao, *Appl. Phys. Lett.* **2005**, *87*, 261905.
[168] C.-H. Huang, Y.-H. Chang, C.-Y. Lee, H.-T. Chiu, *Langmuir* **2006**, *22*, 10.
[169] X. Y. Kong, Y. Ding, Z. L. Wang, *J. Phys. Chem. B* **2004**, *108*, 570.
[170] Y. Ding, X. Y. Kong, Z. L. Wang, *J. Appl. Phys.* **2004**, *95*, 306.
[171] X. Feng, X. Yuan, T. Sekiguchi, W. Lin, J. Kang, *J. Phys. Chem. B* **2005**, *109*, 15786.
[172] Z. Jiang, T. Xie, B. Y. Geng, G. Z. Wang, G. S. Wu, X. Y. Yuan, G. W. Meng, L. D. Zhang, *Inorg. Chem. Commun.* **2004**, *7*, 812.
[173] J. Li, D. Zhao, X. Meng, Z. Zhang, J. Zhang, D. Shen, Y. Lu, X. Fan, *J. Phys. Chem. B* **2006**, *110*, 14685.
[174] Z.-Y. Jiang, Z.-X. Xie, X.-H. Zhang, R.-B. Huang, L.-S. Zheng, *Chem. Phys. Lett.* **2003**, *378*, 313.
[175] W.-Q. Han, C. W. Chang, A. Zettl, *Nano Lett.* **2004**, *4*, 1355.
[176] S. Yang, X. Wen, W. Zhang, S. Yang, *J. Electrochem. Soc.*, **2005**, *152*, G220.
[177] G. Shen, D. Chen, C. J. Lee, *J. Phys. Chem. B* **2006**, *110*, 15689.
[178] Y. Li, Y. Bando, D. Golberg, *Adv. Mater.* **2004**, *16*, 93.
[179] Y. Chai, X. L. Zhou, P. J. Li, W. J. Zhang, Q. F. Zhang, J. L. Wu, *Nanotechnology* **2005**, *16*, 2134.
[180] Y. Chai, Q. F. Zhang, J. L. Wu, *Carbon* **2006**, *44*, 687.
[181] P. Hu, K. Xiao, Y. Liu, G. Yu, X. Wang, L. Fu, G. Cui, D. Zhu, *Appl. Phys. Lett.* **2004**, *84*, 4932.
[182] X. Ma, E. G. Wang, *Appl. Phys. Lett.* **2001**, *78*, 978.
[183] A. M. Cassell, J. Li, R. M. D. Stevens, J. E. Koehne, L. Delzeit, H. T. Ng, Q. Ye, J. Han, M. Meyyappan, *Appl. Phys. Lett.* **2004**, *85*, 2364.
[184] J. Liu, X. Li, L. Dai, *Adv. Mater.* **2006**, *18*, 1740.
[185] L. H. Chan, K. H. Hong, S. H. Lai, X. W. Liu, H. C. Shih, *Thin Solid Films* **2003**, *423*, 27.
[186] Z. Sun, Z. Liu, Y. Wang, B. Han, J. Du, J. Zhang, *J. Mater. Chem.* **2005**, *15*, 4497.
[187] W.-Q. Han, L. Wu, Y. Zhu, M. Strongin, *Nano Lett.* **2005**, *5*, 1419.
[188] J. Hu, Z. Wang, W. Zhang, Z. Xu, Y. Wu, Z. Zhu, X. Duan, *Carbon* **2006**, *44*, 1581.
[189] Y. Zhang, H. Dai, *Appl. Phys. Lett.* **2000**, *77*, 3015.
[190] J. Cao, T. Matsoukas, *IEEE Trans. Plasma Sci.* **2005**, *33*, 829.
[191] L. Sun, J. Gong, D. Zhu, Z. Zhu, S. He, *Adv. Mater.* **2004**, *16*, 1849.
[192] L.-W. Yin, Y. Bando, Y. C. Zhu, M.-S. Li, C.-C. Tang, D. Golberg, *Adv. Mater.* **2005**, *17*, 213.
[193] X. Chen, D. C. Cantrell, K. Kohlhaas, S. Stankovich, J. A. Ibers, M. Jaroniec, H. Gao, X. Li, R. S. Ruoff, *Chem. Mater.* **2006**, *18*, 753.
[194] Y. Li, P. S. Dorozhkin, Y. Bando, D. Golberg, *Adv. Mater.* **2005**, *17*, 545.
[195] X.-H. Sun, C.-P. Li, W.-K. Wong, N.-B. Wong, C.-S. Lee, S.-T. Lee, B.-K. Teo, *J. Am. Chem. Soc.* **2002**, *124*, 14464.
[196] Z. L. Wang, Z. R. Dai, R. P. Gao, Z. G. Bai, J. L. Gole, *Appl. Phys. Lett.* **2000**, *77*, 3349.
[197] D. J. Milliron, S. M. Hughes, Y. Cui, L. Manna, J. Li, L.-W. Wang, A. P. Alivisatos, *Nature* **2004**, *430*, 190.
[198] P. Peng, D. J. Milliron, S. M. Hughes, J. C. Johnson, A. P. Alivisatos, R. J. Saykally, *Nano Lett.* **2005**, *5*, 1809.
[199] H. G. Yang, H. C. Zeng, *J. Am. Chem. Soc.* **2005**, *127*, 270.
[200] Z. Wei, A. J. Mieszawska, F. P. Zamborini, *Langmuir* **2004**, *20*, 4322.
[201] Z. Wei, F. P. Zamborini, *Langmuir* **2004**, *20*, 11301.
[202] A. J. Mieszawska, F. P. Zamborini, *Chem. Mater.* **2005**, *17*, 3415.
[203] A. J. Mieszawska, G. W. Slawinski, F. P. Zamborini, *J. Am. Chem. Soc.* **2006**, *128*, 5622.
[204] N. Taub, O. Krichevski, G. Markovich, *J. Phys. Chem. B* **2003**, *107*, 11579.
[205] H. Liao, J. H. Hafner, *J. Phys. Chem. B* **2004**, *108*, 19276.
[206] P. L. Gai, M. A. Harmer, *Nano Lett.* **2002**, *2*, 771.
[207] J. Gao, C. M. Bender, C. J. Murphy, *Langmuir* **2003**, *19*, 9065.
[208] C. J. Johnson, E. Dujardin, S. A. Davis, C. J. Murphy, S. Mann, *J. Mater. Chem.* **2002**, *12*, 1765.
[209] N. R. Jana, L. Gearheart, S. O. Obare, C. J. Murphy, *Langmuir* **2002**, *18*, 922.
[210] B. Li, Y. Xie, Y. Xu, C. Wu, Q. Zhao, *J. Phys. Chem. B* **2006**, *110*, 14186.
[211] J. Du, J. Zhang, Z. Liu, B. Han, T. Jiang, Y. Huang, *Langmuir* **2006**, *22*, 1307.
[212] L. Y. Zhao, K. R. Eldridge, K. Sukhija, H. Jalili, N. F. Heinig, K. T. Leung, *Appl. Phys. Lett.* **2006**, *88*, 033111.
[213] D. V. Talapin, R. Koeppe, S. Gotzinger, A. Kornowski, J. M. Lupton, A. L. Rogach, O. Benson, J. Feldman, H. Weller, *Nano Lett.* **2003**, *3*, 1677.
[214] D. V. Talapin, E. V. Shevchenko, C. B. Murray, A. Kornowski, S. Foster, H. Weller, *J. Am. Chem. Soc.* **2004**, *126*, 12984.
[215] L. Manna, E. C. Scher, L.-S. Li, A. P. Alivisatos, *J. Am. Chem. Soc.* **2002**, *124*, 7136.
[216] A. Creti, M. Anni, M. Z. Rossi, G. Lanzani, G. Leo, F. D. Sala, L. Manna, M. Lomascolo, *Phys. Rev. B* **2005**, *72*, 125346.
[217] J. McBride, J. Treadway, L. C. Feldman, S. J. Pennycook, S. J. Rosenthal, *Nano Lett.* **2006**, *6*, 1496.
[218] S. Tavenner-Kruger, Y.-S. Park, M. Lonergan, U. Woggon, H. Wang, *Nano Lett.* **2006**, *6*, 2154.
[219] T. Mokari, U. Banin, *Chem. Mater.* **2003**, *15*, 3955.
[220] J. M. Tsay, S. Doose, F. Pinaud, S. Weiss, *J. Phys. Chem. B* **2005**, *109*, 1669.
[221] Y. Xie, P. Yan, J. Lu, Y. Qian, S. Zhang, *Chem. Commun.* **1999**, *19*, 1969.
[222] S. E. Hunyadi, C. J. Murphy, *J. Phys. Chem. B* **2006**, *110*, 7226.
[223] Z. Yang, Y.-W. Lin, W.-L. Tseng, H.-T. Chang, *J. Mater. Chem.* **2005**, *15*, 2450.
[224] Z. Yang, H.-T. Chang, *Nanotechnology* **2006**, *17*, 2304.
[225] C.-C. Huang, Z. Yang, H.-T. Chang, *Langmuir* **2004**, *20*, 6089.
[226] M. Liu, P. Guyot-Sionnest, *J. Phys. Chem. B* **2004**, *108*, 5882.
[227] J. H. Song, F. Kim, D. Kim, P. Yang, *Chem. Eur. J.* **2005**, *11*, 910.
[228] Y. Sun, Y. Xia, *Adv. Mater.* **2004**, *16*, 264.
[229] M. Tsuji, N. Miyamae, K. Matsumoto, S. Hikino, T. Tsuji, *Chem. Lett.* **2005**, *34*, 1518.
[230] C. S. Ah, S. D. Hong, D.-J. Jang, *J. Phys. Chem. B* **2001**, *105*, 7871.
[231] X. Wen, S. Yang, *Nano Lett.* **2002**, *2*, 451.
[232] S. F. Wang, F. Gu, Z. S. Yang, M. K. Lu, G. J. Zhou, W. G. Zou, *J. Cryst. Growth* **2005**, *282*, 79.
[233] J. Cao, J.-Z. Sun, H.-Y. Li, J. Hong, M. Wang, *J. Mater. Chem.* **2004**, *14*, 1203.
[234] J. Cao, J.-Z. Sun, J. Hong, H.-Y. Li, H.-Z. Chen, M. Wang, *Adv. Mater.* **2004**, *16*, 84.
[235] R. Colorado, A. R. Barron, *Chem. Mater.* **2004**, *16*, 2691.
[236] W.-Q. Han, A. Zettl, *Nano Lett.* **2003**, *3*, 681.
[237] H. C. Choi, M. Shim, S. Bangsaruntip, H. Dai, *J. Am. Chem. Soc.* **2002**, *124*, 9058.
[238] U. Woggon, O. Schops, M. V. Artemyev, C. Arens, N. Rousseau, D. Schikora, K. Lischka, D. Litvinov, D. Gerthsen, *Nano Lett.* **2005**, *5*, 483.
[239] C. Arens, N. Rousseau, D. Schikora, K. Lischka, O. Schops, E. Herz, U. Woggon, D. Litvinov, D. Gerthsen, M. V. Artemyev, *Phys. Status Solidi C* **2006**, *3*, 861.
[240] N. S. Gajbhiye, S. Bhattacharyya, *Nanotechnology* **2005**, *16*, 2012.
[241] K. Huang, Y. Zhang, Y. Long, J. Yuan, D. Han, Z. Wang, L. Niu, Z. Chen, *Chem. Eur. J.* **2006**, *12*, 5314.
[242] A. Chen, K. Kamata, M. Nakagawa, T. Iyoda, H. Wang, X. Li, *J. Phys. Chem. B* **2005**, *109*, 18283.

[243] H.-S. Qian, L.-B. Luo, J.-Y. Gong, S.-H. Yu, T.-W. Li, L.-f. Fei, *Cryst. Growth Des.* **2006**, *6*, 607.
[244] M. J. Mulvihill, B. L. Rupert, R. He, A. Hochbaum, J. Arnold, P. Yang, *J. Am. Chem. Soc.* **2005**, *127*, 16040.
[245] Y.-J. Kim, J. H. Song, *Bull. Korean Chem. Soc.* **2005**, *26*, 227.
[246] K. S. Mayya, D. I. Gittins, A. M. Dibaj, F. Caruso, *Nano Lett.* **2001**, *1*, 727.
[247] H. Kong, W. Li, C. Gao, D. Yan, Y. Jin, D. R. M. Walton, H. W. Kroto, *Macromolecules* **2004**, *37*, 6683.
[248] Y. Yu, B. Che, Z. Si, L. Li, W. Chen, G. Xue, *Synth. Met.* **2005**, *150*, 271.
[249] Y. Liu, J. Tang, J. H. Xin, *Chem. Commun.* **2004**, *24*, 2828.
[250] E. D. Sone, E. R. Zubarev, S. I. Stupp, *Angew. Chem.* **2002**, *114*, 1781; *Angew. Chem. Int. Ed.* **2002**, *41*, 1705. .
[251] O. Carny, D. E. Shalev, E. Gazit, *Nano Lett.* **2006**, *6*, 1594.
[252] X.-f. Qiu, J.-J. Zhu, L. Pu, Y. Shi, Y.-D. Zheng, H.-Y. Chen, *Inorg. Chem. Commun.* **2004**, *7*, 319.
[253] T. Gao, T. Wang, *Chem. Commun.* **2004**, *22*, 2558.
[254] T. Gao, Q. Li, T. Wang, *Chem. Mater.* **2005**, *17*, 887.
[255] X. Qiu, C. Burda, R. Fu, L. Pu, H. Chen, J. Zhu, *J. Am. Chem. Soc.* **2004**, *126*, 16276.
[256] D.-F. Zhang, L.-D. Sun, C.-J. Jia, Z.-G. Yan, L.-P. You, C.-H. Yan, *J. Am. Chem. Soc.* **2005**, *127*, 13492.
[257] J. Zhang, Z. Liu, B. Han, T. Jiang, W. Wu, J. Chen, Z. Li, D. Liu, *J. Phys. Chem. B* **2004**, *108*, 2200.
[258] X. Jiang, B. Mayers, Y. Wang, B. Cattle, Y. Xia, *Chem. Phys. Lett.* **2004**, *385*, 472.
[259] X. Jiang, B. Mayers, T. Herricks, Y. Xia, *Adv. Mater.* **2003**, *15*, 1740.
[260] K. Peng, Z. Huang, J. Zhu, *Adv. Mater.* **2004**, *16*, 73.
[261] Y. Fang, X. Wen, S. Yang, *Angew. Chem.* **2006**, *118*, 4771; *Angew. Chem. Int. Ed.* **2006**, *45*, 4655. .
[262] C. J. Brumlik, C. R. Martin, *J. Am. Chem. Soc.* **1991**, *113*, 3174.
[263] C. R. Martin, *Chem. Mater.* **1996**, *8*, 1739.
[264] L. Piraux, J. M. George, J. F. Despres, C. Leroy, E. Ferain, R. Legras, K. Ounadjela, A. Fert, *Appl. Phys. Lett.* **1994**, *65*, 2484.
[265] L. Piraux, S. Dubois, A. Fert, *J. Magn. Magn. Mater.* **1996**, *159*, L287.
[266] L. Piraux, S. Dubois, A. Fert, L. Belliard, *Eur. Phys. J. B* **1998**, *4*, 413.
[267] S. Dubois, C. Marchal, J. M. Beuken, L. Piraux, J. L. Duvail, A. Fert, J. M. George, J. L. Maurice, *Appl. Phys. Lett.* **1997**, *70*, 396.
[268] K. Liu, K. Nagodawithana, P. C. Searson, C. L. Chien, *Phys. Rev. B* **1995**, *51*, 7381.
[269] M. Chen, P. C. Searson, C. L. Chien, *J. Appl. Phys.* **2003**, *93*, 8253.
[270] M. Chen, L. Sun, J. E. Bonevich, D. H. Reich, C. L. Chien, P. C. Searson, *Appl. Phys. Lett.* **2003**, *82*, 3310.
[271] M. Chen, C.-L. Chien, P. C. Searson, *Chem. Mater.* **2006**, *18*, 1595.
[272] M. Tanase, D. M. Silevitch, A. Hultgren, L. A. Bauer, P. C. Searson, G. J. Meyer, D. H. Reich, *J. Appl. Phys.* **2002**, *91*, 8549.
[273] W. Schwarzacher, K. Attenborough, A. Michel, G. Nabiyouni, J. P. Meier, *J. Magn. Magn. Mater.* **1997**, *165*, 23.
[274] G. P. Heydon, S. R. Hoon, A. N. Farley, S. L. Tomlinson, M. S. Valera, K. Attenborough, W. Schwarzacher, *J. Phys. D* **1997**, *30*, 1083.
[275] P. R. Evans, G. Yi, W. Schwarzacher, *Appl. Phys. Lett.* **2000**, *76*, 481.
[276] A. Robinson, W. Schwarzacher, *J. Appl. Phys.* **2003**, *93*, 7250.
[277] Y.-G. Guo, L.-J. Wan, J.-R. Gong, C.-L. Bai, *Phys. Chem. Chem. Phys.* **2002**, *4*, 3422.
[278] Y.-G. Guo, L.-J. Wan, C.-F. Zhu, D.-L. Yang, D.-M. Chen, C.-L. Bai, *Chem. Mater.* **2003**, *15*, 664.
[279] H.-P. Liang, Y.-G. Guo, J.-S. Hu, C.-F. Zhu, L.-J. Wan, C.-L. Bai, *Inorg. Chem.* **2005**, *44*, 3013.
[280] L. Wang, K. Yu-Zhang, A. Metrot, P. Bonhomme, M. Troyon, *Thin Solid Films* **1996**, *188*, 86.
[281] S. Valizadeh, L. Hultman, J.-M. George, P. Leisner, *Adv. Funct. Mater.* **2002**, *12*, 766.
[282] T. Ohgai, X. Hoffer, L. Gravier, J.-E. Wegrowe, J.-P. Ansermet, *Nanotechnology* **2003**, *14*, 978.
[283] Y.-K. Su, D.-H. Qin, H.-L. Zhang, H. Li, H.-L. Li, *Chem. Phys. Lett.* **2004**, *388*, 406.
[284] A. K. Bentley, J. S. Trethewey, A. B. Ellis, W. C. Crone, *Nano Lett.* **2004**, *4*, 487.
[285] F. H. Xue, G. T. Fei, B. Wu, P. Cui, L. D. Zhang, *J. Am. Chem. Soc.* **2005**, *127*, 15348.
[286] A. Blondel, B. Doudin, J.-P. Ansermet, *J. Magn. Magn. Mater.* **1997**, *165*, 34.
[287] B. R. Martin, D. J. Dermody, B. D. Reiss, M. Fang, L. A. Lyon, M. J. Natan, T. E. Mallouk, *Adv. Mater.* **1999**, *11*, 1021.
[288] S. R. Nicewarner-Peña, R. G. Freeman, B. D. Reiss, L. He, D. J. Peña, I. D. Walton, R. Cromer, C. D. Keating, M. J. Natan, *Science* **2001**, *294*, 137.
[289] B. D. Reiss, R. G. Freeman, I. D. Walton, S. M. Norton, P. C. Smith, W. G. Stonas, C. D. Keating, M. J. Natan, *J. Electroanal. Chem.* **2002**, *522*, 95.
[290] I. D. Walton, S. M. Norton, A. Balasingham, L. He, D. F. Oviso, D. Gupta, P. A. Raju, M. J. Natan, R. G. Freeman, *Anal. Chem.* **2002**, *74*, 2240.
[291] C. D. Keating, M. J. Natan, *Adv. Mater.* **2003**, *15*, 451.
[292] S. R. Nicewarner-Peña, A. J. Carado, K. E. Shale, C. D. Keating, *J. Phys. Chem. B* **2003**, *107*, 7360.
[293] R. L. Stoermer, J. A. Sioss, C. D. Keating, *Chem. Mater.* **2005**, *17*, 4356.
[294] R. L. Stoermer, C. D. Keating, *J. Am. Chem. Soc.* **2006**, *128*, 13243.
[295] D. J. Peña, K. N. Mbindyo, A. J. Carado, T. E. Mallouk, C. D. Keating, B. Razavi, T. S. Mayer, *J. Phys. Chem. B* **2002**, *106*, 7458.
[296] J.-G. Wang, M.-L. Tian, T. E. Mallouk, M. H. W. Chan, *Nano Lett.* **2004**, *4*, 1313.
[297] W. F. Paxton, K. C. Kistler, C. C. Olmeda, A. Sen, S. K. St. Angelo, Y. Cao, T. E. Mallouk, P. E. Lammert, V. H. Crespi, *J. Am. Chem. Soc.* **2004**, *126*, 13424.
[298] T. R. Kline, W. F. Paxton, T. E. Mallouk, A. Sen, *Angew. Chem.* **2005**, *117*, 754; *Angew. Chem. Int. Ed.* **2005**, *44*, 744. .
[299] S. Fournier-Bidoz, A. C. Arsenault, I. Manners, G. A. Ozin, *Chem. Commun.* **2005**, *4*, 441.
[300] J. C. Love, A. R. Urbach, M. G. Prentiss, G. M. Whitesides, *J. Am. Chem. Soc.* **2003**, *125*, 12696.
[301] A. R. Urbach, J. C. Love, M. G. Prentiss, G. M. Whitesides, *J. Am. Chem. Soc.* **2003**, *125*, 12704.
[302] L. A. Bauer, D. H. Reich, G. J. Meyer, *Langmuir* **2003**, *19*, 7043.
[303] N. S. Birenbaum, B. T. Lai, C. S. Chen, D. H. Reich, G. J. Meyer, *Langmuir* **2003**, *19*, 9580.
[304] D. H. Reich, M. Tanase, A. Hultgren, L. A. Bauer, C. S. Chen, G. J. Meyer, *J. Appl. Phys.* **2003**, *93*, 7275.
[305] C. M. Hangarter, N. V. Myung, *Chem. Mater.* **2005**, *17*, 1320.
[306] D. S. Xue, H. G. Shi, M. S. Si, *J. Phys. Condens. Matter* **2004**, *16*, 8775.
[307] F. Liu, J. Y. Lee, W. Zhou, *J. Phys. Chem. B* **2004**, *108*, 17959.
[308] F. Liu, J. Y. Lee, W. Zhou, *Adv. Funct. Mater.* **2005**, *15*, 1459.
[309] A. K. Salem, J. Chao, K. W. Leong, P. C. Searson, *Adv. Mater.* **2004**, *16*, 268.
[310] A. K. Salem, C. F. Hung, T. W. Kim, T. C. Wu, P. C. Searson, K. W. Leong, *Nanotechnology* **2005**, *16*, 484.
[311] M. Chen, P. C. Searson, *Adv. Mater.* **2005**, *17*, 2765.
[312] M. Chen, L. Guo, R. Ravi, P. C. Searson, *J. Phys. Chem. B* **2006**, *110*, 211.
[313] B.-K. Oh, S. Park, J. E. Millstone, S. W. Lee, K.-B. Lee, C. A. Mirkin, *J. Am. Chem. Soc.* **2006**, *128*, 11825.

These are not the final page numbers! ↗↗

[314] S. Park, S.-W. Chung, C. A. Mirkin, *J. Am. Chem. Soc.* **2004**, *126*, 11772.
[315] M. Lahav, E. A. Weiss, Q. Xu, G. M. Whitesides, *Nano Lett.* **2006**, *6*, 2166.
[316] Y. Xi, J. Zhou, H. Guo, C. Cai, Z. Lin, *Chem. Phys. Lett.* **2005**, *412*, 60.
[317] J. Luo, Z. Huang, Y. Zhao, L. Zhang, J. Zhu, *Adv. Mater.* **2004**, *16*, 1512.
[318] J. Luo, Y. Xing, J. Zhu, D. Yu, Y. Zhao, L. Zhang, H. Fang, Z. Huang, J. Xu, *Adv. Funct. Mater.* **2006**, *16*, 1081.
[319] J. Luo, J. Zhu, *Nanotechnology* **2006**, *17*, S262.
[320] J. Luo, L. Zhang, Y. Zhang, J. Zhu, *Adv. Mater.* **2002**, *14*, 1413.
[321] J. Luo, L. Zhang, J. Zhu, *Adv. Mater.* **2003**, *15*, 579.
[322] N. I. Kovtyukhova, B. R. Martin, J. K. N. Mbindyo, T. E. Mallouk, M. Cabassi, T. S. Mayer, *Mater. Sci. Eng. C* **2002**, *19*, 255.
[323] N. I. Kovtyukhova, B. R. Martin, J. K. N. Mbindyo, P. A. Smith, B. Razavi, T. S. Mayer, T. E. Mallouk, *J. Phys. Chem. B* **2001**, *105*, 8762.
[324] J. J. Mock, S. J. Oldenburg, D. R. Smith, D. A. Schultz, S. Schultz, *Nano Lett.* **2002**, *2*, 465.
[325] J. S. Tresback, A. L. Vasiliev, N. P. Padture, *J. Mater. Res.* **2005**, *20*, 2613.
[326] A. Sokolov, I. F. Sabirianov, E. Y. Tsymbal, B. Doudin, X. Z. Li, J. Redepenning, *J. Appl. Phys.* **2003**, *93*, 7029.
[327] F. Li, J. B. Wiley, *J. Mater. Chem.* **2004**, *14*, 1387.
[328] W. Lee, R. Scholz, K. Nielsch, U. Gösele, *Angew. Chem.* **2005**, *117*, 6055; *Angew. Chem. Int. Ed.* **2005**, *44*, 6050.
[329] A. Kolmakov, Y. Zhang, M. Moskovits, *Nano Lett.* **2003**, *3*, 1125.
[330] K. Chatterjee, S. Basu, D. Chakravorty, *J. Mater. Res.* **2006**, *21*, 34.
[331] J.-G. Wang, M.-L. Tian, N. Kumar, T. E. Mallouk, *Nano Lett.* **2005**, *5*, 1247.
[332] L. Qin, S. Park, L. Huang, C. A. Mirkin, *Science* **2005**, *309*, 113.
[333] J. A. Sioss, C. D. Keating, *Nano Lett.* **2005**, *5*, 1779.
[334] N. I. Kovtyukhova, B. K. Kelley, T. E. Mallouk, *J. Am. Chem. Soc.* **2004**, *126*, 12738.
[335] N. I. Kovtyukhova, T. E. Mallouk, *Adv. Mater.* **2005**, *17*, 187.
[336] N. I. Kovtyukhova, T. E. Mallouk, T. S. Mayer, *Adv. Mater.* **2003**, *15*, 780.
[337] V. M. Cepak, J. C. Hulteen, G. Che, K. B. Jirage, B. B. Lakshmi, E. R. Fisher, C. R. Martin, *Chem. Mater.* **1997**, *9*, 1065.
[338] J.-R. Ku, R. Vidu, R. Talroze, P. Stroeve, *J. Am. Chem. Soc.* **2004**, *126*, 15022.
[339] Y. Wu, T. Livneh, Y. X. Zhang, G. Cheng, J. Wang, J. Tang, M. Moskovits, G. D. Stucky, *Nano Lett.* **2004**, *4*, 2337.
[340] Y. Wang, K. Takahashi, K. Lee, G. Cao, *Adv. Funct. Mater.* **2006**, *16*, 1133.
[341] K. Takahashi, Y. Wang, G. Cao, *J. Phys. Chem. B* **2005**, *109*, 48.
[342] G. Cao, *J. Phys. Chem. B* **2004**, *108*, 19921.
[343] S. J. Limmer, T. P. Chou, G. Cao, *J. Phys. Chem. B* **2003**, *107*, 13313.
[344] C. H. Liu, W. C. Yiu, F. C. K. Au, J. X. Ding, C. S. Lee, S. T. Lee, *Appl. Phys. Lett.* **2003**, *83*, 3168.
[345] M. Lu, M. K. Li, H. L. Li, X.-Y. Guo, *J. Mater. Sci. Lett.* **2003**, *22*, 1107.
[346] S. J. Son, J. Reichel, B. He, M. Schuchman, S. B. Lee, *J. Am. Chem. Soc.* **2005**, *127*, 7316.
[347] X.-R. Ye, Y. Lin, C. Wang, C. M. Wai, *Adv. Mater.* **2003**, *15*, 316.
[348] L. Fu, Z. Liu, Y. Liu, B. Han, J. Wang, P. Hu, L. Cao, D. Zhu, *J. Phys. Chem. B* **2004**, *108*, 13074.
[349] B. W. Maynor, J. Li, C. Lu, J. Liu, *J. Am. Chem. Soc.* **2004**, *126*, 6409.
[350] C. J. Barrelet, J. Bao, M. Lončar, H.-G. Park, F. Capasso, C. M. Lieber, *Nano Lett.* **2006**, *6*, 11.
[351] Y. Wu, J. Xiang, C. Yang, W. Lu, C. M. Lieber, *Nature* **2004**, *430*, 61.
[352] Y. Huang, X. Duan, Q. Wei, C. M. Lieber, *Science* **2001**, *291*, 630.
[353] F. Patolsky, B. P. Timko, G. Yu, J. Fang, A. B. Greytak, G. Zheng, C. M. Lieber, *Science* **2006**, *313*, 1100.
[354] Y. Cui, C. M. Lieber, *Science* **2001**, *291*, 851.
[355] M. C. McAlpine, R. S. Friedman, S. Jin, K. Lin, W. U. Wang, C. M. Lieber, *Nano Lett.* **2003**, *3*, 1531.
[356] Y. Huang, X. Duan, Y. Cui, L. J. Lauhon, K.-H. Kim, C. M. Lieber, *Science* **2001**, *294*, 1313.
[357] O. Hayden, C. K. Payne, *Angew. Chem.* **2005**, *117*, 1419; *Angew. Chem. Int. Ed.* **2005**, *44*, 1395. .
[358] Y. Zhang, T. Ichihashi, E. Landree, F. Nihey, S. Iijima, *Science* **1999**, *285*, 1719.
[359] C.-H. Hsia, M.-Y. Yen, C.-C. Lin, H.-T. Chiu, C.-Y. Lee, *J. Am. Chem. Soc.* **2003**, *125*, 9940.
[360] B. Park, Y. Ryu, K. Yong, *Surf. Rev. Lett.* **2004**, *11*, 373.
[361] R. Ostermann, D. Li, Y. Yin, J. T. McCann, Y. Xia, *Nano Lett.* **2006**, *6*, 1297.
[362] Y. Huang, X. Duan, Y. Cui, L. J. Lauhon, K.-H. Kim, C. M. Lieber, *Science* **2001**, *294*, 1313.
[363] P. Avouris, J. Chen, *Mater. Today* **2006**, *9*, 46.

Received: December 22, 2006
Published online on ■■ ■■, 2007

Up the junction: Nanoscale heterojunctions represent one of the most exciting areas of research into nanoscale materials; the various methods of their preparation and their utililty for a multitude of applications render this subject to be of immense current interest, and hence the subject of this Review. The Au nanorod (NR)/GaAs nanowire (NW) heterojunction shown in the figure represents work in our laboratory accomplished by combining vapor-phase and solution-phase methods.

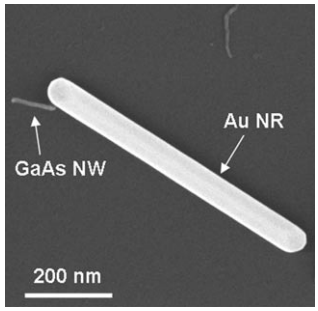

Nanoscale heterojunctions

■. a. t. p. J. Mieszawska, R. Jalilian, G. U. Sumanasekera, F. P. Zamborini* _____ ■■■■ – ■■■■

The Synthesis and Fabrication of One-Dimensional Nanoscale Heterojunctions